UNIVERSITY OF CALIFORNIA
RIVERSIDE

# Biogeochemical Signatures in Precambrian Black Shales: Window Into the Co-Evolution of Ocean Chemistry and Life on Earth

A Dissertation completed in partial satisfaction
of the requirements for the degree of

Doctor of Philosophy

in

Geological Sciences

by

Clinton Thomas Scott

December 2009

Dissertation Committee

Dr. Timothy Lyons, Chairperson
Dr. Gordon Love
Dr. Michael McKibben

This dissertation of Clinton Thomas Scott is approved:

---

---

---

Committee Chairperson

University of California, Riverside

ABSTRACT OF THE DISSERTATION

Biogeochemical Signatures in Precambrian Black Shales: Window Into the Co-Evolution of Ocean Chemistry and Life on Earth

by

Clinton Thomas Scott

Doctor of Philosophy, Graduate Program in Geological Science
University of California, Riverside, December 2009
Dr. Timothy Lyons, Chairperson

The degradation of sedimentary organic matter drives a suite of biologically-mediated redox reactions that in turn reflect the chemical composition of pore waters and bottom waters on local to global scales. By analyzing the chemical and isotopic composition of modern sediments and ancient black shales, biogeochemists can track the evolution of ocean/atmosphere redox conditions, the chemical composition of the oceans, and the evolutionary course of life throughout Earth history. Chapter 1 introduces the concepts of suboxic versus euxinic depositional environments and details the cycling of the transition metal molybdenum in each of these environments. A method for using Mo enrichments in ancient suboxic black shales as an environmental paleoproxy is proposed. Chapter 2 is a temporal survey of Mo enrichments in euxinic sediments and ancient black

shales, throughout Earth's history. The purpose of this study is to test the hypothesis that widespread euxinic conditions during the Proterozoic would lead to Mo drawdown on a global scale, affecting the global nitrogen cycle. Chapter 3 is a biogeochemical description of the Mesoproterozoic Newland Formation, a non-euxinic black shale. Chapter 4 is a biogeochemical description of the Archean Jeerinah Formation, Earth's earliest known euxinic basin.

# Table of Contents

# List of Figures

**Chapter 1**



**Chapter 2**

**Chapter 3**



**Chapter 4**

# List of Tables

Chapter 1

# *Molybdenum Geochemistry in Modern Suboxic Sediments and Ancient Suboxic Black Shales*

## 1.1 Abstract

The transition element molybdenum is present in the Earth's crust at trace concentrations but is abundant in seawater and many marine sediments and ancient marine sedimentary rocks. These occurrences have lead to the development of a suite of paleoproxies based on the Mo geochemistry of ancient black shales. These proxies have focused exclusively on the isotopic composition, bulk concentration, and covariation of Mo with total organic carbon in euxinic black shales, deposited beneath an anoxic and sulfidic water column. Here the geochemistry of Mo in suboxic sediments is considered and a new set of paleoproxies is proposed based on the identification and interpretation of ancient black shales from suboxic environments, where sulfide is present but restricted to the pore waters.

## 1.2 Introduction

The transition element molybdenum is a minor constituent of the Earth's crust (1 ppm; Taylor and McLennan, 1995) but is conspicuously enriched, up to 100s of ppm, in sulfidic marine sediments and ancient black shales (Bertine and Turekian, 1973; Brumsack, 1980; Francois, 1988; Dean et al., 1999; Lyons et al., 2002; Werne et al., 2002; Zheng et al., 2002; Algeo and Lyons, 2005; McManus et al., 2006; Poulson et al., 2006; Scott et al., 2008; Gill, 2009). These occurrences have motivated a great deal of research on Mo cycling in modern environments and Mo analyses have joined classic C-S-Fe systematics as a routine tool in the characterization and interpretation of ancient black shales, particularly as applied to the question of the initial oxygenation of the

biosphere and periods of relative ocean anoxia (Werne et al., 2002; Cruse and Lyons, 2004; Wilde et al., 2004; Anbar et al, 2007; Scott et al., 2008; Gill, 2008).

Black shales preserving bulk Mo concentrations of 100's of ppm are typical of localized Phanerozoic euxinic basins, where bottom waters are anoxic and contain hydrogen sulfide (Werne et al., 2002; Cruse and Lyons, 2004; Wilde et al. 2004). Thus, Mo concentrations can be used as an excellent indicator of past euxinic conditions. In addition to high enrichments of Mo, black shales often display a striking covariation between Mo concentrations and the concentration of total organic carbon or TOC (Lyons et al, 2002; Werne et al., 2002; Cruse and Lyons, 2004). Algeo and Lyons (2006) show that in modern euxinic environments, the value of Mo/TOC (ppm/wt. %) is proportional to the concentration of dissolved Mo in the euxinic basin and that Mo/TOC in ancient euxinic shales should likewise reflect the concentration of Mo in the ancient water column. Furthermore, when local euxinia is otherwise constrained by C-S-Fe proxies and where euxinic basins are open to resupply of Mo from the open ocean (e.g. Cariaco Basin, Venezuela; Lyons et al., 2002), Mo/TOC can reflect the global concentration of Mo. This is important for two reasons. First, because sulfidic environments are efficient at removing Mo from seawater, Mo/TOC, reflects the global extent of sulfidic conditions. Second, because Mo is also a micronutrient utilized in the fixation and assimilation of N, temporal trends in the Mo concentration of sea water provides information on global nutrient cycles (Anbar and Knoll, 2002). Application of this proxy to Phanerozoic and Precambrian euxinic black shales has confirmed the hypothesis of Anbar and Knoll

(2002), that persistent euxinic conditions can significantly deplete the global oceanic reservoir of Mo (Scott et al., 2008; Gill, 2009).

Motivated in part by the biological implications of global depletion of dissolved Mo during the Proterozoic Eon (Anbar and Knoll, 2002), Arnold et al (2004) proposed a method of quantifying the spatial extent of euxinic deposition based on Mo isotope signatures in euxinic black shales. In their model, the isotopic composition of sea water is dependent upon the relative influence of oxic versus euxinic depositional environments while suboxic sediments are considered a minor sink for Mo and are excluded from their calculations. Oxic environments record a strong, negative fractionation relative to seawater (Barling et al., 2001; Barling and Anbar, 2004) while euxinic environments record little or no fractionation (Siebert et al., 2003), approaching the seawater value. A simple mass balance calculation places an estimate on the euxinic fraction of the seafloor. This approach has been used to infer the extent of euxinia in the Proterozoic and Phanerozoic (Arnold et al, 2004; Lehman et al., 2007).

Each of these paleoproxy applications focus exclusively on black shales deposited under euxinic conditions. However, euxinia is rare on Earth today and it is likely that many of the pyritic black shales preserved in the rock record actually represent ancient suboxic sediments where sulfate reduction and sulfide accumulation were restricted to discrete zones below the sediment water interface. It is important to be able to identify Mo cycling in suboxic shales in order to avoid associating Mo concentrations and Mo/TOC to Mo availability and redox conditions in the water column. This is particularly

true for the Precambrian, where the absence of bioturbation would allow suboxic sediments to preserve lamination.

Here it is demonstrated that pyritic black shales with bulk Mo concentrations consistently < 20 ppm and Mo/TOC < 5 ppm/wt. % are characteristic of suboxic depositional environments. Thus, when used in concert with Fe speciation, Mo enrichments and Mo/TOC can be used to distinguish between euxinic and suboxic black shales. Furthermore, since modern suboxic environments account for half of Mo removed from the ocean annually, with a commensurate influence of the isotopic composition of seawater, future applications of the Mo isotope proxy for global euxinia must take the suboxic contribution into consideration. Under some circumstances, the Mo isotopic composition of suboxic black shales may capture evidence of Mn oxide cycling in ancient sediments, even in the absence of preserved Mn enrichments, further constraining bottom water redox conditions.

## 1.3 Molybdenum Geochemistry

Oxidative weathering of continental crust is the primary source of Mo in the oceans, and a single dissolved species, molybdate ($MoO_4^{2-}$), dominates in oxygenated waters (Manheim and Landergren, 1978) Due to the low reactivity of $MoO_4^{2-}$, oceanic Mo concentrations are on the order of 100 nM (Collier et al., 1985; Barling et al., 2001), the highest of any transition element. A number of essential cellular functions require Mo (Scherer, 1989; Kessler et al., 1997; Raymond et al., 2004; Zerkle et al., 2006; Glass et al., 2009), but in the modern ocean the biological demand is far exceeded by the size of

the oceanic reservoir such that Mo concentrations vary less than 5% throughout the world's oceans. The residence time of Mo is nearly 800,000 years (Emerson and Huested, 1991; Morford and Emerson, 1999; Scott et al., 2008), compared to an ocean mixing cycle of 2,000 years.

The primary sink for $MoO_4^{2-}$ is coprecipitation/adsorption with Mn-oxides (Mn nodules, ferromanganese crusts and pelagic clays) on the deep seafloor where sedimentation rates are extremely low (Bertine and Turekian, 1973; Krishnaswami, 1976). Interestingly, the ratio of total Mo to total Mn (Mo/Mn) in each of these lithologies is remarkably consistent 0.002 (Shimmield and Price, 1999). Due to the low burial rate of Mn oxides, and despite the global extent of oxic environments, most of the ocean's Mo is removed by a relatively small fraction of the seafloor (1-2 %; Scott et al., 2008) where $MoO_4^{2-}$ is not stable.

Mo speciation is subject to change where sulfide is produced as a byproduct of bacterial sulfate reduction (BSR). In the presence of minor amounts of dissolved sulfide, $MoO_4^{2-}$ is converted to a series of particle-reactive thiomolybdates ($MoS_{4-x}O_x^{2-}$) (Helz et al., 1996). Where sulfide reaches just 10 μM, tetrathiomolydate ($MoS_4^{2-}$) forms and Mo is rapidly sequestered into the organic fraction and/or precipitated with authigenic sulfide minerals (Huerta-Diaz and Morse, 1992; Crusius et al., 1996; Helz et al., 1996; Erickson and Helz, 2000; Vorlicek and Helz, 2002; Bostick et al., 2003; Tribovillard et al., 2004; Vorlicek et al., 2004). In environments where sulfide is present and thiomolybdates are forming, the burial rate of Mo is two to three orders of magnitude higher than in oxic

environments (Bertine and Turekian, 1973; Scott et al., 2008). One manifestation of efficient thiomolybdate sequestration is the significant enrichment of Mo in sulfidic sediments and ancient black shales, where concentrations can exceed 200x the crustal average (Werne et al., 2002; Lyons et al., 2003; Cruse and Lyons, 2004; Algeo and Lyons 2006). Rapid removal of thiomolybdates, particularly $MoS_4^{2-}$, from solution has the potential to severely deplete the local or even global reservoir of dissolved Mo (Algeo, 2004; Algeo and Lyons, 2006). This phenomenon is best expressed in the euxinic Black Sea where below 200 m, hydrogen sulfide exceeds 100 μM, and dissolved Mo drops dramatically to ~3 nM or about 3% of the open ocean average (Emerson and Huested, 1991). Thus, the large size of modern oceanic reservoir requires that thiomolybdates are confined to a small fraction of the seafloor.

Another prominent feature of many euxinic basins and euxinic black shales is a strong co-variation between the concentrations of Mo and TOC (Werne et al., 2002; Lyons et al., 2002; Cruse and Lyons, 2004; Algeo and Lyons, 2006; Scott et al., 2008; Gill, 2009). The mechanisms responsible for this relationship are not yet known, but it is clear that the average value of Mo/TOC is sensitive to the concentration of Mo in the euxinic portion of the water column (Algeo and Lyons, 2006). This relationship has been used to track the size of local, or even global, Mo reservoir (Scott et al., 2008; Gill, 2009), with important implications for both ocean redox conditions and nutrient cycles. However, not all sulfidic environments and not all black shales display this conspicuous

co-variation, and as described below, care must be taken to exclude non-euxinic shales when relating Mo/TOC to dissolved Mo concentrations in the water column.

In modern sulfidic settings, Mo concentrations cover a wide range, from just above the crustal average of 1-2 ppm (Taylor and McLennan, 1995) up to 100's of ppm (Lyons et al., 2002; Algeo and Lyons, 2006). However, a distinct bimodal distribution appears if we consider suboxic and euxinic locations separately (Fig. 1.1). The average concentration of Mo in modern suboxic environments, where hydrogen sulfide is restricted to the pore waters is 10 ppm. Furthermore, Mo rarely exceeds 20 ppm, and never exceeds 40 ppm. In contrast, in normal euxinic environments, where hydrogen sulfide is present in the water column throughout the year and dissolved Mo is abundant, enrichments display a much wider range, with an average of ~100 ppm, but never fall below 60 ppm. Importantly, there is no overlap in the concentration of Mo between these distinct environments. This bimodal relationship suggests that there is a mechanistic difference in the enrichment of Mo between these environments. In seasonally euxinic locations like Saanich Inlet, British Columbia (Francois et al., 1988) and intermittently euxinic locations like the Namibian Shelf (Brongersma-Sanders et al., 1980; Algeo and Lyons, 2006), Mo concentrations fall between the end-members of suboxia and euxinia, presumably representing a mixture of enrichment mechanisms. Mo concentrations in sediments from the restricted and euxinic Black Sea also fall in this intermediate range reflecting extreme water column Mo depletion (Algeo and Lyons, 2006), and is our best analogue to a Mo-limited Proterozoic (Scott et al., 2008).

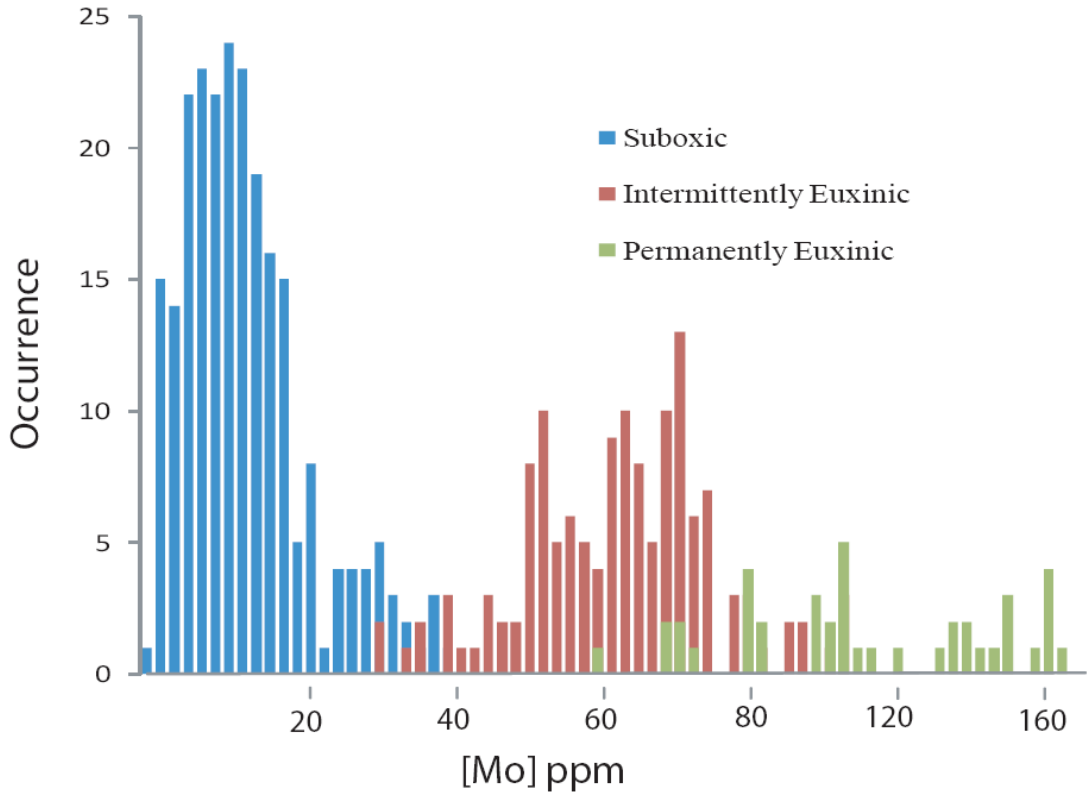


Figure 1.1: Mo concentrations in modern sulfidic sediments. Blue bars are suboxic sediments. Red bars are intermittently euxinic or permanently euxinic and Mo deficient. Green bars are permanently euxinic and Mo replete.

As is the case with Mo enrichments and Mo/TOC, Mo isotope systematics are dominated by the speciation of dissolved Mo in the sedimentary environment. Riverine delivery is the primary source of $MoO_4^{2-}$ to the oceans, and displays a considerable range of isotopic compositions, averaging $\delta^{98/95}$ +0.7 ± 0.2‰ (Archer and Vance, 2007). Dissolved Mo in the open ocean is comparatively enriched (+2.3‰; Barling et al., 2001; Siebert et al., 2003). $MoO_4^{2-}$ adsorption onto Mn nodules and ferromanganese crusts results in a relatively large fractionation of -3‰ from sea water, and Mo burial in association with Mn nodules and crusts is thought to be the primary driver behind the isotopic enrichments observed in the open ocean. Conversely, in euxinic environments, $MoS_4^{2-}$ is removed from the water column with a much smaller fractionation relative to sea water; -0.6‰ in the Cariaco Basin, Venezuela and 0‰ in the Black Sea (Barling et al., 2001; Siebert et al., 2003; Arnold et al., 2004). Since euxinic black shales record little or no fractionation, they approximate the paleo-seawater value which can then be used to estimate the euxinic fraction of the global seafloor using a simple three-box model (ocean reservoir, oxic sink, euxinic sink) that excludes suboxic sediments (Arnold et al., 2004; Lehman et al., 2007; Wille et al.., 2008). However, a recently updated Mo budget demonstrates that suboxic sediments actually remove half of the riverine flux (Scott et al., 2008), with a commensurate influence (Poulson et al., 2006) on the isotopic composition of seawater that necessitates a reworking of the isotopic mass balance.

## 1.4 Suboxic Marine Sediments

Suboxia is commonly defined by some minimum threshold of dissolved oxygen in the water column or depth of oxygen penetration into the sediments (Luther and Church, 1988; Murray et al., 1992; Morford and Emerson, 1999; Zheng et al., 2000). However, this parameter is the primary unknown in paleoredox studies. In order to develop useful paleopreoxies, modern analogues should be defined in terms of variables that are available in the rock record. Thus, for the purpose of paleoproxy, suboxic environments are here defined as those where oxidants other than oxygen (e.g., $NO_3^-$, $Mn^{2+}$, $Fe^{2+}$, $SO_4^{2-}$) are consumed in the degradation of sedimentary organic matter and which are not euxinic, adding sulfate reduction to the classic description of suboxic sediments by Froelich et al. (1979). Suboxic sediments develop beneath a range of bottom water conditions (Murnane et al., 1989; Shaw et al., 1990; Johnson et al., 1992; Kuwabara et al., 1999; Zhang et al., 2000), including those where oxygen penetrates into the pore waters and those where bottom waters are anoxic.

As described by Froelich et al. (1979), the remineralization of organic matter in suboxic marine sediments will theoretically proceed through the utilization of the following sequence of oxidants: $O_2$, Mn-oxides/nitrate, Fe-oxides and sulfate. The oxidant yielding the highest free energy gain is utilized first and exclusively until it is completely consumed, after which, the next most efficient oxidant is utilized and so on until all oxidants or labile organic matter are exhausted. Under ideal conditions, the complete sequence is utilized and discrete redox zones develop in the sediment profile as reduced products ($Mn^{2+}$, $Fe^{2+}$, $S^{2-}$) are re-oxidized by oxidants higher in the sequence

(Fig. 1.2). This mechanism behaves as an electron pump linking reduced carbon buried in the sediments to the seawater source of electron accepters (Postma, 1985; Aller and Rude, 1988; Myers and Nealson, 1988; Yao and Millero, 1993; Canfield et al., 1993; Yao and Millero, 1996).

This theoretical model of suboxic diagenesis is expressed to varying degrees in natural environments in response to varying inputs of organic matter and oxidants as well as the influence of bacterial and infaunal communities. Commonly, not all oxidants are utilized in the sediments. For example, where the delivery of oxidants is high, and delivery of reduced carbon is relatively low, sulfate reduction is not favorable in the sediments and no sulfide zone will develop. This scenario is exemplified by the suboxic sediments of Santa Cruz Basin, California and others locations in the eastern Pacific Ocean (Shaw et al., 1990; Shimmield and Price, 1986; Crusius et al., 1996), among others. Conversely, where there is a high demand for oxidants in the water column, bottom waters can become sufficiently depleted in oxygen (<10 to 100 μM) that $MnO_2$ is excluded from the sediments and the sulfide zone may approach the sediment water interface (Brumsack and Gieskes, 1983; Pedersen et al. 1989; Zheng et al., 2000; McManus et al, 2006). Suboxic sediments suitable for both Mn-oxide and sulfate reduction zones require both oxygenated bottom waters and a high flux of organic matter. (Fig. 1.3; Brumsack and Gieskes, 1983; Malcolm, 1985; Canfield et al., 1993; Nameroff et al., 1999; Elbaz-Poulichet et al., 2006).

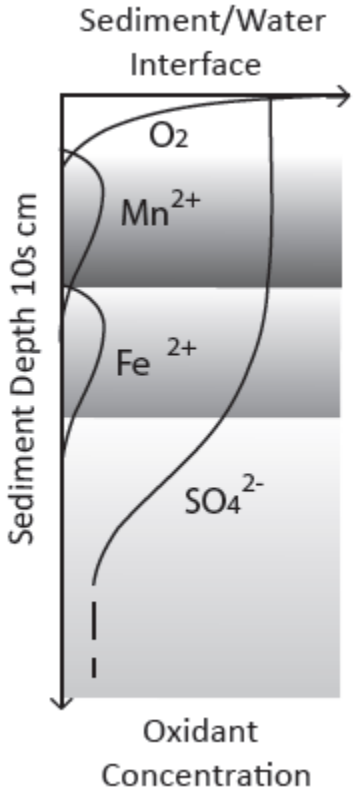


Figure 1.2. Schematic of idealized suboxic sediments. After Froelich et al., (1979).

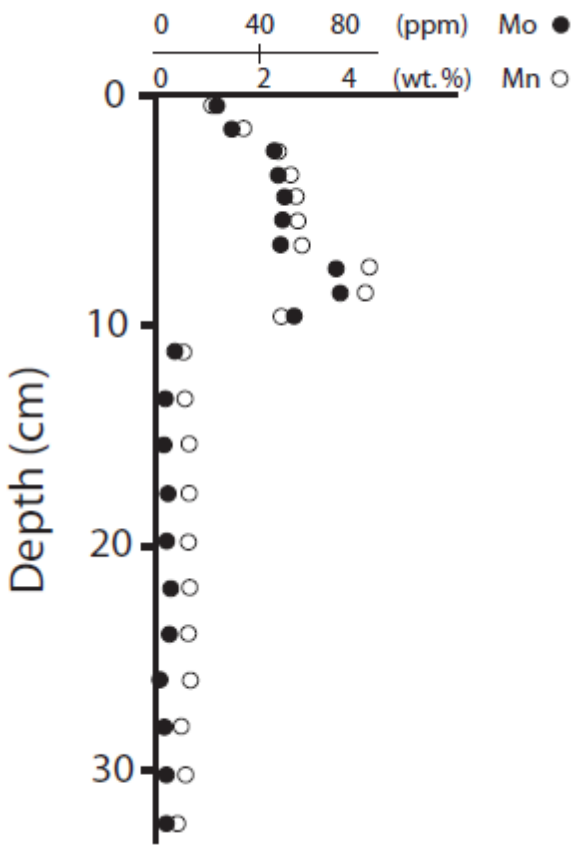


Figure 1.3. Sediment profile of suboxic sediments off the coast of Baja California. After Shimmield and Price (1986).

Due to the affinity of $MoO_4^{2-}$ for Mn-oxides, the Mn cycle is particularly important in understanding how Mo is cycled in suboxic sediments. Where Mn-oxides are actively cycled in the sediments two constraints must be met: the water column must be sufficiently oxygenated to allow for Mn-oxides to accumulate at the sediment water interface and the pore waters must be sufficiently reducing to promote dissolution. In the natural environment, Mn-oxides begin to dissolve in the water column where oxygen falls below 100 μM (Klinkhammer and Bender, 1980; Calvert and Pedersen, 1996) but due to sluggish dissolution, can persist and become buried where oxygen is as low as 10 μM (Shaw et al., 1990), highlighting the importance of exposure time on the burial of metal oxides. Below 10 μM $O_2$, Mn-oxides are not known to persist. Where Mn-oxides are buried, a distinct subsurface maximum in Mn particulates is a common feature (Fig. 1.3; Burdige and Gieskes, 1983; Malcolm, 1985; Canfield et al., 1993; Calvert and Pedersen, 1996). Such maxima are the result of reductive dissolution of Mn-oxides upon further burial, upward diffusion of $Mn^{2+}$, and reprecipitation of Mn-oxides at the maximum depth of oxygen penetration (Burdige and Gieskes, 1983). These subsurface maxima of Mn-oxides are not preserved in the rock record but they play an important role in the remineralization of organic matter. Canfield et al. (1993) estimated that a single atom of Mn may be recycled hundreds of time before being lost from the system.

## 1.5 Molybdenum in Suboxic Sediments

As defined above, suboxic sediments are those where oxidation of sedimentary

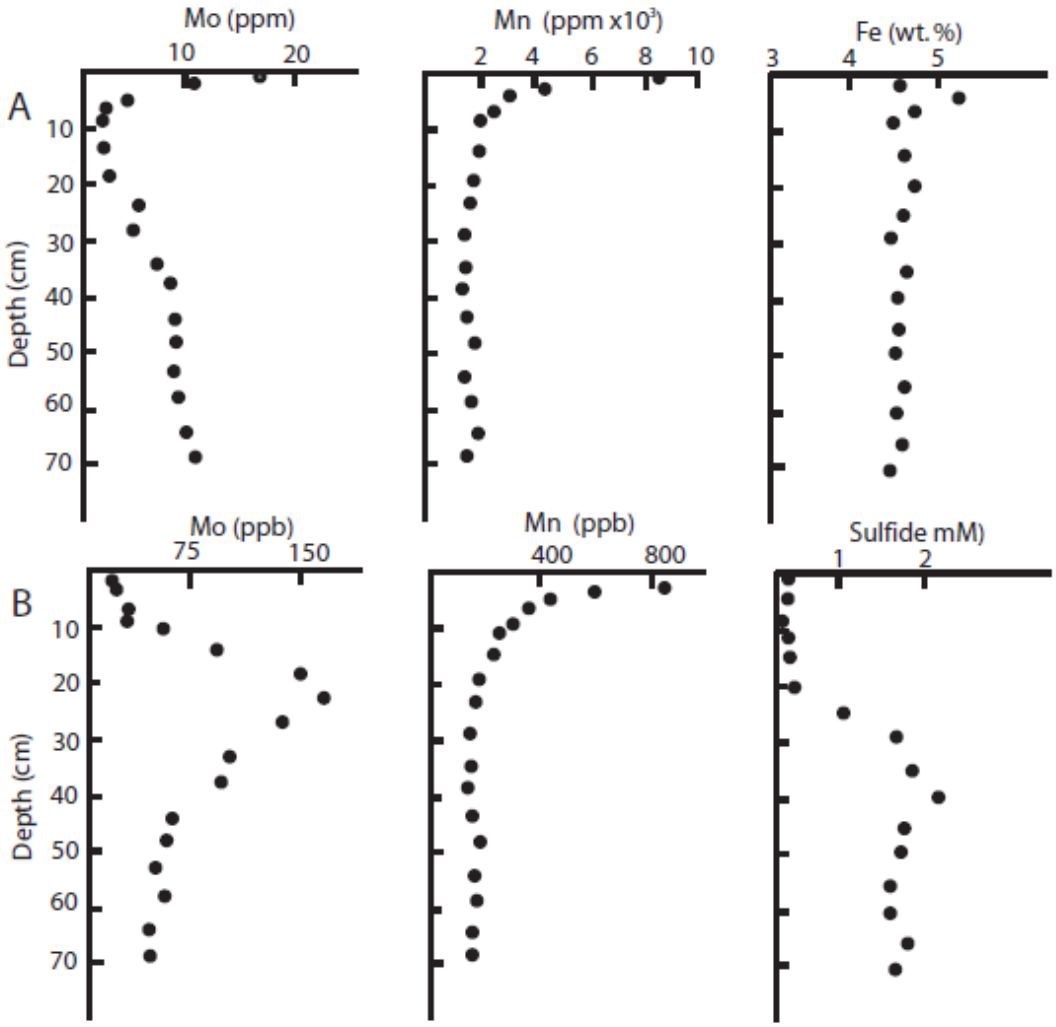


Figure 1.4. Sediment profile of suboxic sediments from Loch Etive, Scotland. A. Particulate metal concentrations. B. Dissolved pore water constituents. After Malcom (1985).

organic matter is coupled to the reduction of oxidants other than oxygen, including any or all of the following: Mn-oxides, Fe-oxides and sulfate. This definition is based on sedimentary processes because it is the sediments that are ultimately preserved in the rock record and it is intended to facilitate the identification of ancient suboxic black shales. However, this definition of suboxia is also well suited for the study of Mo cycling in general. Mo is sequestered from seawater by one of two pathways, as $MoO_4^{2-}$ where Mn oxides are buried, and as $MoS_{4-x}O_x^{2-}$ where sulfides are buried. These two environments are essentially mutually exclusive because Mn-oxides will not persist in sulfidic pore waters. Importantly, where Mn-oxides (and adsorbed $MoO_4^{2-}$) are permanently buried they are not being reduced in association with organic matter oxidation and the environment is considered to be oxic, not suboxic. Conversely, where thiomolybdates are forming in, and sequestered from the water column, the environment is considered to be euxinic, not suboxic. Thus, from the perspective of Mo burial, suboxic sediments are specifically those where sulfide is present, but restricted to the pore waters.

Suboxic sediments where sulfate reduction is not occurring are not meaningful sinks for seawater Mo because thiomolybdates are not forming (Crusius et al., 1996; Morford and Emerson, 1999). However, due to the strong affinity of $MoO_4^{2-}$ for Mn-oxides, these sediments will often display a significant surficial enrichment of Mo if robust Mn-oxide recycling is occurring below the sediment/water interface. These surface features can reach 100s of ppm Mo and the ratio of Mo/Mn is typically 0.002, the same

ratio observed in oxic sediments. While these surficial enrichments may constitute a substantial reservoir of Mo, they are not permanently buried.

An excellent example of this relationship is expressed in cores from the suboxic Pacific Margin off Baja California (Fig. 1.3; Shimmield and Price, 1986). Here, bottom waters are mildly oxygenated and Mn-oxides reach 6 wt. % in the surface sediments, while Mo concentrations reach 120 ppm (Mo/Mn = 0.002). As Mn-oxides are further buried into organic matter-containing sediments, they experience reductive dissolution, and liberate adsorbed $MoO_4^{2-}$ into the pore waters. In the absence of pore water sulfide, $MoO_4^{2-}$ will diffuse into the overlying water column and Mo is not permanently buried (Johnson et al., 1992; Morford and Emerson, 1999). This example highlights two important points. First, not all suboxic environments are sinks for Mo. This perspective was explored by Crusius et al. (1996) who showed that Re is highly enriched in such in sediments while Mo is not, such that the ratio Re/Mo can be used as an indicator for suboxia in non-sulfidic black shales. Second, while some suboxic sediments appear to be a source of dissolved Mo to the ocean (Bertine and Turekian, 1973; Morford and Emerson, 1999), they do not represent a net source of Mo, rather they reflect a failed sink of Mo.

In suboxic environments where the redox gradient is highly compressed, such that both Mn-oxides and sulfate are reduced in the sediments, two zones of Mo enrichment can develop. A transient enrichment zone is again established where Mn-oxides accumulate in the surface sediments (Fig. 1.4). A second, permanent enrichment zone is coincident with the zone of sulfide accumulation as thiomolybdates are formed in,

and removed from, the pore waters. From the perspective of the Froelich (1979) model, these two horizons are separated by the zone of Fe-oxide cycling (Fig. 1.2).

An excellent example is the suboxic sediments in Lock Etive, a fjordic estuary on the west coast of Scotland (Fig. 1.4; Malcolm, 1986). In Loch Etive sediments, Mo concentrations are highest at the sediment water interface, reaching 20 ppm, coincident with a surface enrichment of Mn-oxides. Below the Mn-oxide reduction zone, particulate Mo drops to crustal levels, while pore water $MoO_4^{2-}$ accumulates to twice the open ocean concentration. This is the result of reductive dissolution of Mn-oxides and release of $MoO_4^{2-}$ in the zone of Fe-oxide reduction. In the sulfate reduction zone, sulfide accumulates in the pore waters while the concentration of dissolved Mo decreases. Mo enrichments rebound from crustal levels to approximately 10 ppm, a concentration that is typical of suboxic sediments (Fig. 1.1).

The dissolved Mo maximum in the Fe-oxide reduction zone of Loch Etive sediments highlights the fact that there are two sources of Mo in many suboxic pore waters, sea water $MoO_4^{2-}$ that is supplied through diffusion and $MoO_4^{2-}$ released to pore waters upon reductive dissolution of Mn-oxides. This augmented pore water reservoir is the source of the Mo that is ultimately sequestered in the sulfidic zone. Because Mn-oxides are known to adsorb isotopically light $MoO_4^{2-}$, in cases where Mn-oxides are recycled in the surface sediments, it is expected that permanently buried Mo will record an isotopic signal of Mn-oxide recycling, even though Mn-oxide/ $MoO_4^{2-}$ maxima are not preserved.

In sediments where Mn-oxides are excluded, due to a combination of water column redox conditions and transit time for Mn-oxides through the oxygen minimum zone, transient surface enrichments of Mo are not observed and if sulfate reduction is also absent, no Mo enrichments will occur (Zheng et al., 2000). Where Mn-oxides are excluded and sulfide is present, thiomolybdates will form from a pore water source that is not augmented through Mn-oxide dissolution. These processes are well expressed in sediments below the oxygen minimum zone of the continental margin near Mazatlan, Mexico (Fig. 1.5; McManus et al., 2006) where bottom water oxygen concentration is essentially zero and sulfide accumulates close to the sediment water interface.

While such environments are at the reducing extreme of suboxia as defined above, the magnitude of Mo enrichment is not significantly higher than in less reducing suboxic examples (Fig. 1.1) and they lack the strong covariation between Mo concentrations and organic matter that are common in euxinic sediments (Fig. 1.6). In euxinic sediments and shales the average value of Mo/TOC (ppm/wt. %) is typically in the range of 25 to 30 and values of 10 to 15 suggest water column Mo depletion (Algeo and Lyons, 2006; Scott et al., 2008; Gill, 2009). By comparison, in suboxic sediments off of Mazatlan, average Mo/TOC is less than 2 (Fig. 1.6).

The isotopic value of Mo in modern suboxic sediments covers a wide a range of $\delta^{98/95}$Mo (-0.5 to +1.6‰) that spans from close to the oxic end-member (-0.7‰) to close to the euxinic end-member (+1.8 ‰; Poulson et al., 2006; Siebert et al. 2006). Furthermore, $\delta^{98/95}$Mo correlates negatively with bottom water oxygen concentration (Fig. 1.7). As described by Reitz et al. (2007), the mechanism driving the observed range

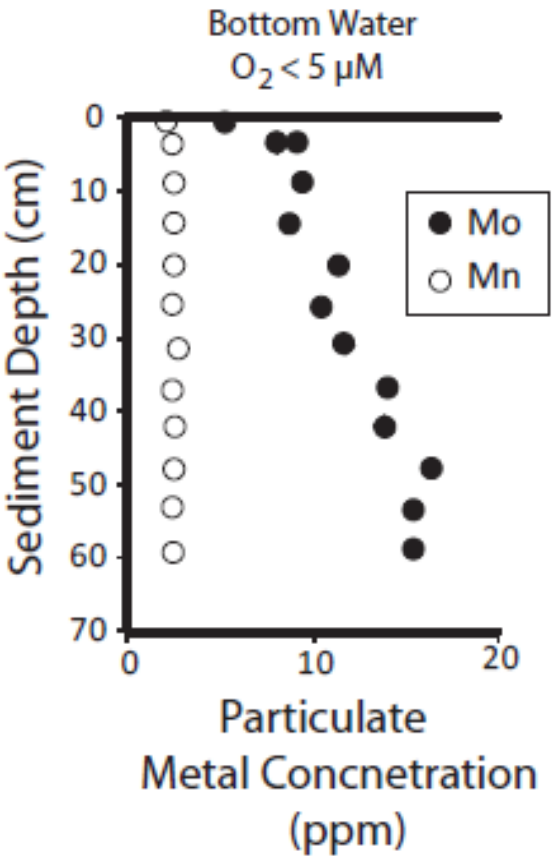


Figure 1.5. Sediment profile of suboxic sediments off the coast of Mazatlan, Mexico. McManus et al. (2006).

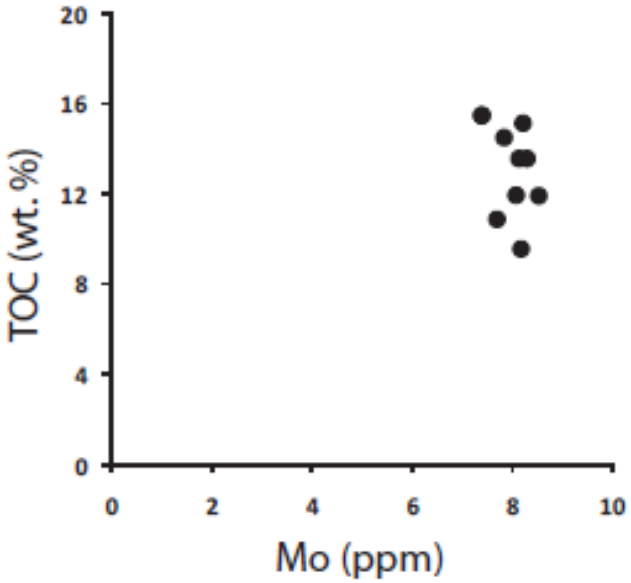


Figure 1.6. Mo/TOC in suboxic sediments off the coast of Mazatlan, Mexico. McManus et al. (2006).

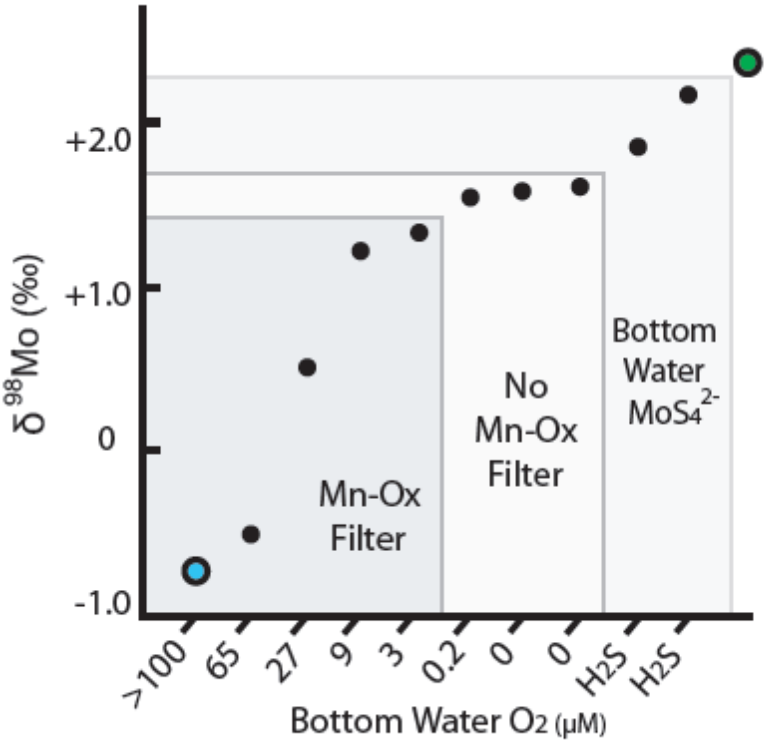


Figure 1.7. Isotopic composition of suboxic and euxinic sediments. Green circle is the isotopic composition of seawater. Blue circle is the isotopic composition of Mn nodules. Data from Barling et al. (2001); Siebert et al. (2003); Poulson et al. (2006); Siebert et al. (2006).

in $\delta^{98/95}$Mo and the correlation with bottom water oxygen is likely the presence or absence of Mn-oxides recycling in the sediments.

## 1.6 Discussion

### 1.6.1 A Model for Molybdenum Cycling in Suboxic Sediments

Figure 8 is a schematic of four idealized depositional environments where Mo is cycled, three of them are suboxic (Fig. 1.8a-1.8c) and one euxinic (Fig. 1.8d). The suboxic examples are based on the three specific environments discussed in Section 1.5: the Pacific Margin off of the Baja California Peninsula (Shimmield and Price, 1985) where Mo is cycled with Mn-oxides but sulfide is absent such that Mo is not permanently buried; Loch Etive, Scotland (Malcolm, 1985) where Mo is cycled with Mn-oxides in the surface sediments and is permanently buried in the sulfate reduction zone; the Pacific Margin off of Mazatlan, Mexico (McManus et al., 2006) where Mo is buried in sulfidic sediments and in the absence of Mn-oxide cycling. Figure 1.8d is a euxinic environment where $MoS_4^{2-}$ is stable in the bottom waters throughout the year.

In the least reducing suboxic environments (Fig. 1.8a) Mn-oxides are recycled in the surface sediments and sulfate reduction is absent. Mo concentrations associated with surficial Mn-oxide recycling can exceed 100 ppm (Bertine and Turekian, 1973; Shimmield and Price, 1986). The affinity of molybdate for Mn-oxides is well known. Not only are Mn nodules and crusts the largest sink for oceanic Mo, but a constant ratio (Mo/Mn≈ 0.002) is observed in a variety of sediments types where Mn oxides are

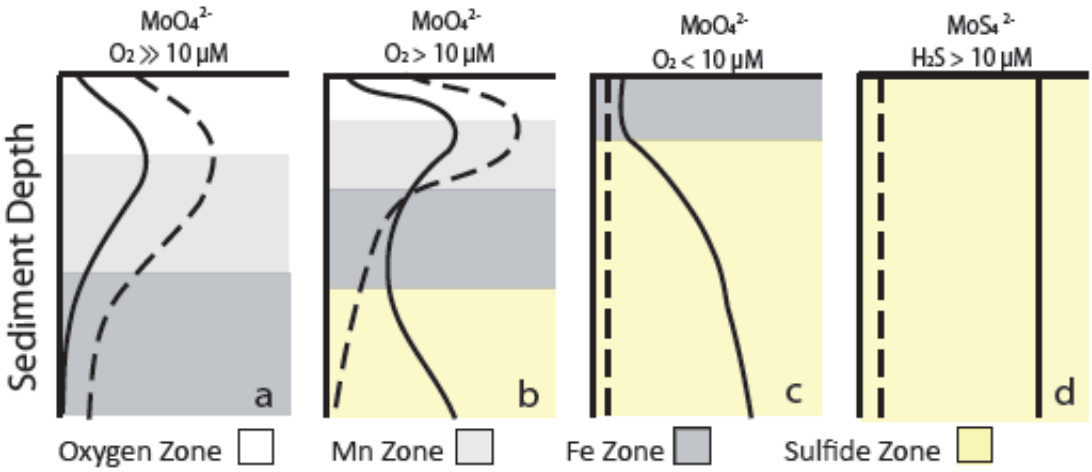


Figure 1.8. Idealized model for Mo enrichments in suboxic sediments. Dashed line represents concentration of particulate Mn-oxides. Solid line represents concentration of particulate Mo. a. Suboxic sediments with ephemeral surficial enrichments of both Mn-oxides and Mo. b. Suboxic sediments with ephemeral surficial enrichment of both Mn-oxides and Mo particulates and permanent enrichments of Mo in the sulfidic zone. c. Suboxic sediments where Mn-oxides are excluded from the sediments due to low bottom water oxygen and with permanent enrichments of Mo in the sulfidic zone. d. Euxinic sediments where thiomolybdates are present in the bottom waters.

present, to include Mn nodules and crusts, the Mn-oxide zone of suboxic sediments, and sediment traps from oxygenated waters (Shimmield and Price, 1986; Nameroff et al., 1999). Because Mn-oxides do not persist as they are progressively buried, Mo is not permanently buried in these environments. Such suboxic environments, upon preservation in the rock record, will record no Mo enrichments. Rather, they will be enriched in Re relative to Mo, as described by Crusius et al. (1996). It is important to recognize that environments demonstrating large surficial enrichments of Mo are not necessarily sinks for dissolved Mo.

In environments with a compressed redox gradient both Mn-oxides and sulfate are reduced in the sediments (Fig. 1.8b). This co-occurrence requires a unique combination of oxygenated bottom waters and sulfidic pore waters and may speak to a productivity control on organic matter burial. Based on the variable chemistries of the California Borderland Basins, Mn-oxide recycling requires that bottom water oxygen $\geq 10$ μM (Shaw et al, 1990). Two zones of Mo enrichment occur in these sediments, a transient upper zone of enrichment and a lower zone of permanent enrichments where thiomolybdates are formed. Reductive dissolution of Mn-oxides contributes significantly to the pore water reservoir of dissolved Mo. It is well known that Mn-oxides preferentially adsorb isotopically light $MoO_4^{2-}$; the - 3‰ fractionation from sea water observed in Mn-oxides covers nearly the entire range of Mo isotopes in modern marine environments (Barling et al., 2001; Arnold et al., 2004; Reitz et al., 2007). Mn-oxide recycling augments the pore water reservoir form which thiomolybdates form, and the Mo that is permanently buried in these suboxic environments should record isotopic

evidence for Mn-oxide recycling (Reitz et al., 2007). More vigorous Mn-oxide recycling would hypothetically have a greater influence on pore water chemistry.

At the more reducing extreme of suboxic environments Mn-oxides are excluded from the sediments and sulfide accumulates very near the sediment water interface (Fig. 1.8c). Because Mn-oxide recycling is absent from the sediments, the isotopic composition of pore water Mo will mirror that of the bottom waters. While these conditions are very near to euxinia, the concentration of preserved Mo will still remain well below 20 ppm on average.

### 1.6.2 The Influence of Molybdenum Speciation at the Sediment Water Interface

The distinct bimodality of Mo enrichments between suboxic sediments and euxinic basins, and the lack of Mo/TOC covariation in suboxic sediments, suggests that there is a first-order variable that controls the rate and magnitude of Mo enrichment and its sensitivity to the abundance of organic matter. The most important variable that differs between suboxic and euxinic environments, as described above, is the speciation of Mo at the sediment water interface. $MoO_4^{2-}$ is the dominant species of Mo at the sediment water interface of all suboxic environments. This is true despite a considerable range in water column oxygen and pore water sulfide concentrations. Where thiomolybdates ($MoS_{4-x}O_x^{2-}$) are present at the sediment water interface, the environments is euxinic. In euxinic environments, thiomolybdates may precipitate directly on this horizon, without diffusing into the pore waters, or may be scavenged directly from seawater, joining the detrital

fraction. Thus, in euxinic environments, diffusion of dissolved Mo into the sediments is not necessary. However, this is not the case in suboxic environments.

Many suboxic sediments lack sufficiently high rates of sulfate reduction required to exhaust the pore waters of dissolved Mo and should be considered effectively sulfide limited with respect to Mo enrichments. These settings likely produce intermediate thiomolybdates which are less particle reactive than is tetrathiomolybdate (Zheng et al., 2000). In cases where pore water Mo is depleted as a result of efficient thiomolybdate sequestration, $MoO_4^{2-}$ must diffuse into the sulfidic zone, where conversion to thiomolybdates occurs, in order to promote continued enrichment. It is likely this requirement for diffusion, combined with the sluggish conversion to thiomolybdates (Helz et al., 1996) that limits the magnitude of Mo enrichment in suboxic sediments, even where pore water sulfide is abundant.

Organic matter burial acts as a control for the concentration of Mo in euxinic black shales (Lyons et al, 2002; Tribovillard et al., 2004; Algeo and Lyons, 2006), as expressed by the conspicuous covariation between Mo and TOC (e.g. Oatka Creek Formation, Devonian; Werne et al. 2002). As described by Algeo and Lyons (2006), the sensitivity of Mo enrichment to the abundance of organic matter decreases as Mo becomes depleted from the euxinic water column, and Mo/TOC in euxinic black shales can be used to track the supply of dissolved Mo on local to global scales (Scott et al., 2008; Gill, 2009). For example, average Mo/TOC for Phanerozoic euxinic black shales is 25 ppm/wt. %, reflecting Mo replete oceans resulting from oxygenation of the deep

ocean, compared to Mo/TOC of 15 ppm/wt. % for the Proterozoic, owing to more reducing oceans and efficient removal of Mo (Scott et al., 2008).

However, in suboxic sediments from Mazatlan, Mexico, (Fig. 1.6), where conditions are nearly euxinic, and organic matter covers a relatively wide range for suboxic sediments, Mo/TOC averages just 2 ppm/wt. %, reflecting a greatly diminished influence of TOC on the concentration of Mo in the sediments (McManus et al, 2006; Poulson et al, 2006). Here, Mo enrichments are essentially decoupled from the abundant organic matter. This decoupling is also consistent with a diffusional barrier to the resupply of $MoO_4^{2-}$ to pore waters. Thus, both the magnitude of Mo enrichment and the lack of Mo/TOC in suboxic are best explained by the speciation of Mo at the sediment water interface.

### 1.6.3 Molybdenum Concentrations and Mo/TOC in Ancient Shales as a Proxy for Suboxic Sediments

The bimodal expression of Mo concentrations in modern sulfidic sediments, and the lack of Mo/TOC covariation in modern suboxic sediments, allow for the unique characterization of ancient suboxic environments based on Mo geochemistry. For ancient black shales, Mo concentrations consistently below 20 ppm and with no covariation between the concentrations of Mo and TOC suggest an environment where bacterial sulfate reduction and sulfide accumulation were restricted to the pore waters and was thus suboxic. Importantly, other oxidants, perhaps even oxygen, were likely utilized in the remineralization of sedimentary organic matter as well.

Conversely, black shales with Mo concentrations greater than 100 ppm and which co-vary with the concentration of organic matter, are indicative of euxinic conditions where hydrogen sulfide and thiomolybdates were present above the sediment water interface. Black shales with intermediate Mo enrichments (20 to 100 ppm) are more ambiguous. Modern examples include intermittently euxinic environments such as restricted Saanich Inlet, British Columbia (Francois, 1988), and highly productive upwelling regions like the Namibian Shelf (Brongersma-Sanders et al., 1980) and the Peru Margin (Bonning et al, 2004; McManus et al, 2006). These locations are essentially fluctuating between suboxia and euxinia over variable timescales and Mo enrichments reflect a time-average of the two depositional mechanisms.

The use of Mo concentration as a proxy for suboxia is supported by the work of Scott et al., (2008) who demonstrated that euxinic black shales with Mo concentrations consistently below 20 ppm are only known in the Archean, before oxidative weathering of the continents, and thus supply of $MoO_4^{2-}$ to the oceans, was initiated. Furthermore, this interpretation is apparently insensitive to high rates of sedimentation. In the modern Black Sea, where sedimentation rates are high (15-20 cm/1000 yr; Lyons and Severmann, 2006) and dissolved Mo is less than 3% of the open ocean average (Emerson and Huested, 1991), Mo concentrations are still well above 20 ppm and still display at least a weak covariation with the concentration of organic matter (Algeo and Lyons, 2006). Thus, extreme rates of sedimentation are required to give a false positive (euxinia disguised as suboxia).

Black shales with Mo concentrations and Mo/TOC ratios intermediate to those of modern suboxic and euxinic end-members are common in the rock record (Algeo, 2004; Algeo and Lyons, 2006; Scott et al., 2008; Gill, 2009). Where independent evidence for euxinia exists (i.e. classis C-S-Fe chemistry) these black shales should be interpreted as representing a Mo deficient water column (Algeo and Lyons, 2006; Scott et al., 2008). In the absence of conclusive evidence for euxinia, intermittent euxinia on season timescales should also be considered.

In order to make a robust characterization of the paleoenvironment, this Mo proxy should be used in concert with additional proxies based on other elements of redox significance (C, S, Fe, Mn). In terms of reconstructing the paleoenvironment as a whole, the strength of the interpretation should reflect the degree to which the multiple proxies agree.

### 1.6.4 Molybdenum Isotopes in Suboxic Sediments and Suboxic Black Shales

To date, Mo isotopes studies of ancient black shales have focused on the isotopic composition of authigenic Mo in euxinic black shales. The goal of these studies is to estimate the global extent of euxinic deposition using a simple three-box model that makes two important assumptions. The first assumption is that the isotopic composition of authigenic Mo preserved in a euxinic shale is a faithful record of the isotopic composition of seawater at the time of deposition, as is apparently the case in the modern Black Sea, the largest euxinic basin on Earth today. However, the isotopic composition of Mo in the Cariaco Basin, the second largest euxinic basin today, demonstrates a -0.6 ‰

fractionation ($\delta^{98/95}$Mo) from the seawater value (Arnold et al., 2004; Nagler et al., 2005). The difference between these two basins appears to be that Mo is quantitatively removed in the highly restricted Black Sea, while it is not in the Cariaco Basin. Thus, quantitative removal of Mo is essential for a faithful recording of the seawater value, yet it is difficult to constrain quantitative removal in ancient black shales. The second assumption made in the Mo isotope proxy for ancient euxinia is that suboxic environments account for a trivial amount of Mo removed from seawater, and are thus excluded from the three-box model used to relate the preserved signature to the extent of euxinic deposition. However, Scott et al. (2008) published an updated modern Mo budget indicating that suboxic sediments in fact remove about half of the annual riverine flux of Mo. Clearly, suboxic environments should not be ignored in the Mo isotope proxy for global euxinia.

Modern suboxic sediments demonstrate a range of $\delta^{98/95}$Mo (-0.5 to +1.6‰; Poulson et al., 2006; Siebert et al. 2006) that spans from near the oxic end-member where $MoO_4^{2-}$ is buried in association with Mn-oxides ($\delta^{98/95}$Mo = -0.7 ‰; Barling et al., 2001; Seibert et al., 2003), to near the isotopic value of the euxinic Cariaco Basin, Venezuela ($\delta^{98/95}$Mo = +1.8‰; Arnold et al., 2004; Nagler et al., 2005). Furthermore, $\delta^{98/95}$Mo correlates negatively with bottom water oxygen concentration (Fig. 1.7). The mechanism driving the observed range in $\delta^{98/95}$Mo and the negative correlation with bottom water oxygen is likely the influence of Mn-oxide recycling in the sediments (Reitz et al., 2007). As described above, the reductive dissolution and re-precipitation of Mn-oxides in suboxic sediments can drive high concentrations of $MoO_4^{2-}$ in the pore waters. Since Mn-oxides prefer isotopically light $MoO_4^{2-}$, the pore waters become increasingly enriched in

the light isotope as a result of Mn-oxide recycling. Their contribution to the pore water chemistry is then preserved upon conversion of $MoO_4^{2-}$ to $MoO_xS_{4-x}$ in the sulfidic zone and ultimate sequestration in the sediments (Reitz et al., 2007). More vigorous Mn recycling, reflecting both high bottom water oxygen concentrations and reducing sediments at depth, would presumably have a greater influence on pore water chemistry. Conversely, where Mn-oxides are excluded from the sediments, such as the in oxygen minimum zone off of Mazatlan, Mexico (Fig. 5; McManus et al., 2006; Poulson et al., 2006) this mechanism is absent and $\delta^{98/95}$Mo is within 0.2‰ of the euxinic Cariaco Basin, Venezuela (Arnold et al., 2004; Nagler et al., 2005).

The Mo isotope proxy for global euxinia assumes that the degree of enrichment of the oceanic reservoir is dependant primarily on the burial of $MoO_4^{2-}$ in oxic environments. However, due to the recycling of Mn-oxides in some suboxic sediments, such environments are also a sink for the light isotope. While the magnitude of fractionation in suboxic sediments is, on average, much smaller than for Mn nodules and ferromanganese crusts, the rate of Mo burial in suboxic sediments is two orders of magnitude greater than in oxic sediments (Scott et al., 2008). Scott et al. (2008) presented a revised modern Mo budget highlighting the influence of suboxic deposition as a sink for oceanic Mo. Table 1.1 builds upon this budget to create an isotopic mass-balance of Mo in the modern ocean. The fractionations reported from Mn nodules and the Cariaco Basin, Venezuela are used to represent normal oxic and normal euxinic deposition respectively, and a recently reported riverine composition of +0.7‰ is used for the input term (Archer and Vance, 2007). The isotopic budget is balanced if suboxic

sediments record an average $\delta^{98/95}$Mo of ~ +1.0 ‰. This is an intermediate value for modern suboxic environments (Fig. 1.7). This mass balance complicates the use of Mo isotope signature in ancient euxinic black shales as a proxy for ancient euxinia because it demonstrates that the oceanic reservoir is far more sensitive to the expansion or contraction of suboxic sediments than it is for euxinic environments.

Fortunately, the suboxic model for Mo cycling described above suggests an alternative role for Mo isotopes as a proxy for redox conditions in ancient environments. Even though Mn-oxide maxima are not permanently buried, their influence on the isotopic composition of authigenic Mo can be preserved. Identification of this signal in the rock record would provide an additional set of constraints on the paleoenvironment. First of all, they describe an environment with a compressed redox gradient where both Mn-oxides and sulfate are reduced in the sediments, requiring rapid transport of organic matter to the sediment water interface. Second, an indication of the former presence of Mn-oxides in the paleo-sedimentary environment can provide a valuable constraint on the minimum concentration of dissolved oxygen at the sediment/water interface. Earlier work from the California Borderland Basins demonstrates that Mn oxides begin to dissolve where oxygen falls below 100 μM (Johnson et al., 1992) but can persist, and become buried, beneath bottom waters where oxygen is as low as 10 μM (Shaw et al., 1990; Klinkhammer and Bender, 1980; Calvert and Pedersen, 1996)). Since Mn-oxides are not permanently buried in black shales, there is rarely direct evidence for their influence on the remineralization of organic matter (see Calvert and Pedersen, 1996 for exceptions). Under ideal conditions, Mo isotope analyses may provide evidence for their former

presence in the paleo-environment, and thus, a minimum of 10 μM dissolved $O_2$ at the sediment/water interface.

## 1.7 References

Algeo, T. J., 2004. Can marine anoxic events draw down the trace element inventory of seawater? Geology 32, 1057-1060.

Algeo, T. J, Lyons, T. W., 2006. Mo-total organic carbon covariation in modern anoxic marine environments: Implications for analysis of paleoredox and paleohydrographic conditions. Paleoceanography 21, doi:10.1029/2004PA001112 (2006).

Aller, R. C., Rude, P. D., 1988. Complete oxidation of solid phase sulfides by manganese and bacteria in anoxic marine sediments. Geochimica et Cosmochimica Acta 52, 751-765.

Anbar, A. D., Duan, Y., Lyons, T. W., Arnold, G. L., Kendall, B., Creaser, R. A., Kaufman, A. J., Gordon, G. W., Scott, C., Garvin, J., Buick, R., 2007. A whiff of oxygen before the great oxidation event? Science 317, 1903-1906.

Archer, C., Vance, D., 2006. Coupled Fe and S isotope evidence for Archean microbial Fe(III) and sulfate reduction. Geology 34, 153-156.

Arnold, G. L., Anbar, A. D., Barling, J., Lyons, T. W., 2004. Molybdenum isotope evidence for widespread anoxia in Mid-Proterozoic oceans. Science 304, 87-90.

Balzer, W., 1982. On the distribution of iron and manganese at the sediment/water interface: thermodynamic versus kinetic control. Geochimica et Cosmochimica Acta 46, 1153-1161.

Barling, J., Anbar, A.D., 2004. Molybdenum isotope fractionation during adsorption by manganese oxides. Earth and Planetary Science Letters 217, 315–329.

Barling, J., Arnold, G.L., Anbar, A.D., 2001. Natural mass-dependent variations in the isotopic composition of molybdenum. Earth and Planetary Science Letters 193, 447–457.

Bender, M. L., Klinkhammer, G. P., Spender, D. W., 1977. Manganese in seawater and the marine manganese balance. Deep-Sea Reasearch 24, 799-812.

Bertine, K. K., 1972. The deposition of molybdenum in anoxic waters. Marine Chemistry 1, 43-53.

Bertine, K. K., Turekian, K. K., 1973. Molybdenum is marine deposits. Geochimica et Cosmochimica Acta 37, 1415-1434.

Berrang, P. G. and Grill, E. V., 1974. The effect of manganese oxide scavenging on molybdenum in Saanich Inlet, British Columbia. Marine Chemistry 2, 125-148.

Bonning, P., Brumsack, H. J., Bottcher, M. E., Schnetger, B., Kriete, C., Kallmeyer, J., Borchers, S. L., 2004. Geochemistry of Peruvian near-surface sediments. Geochimica et Cosmochimica Acta 68, 4429-4451.

Bostick, B. C., Fendorf, S., Helz, G. R., 2002. Differential adsorption of molybdate and tetrathiomolybdate on pyrite ($FeS_2$). Environmental Science and Technology 37, 285-291.

Brongersma-Sanders, M., Stephan, K. M., Kwee, T. G., De Bruin, M., 1980. Distribution of minor elements in cores from the Southwest Africa shelf with nores on plankton and fish mortality. Marine Geology 37, 91-132.

Brumsack, H. J., 1980. Geochemistry of Cretaceous black shales from the Atlantic Ocean (DSDP legs 11, 14, 36 and 41). Chemical Geology 31, 1-2.

Brumsack, H. J., Geiskes, J. M., 1983. Interstitial water trace-metal chemistry of laminated sediments from the Gulf of California, Mexico. Marine Chemistry 14, 89-106.

Bodin, S., Godet, A., Matera, V., Steinmann, P., Vermeulen, J., Gardin, S., Adatte, T., Coccioni, R., Föllmi, K. B., 2007. Enrichment of redox-sensitive trace metals (U, V, Mo, As) associated with the late Hauterivian Faraoni oceanic anoxic event. International Journal of Earth Science 96, 327-341.

Burdige, D. J., Gieskes, J. M., 1983. A pore water/solid phase diagenetic model for manganese in marine sediments. American Journal of Science 283, 29-47.

Caccia, V. G., Millero, F. J., Palanques, A., 2003. The distribution of trace metals in Florida Bay sediments. Marine Pollution Bulletin 46, 1420-1433.

Calvert, S. E., Pedersen, T. F., 1996. Sedimentary geochemistry of manganese: implications for the environment of formation of manganiferous black shales. Economic Geology 91, 3-37.

Canfield, D. E., Thamdrup, B., Hansen, J. W., 1993. The anaerobic degradation of organic matter in Danish coastal sediments: iron reduction, manganese reduction, and sulfate reduction. Geochimica et Cosmochmia Acta 57, 3867-3883.

Collier, R. W., 1985. Molybdenum in the Northeast Pacific Ocean. Limnology and Oceanography 306, 1351-1354.

Cruse, A. M. & Lyons, T. W. Trace metal records of regional paleoenvironmental variability in Pennsylvanian (Upper Carboniferous) black shales. Chemical Geology 206, 319-345 (2004).

Crusius, J., Calvert, S., Pedersen, T., Sage, D., 1996. Rhenium and molybdenum enrichments in sediments as indicators of oxic, suboxic and sulfidic conditions of deposition. Earth and Planetary Science Letters 145, 65-78.

Elbaz-Poulichet, F., Seiel, J. L., Jézéquel, D., Metzger, E., Prévot, F., Simonucci., C., Sarazin, G., Viollier, E., Etcheber, H., Jouaneau, J. M., Weber, O., Radakovitch, O., 2005. Sedimentary record of redox-sensitive elements (U, Mn, Mo) in a transitory anoxic basin (the Thau lagoon, France). Marine Chemistry 95, 271-281

Emerson, S. R. & Huested, S. S. 1991. Ocean anoxia and the concentrations of molybdenum and vanadium in seawater. Marine Chemistry 34, 177-196.

Erickson, B. E., Helz, G. R., 2000. Molybdenum(VI) speciation in sulfidic waters: Stability and lability of thiomolybdates. Geochimica et Cosmochimica Acta 64, 1149-1158.

Froelich, P. N., Klinkhammer, M. L., Bender, M. L., Luedtke, N. A., Heath, G. R., Cullen, D., Dauphin, P., Hammond, D., Hartman, B., Maynard, V., 1979. Early oxidation of organic matter in pelagic sediments of the eastern equatorial Atlantic: suboxic diagenesis. Geochimica et Cosmochimica Acta 43, 1075-1090.

Force, E. R., Cannon, W. F., 1988. Depositional model for shallow-marine manganese deposits around black shale basins. Economic Geology 83, 93-117.

Francois, R., 1988. A study on the regulation of the concentrations of some trace metals (Rb, Sr, Zn, Pb, Cu, V, Cr, Ni, Mn and Mo) in Saanich Inlet sediments, British Columbia, Canada.

Gill, B. C., 2009. High-resolution sulfur isotope records of the Paleozoic and a detailed geochemical study of the Late Cambrian SPICE Event utilizing sulfur isotope stratigraphy, metal chemistry and numerical modeling. Ph.D. thesis, University of California-Riverside.

Habicht, K. S., Canfield, D. E., 1997. Sulfur isotope fractionation during bacterial sulfate reduction in organic-rich sediments. Geochimica et Cosmochimica Acta 61, 5351-5361.

Helz, G. R., Miller, C. V., Charnock, J. M., Mosselmans, J. F. W., Patrick, R. A. D., Garner, D. D., Vaughan, D. J., 1996. Mechanism of molybdenum removal from the sea and its concentration in black shales: EXAFS evidence. Geochimica et Cosmochimica Acta 60, 3631-3642.

Huerta-Diaz, M. A., Morse, J. W., 1992. Pyritization of trace metals in anoxic marine sediments. Geochimica et Cosmochimica Acta 56, 2681-2702.

Hurtgen, M. T., Lyons, T. W., Ingall, E. D., Cruse, A. M., 1999. Anomolous enrichments of iron monosulfide in euxinic marine sediments and the role of $H_2S$ in iron sulfide transformation: examples from Effingham Inlet, Orca Basin, and the Black Sea. American Journal of Science 299, 556-588.

Ingall, E., Kolowith, L., Lyons, T., Hurtgen, M., 2005. Sediment carbon, nitrogen and phosphorus cycling in an anoxic fjord, Effingham Inlet, British Columbia. American Journal of Science 305, 240-258.

Johnson, K. S., Berelson, W. M., Coale, K. H., Coley, T. L., Elrod, V. A., Fairey, W. R., Iams, H. D., Kilgore, T. E., Nowicki, J. L., 1992. Manganese flux from

continental margin sediments in a transect through the oxygen minimum zone. Science 257, 1242-1245.

Jones, G. B., 1974. Molybdenum in a nearshore and estuarine environment, North Wales. Estuarine and Coastal Marine Science 2, 185-189.

Kessler, P.S., McLarnan, J., and Leigh, J.A. 1997. Nitrogenase phylogeny and the molybdenum dependence of nitrogen fixation in Methanococcus maripaludis. Journal of Bacteriology 179: 541-543.

Koide, M., Hodge, V. F., Yang, J. S., Stallard, M., Goldberg, E. G., 1986. Some comparative marine chemistries of rhenium, gold, silver and molybdenum. Applied Geochemistry 1, 705-714.

Klinkhammer, G. P., Bender, M. L., 1980. The distribution of manganese in the Pacific Ocean. Earth and Planetary Science Letters 46, 361-384.

Krishnaswami, S., 1976. Authigenic transition elements in Pacific pelagic clays. Geochimica et Cosmochimica Acta 40, 425-434.

Kuwabara, J. S., Van Green, A., McCorkle, D. C., Bernhard, J. M., 1999. Dissolved sulfide distributions in the water column and sediment pore waters of the Santa Barbara Basin. Geochimica et Cosmochimica Acta 63, 2199-2209.

Landing, W. M., Bruland, K. W., 1980 Manganese in the North Pacific. Earth and Planetary Science Letters 49, 45-46.

Lehmann, B., Nägler, T. F., Holland, H. D., Wille, M., Mao, J., Pan, J., Ma, D., Dulski, P., 2007. Highly metalliferous carbonaceous shales and Early Cambrian seawater. Geology 35, 403-406.

Lipinski, M., Warning, B., Brumsack, H. J., 2003. Trace metal signatures of Jurasic/Cretaceous black shales from the Norwegian Shelf and the Barents Sea. Paleoceanography, Paleoclimatology, Paleoecology 19, 459-475.

Lovley, D. R., Phillips, E. J. P., 1988. Novel mode of microbial energy metabolism: organic carbon oxidation coupled to dissimilatory reduction of iron or manganese. Applied and Environmental Microbiology 54, 1472-1480.

Luther, G.W. and T.M. Church, 1988: Sulfur speciation and possible sulfide oxidation in the water of the Black Sea. EOS 69, 1242.

Lyons, T. W., Severmann, S., 2005. A critical look at iron paleoredox proxies: new insights from modern euxinic marine basins. Geochimica et Cosmochimica Acta 70, 5698-5722.

Lyons, T. W., Werne, J. P., Hollander, D. J. & Murray, R. W., 2003. Contrasting sulfur geochemistry and Fe/Al and Mo/Al ratios across the last oxic-to-anoxic transition in the Cariaco Basin, Venezuela. Chemical Geology 195, 131-157.

Malcolm, S. J., 1985. Early diagenesis of molybdenum in estuarine sediments. Marine Chemistry 16, 213-225.

Manheim, F.T., Landergren, S., 1978. Handbook of Geochemistry II. Section 42. B-O. Springer-Verlag, Berlin.

McManus, J., Nägler, T. F., Siebert, C., Wheat, C. G., Hammond, D. E., 2002. Oceanic molybdenum isotope fractionation: diagenesis and hydrothermal ridge-flank alteration. Geochemistry, Geophysics, Geosystems 3, doi: 10.1029/2002/GC000356.

McManus, J, Berelson, W. M., Severmann, S., Poulson, R. L., Hammond, D. E., Klinkhamer, G. P., Holm, C., 2006. Molybdenum and uranium geochemistry in continental margin sediments: Paleoproxy potential. Geochimica et Cosmochimica Acta, 4643-4662.

Morford, J. L., Emerson, S., 1999. The geochemistry of redox sensitive trace metals in sediments, Geochimia et Cosmochimica Acta,63, 1735-1750.

Murnane, R. J., Leslie, B., Hammond, D. E., Stallard, R. F., 1989. Germanium geochemistry in the Southern California Borderlands. Geochimica et Cosmochimica Acta 53, 2873-2882.

Myers, C. R., Nealson, K. H., 1988. Microbial reduction of manganese oxides: interactions with iron and sulfur. Geochimica et Cosmochimica Acta 52, 2727-2732.

Murray, J.W. , Codispoti, L.A., Friederich, G.E., 1995. Oxidation-reduction environments: The suboxic zone in the Black Sea. In: (C.P. Huang, C.R. O'Melia and J.J. Morgan, eds) Aquatic Chemistry: Interfacial and Interspecies Processes. American Chemical Society.

Nägler, T. F., C. Siebert, H., Lüschen, M. E., Böttcher, 2005, Sedimentary Mo isotope record across the Holocene fresh-brackish water transition of the Black Sea, Chemical Geology, 219, 283-295.

Nameroff, T. J., Balistrieri, L. S., Murray, J. W., 2002. Suboxic trace metal geochemistry in the eastern tropical North Pacific. Geochimica et Cosmochimica Acta 66, 1139-1158.

Nijenhuis, T. A., Schenau, S. J., Van der Weijden, C. H., Hilgen, F. J., Lourens L. J., Zachariasse, W. J., 1996. On the origin of upper Miocence sapropelites: A case study from the Faneromeni section, Crete (Greece). Paleoceanography 11, 633-645.

Pedersen, T. F., Waters, R. D., Macdonald, R. W., 1989. On the natural enrichment of cadmium and molybdenum in the sediments of Ucluelet Inlet, British Columbia. The Science of the Total Environment 79, 125-139.

Poulson, R. L., Siebert, C., McManus, J., Berelson, W. M., 2006. Authigenic molybdenum isotope signatures in marine sediments. Geology 34, 617-620.

Postma, D., 1985. Concentrations of Mn and separation from Fe in sediments. 1. Kinetics and stoichiometry of the reaction between birnessite and dissolved Fe(II) at 10 °C. Geochimica et Cosmochimica Acta, 49, 1023-1033.

Raymond, J., Siefert, J.L., Staples, C.R., and Blankenship, R.E. 2004. The natural history of nitrogen fixation. Molecular Biology and Evolution 21: 541-554.

Reitz, A., Wille, M., Nägler, T. F., de Lange, G. J., 2007. Atypical Mo isotope signatures in eastern Mediterranean sediments. Chemical Geology 245, 1-8.

Roy, S., 1992. Environments and processes of manganese deposition. Economic Geology 87, 1218-1236.

Sageman, B. B., Murphy A. E., Werne, J. P., Ver Straeten, C. A., Hollander, D. J. & Lyons, T. W., 2003. A tale of shales: the relative roles of production, decomposition, and dilution in the accumulation of organic-rich strata, Middle-Upper Devonian, Appalachian basin. Chemical Geology 195, 229-273.

Scherer, P. 1989. Vanadium and molybdenum requirement for the fixation of molecular nitrogen by two Methanosarcina strains. Archives of Microbiology 151, 44-48.

Scott, C., Lyons, T. W., Bekker, A., Shen, Y., Poulton, S. W., Chu, X., Anbar, A. D., 2008. Tracing the stepwise oxygenation of the Proterozoic ocean. Nature 452, 456-459.

Shaw, T. J., Gieskes, J. M., Jahnke, R. A., 1990. Early diagenesis in differing depositional environments: the response of transition metals in pore water. Geochimica et Cosmochimica Acta 54, 1233-1246.

Shimmield, G. B. and Price, N. B., 1986. The behavior of molybdenum and manganese during early sediment diagenesis - offshore Baja California. Marine Chemistry 19, 261-280.

Shultz, H. N., Brinkoff, T., Fedelman, T. G., Hernández Mariné, M., Teske, A., Jorgensen, B. B., 1999. Dense populations of a giant sulfur bacterium in Namibian Shelf Sediments. Science 284, 493-495.

Siebert, C., Nägler, T.F., von Blanckenburg, F., Kramers, J.D., 2003. Molybdenum isotope record as a potential new proxy for paleoceanography. Earth and Planetary Science Letters 211, 159–171.

Siebert, C., McManus, J., Bice, A., Poulson, R., Berelson,W.M., 2006. Molybdenum isotope signatures in continental margin marine sediments. Earth and Planetary Science Letters 241, 723–733.

Taylor, S. R. & McLennan, S. M., 1995. The geochemical evolution of the continental crust. Reviews of Geophysics 33, 241-265.

Tribovillard, N., Riboulleau, S., Lyons, T. W., Baudin, F., 2004. Enhanced trapping of molybdenum by sulfurized organic matter of marine origin in Mesozoic limestones and shales. Chemical Geology 213, 385-401.

Vorlicek, T. P. and Helz, G. R., 2002. Catalysis by mineral surfaces: Implications for Mo Geochemistry in anoxic environments. Geochimica et Cosmochimica Acta 66, 3679-3692.

Vorlicek T. P., Kahn, M. D., Kasuya, Y., Helz, G. R., 2004. Capture of molybdenum in pyrite-forming ligand-induced reduction by polysulfides. Geochimica et Cosmochimica Acta 68, 547-556.

Werne, J. P., Sageman, B. B., Lyons, T. W. & Hollander, D. J., 2002. An integrated assessment of a "type euxinic" deposit: evidence for multiple controls on black shale deposition in the Middle Devonian Oatka Creek Formation. American Journal of Science 302, 110-143.

Wilde, P., Lyons, T. W., Quinby-Hunt, M. S., 2004. Organic carbon proxies in black shales: molybdenum. Chemical Geology 206, 167-176.

Yao, W. S., Millero, F. J., 1993. The rate of sulfide oxidation by $dMnO_2$ in seawater. Geochimica et Cosmochimica Acta 57, 3359-3365.

Yao, W. S., Millero, F. J., 1996. Oxidation of hydrogen sulfide by hydrous Fe(III) oxides in seawater. Marine Chemistry 52, 1-16.

Zerkle, A. L., House, C. H., Cox, R. P., Canfield, D. E., 2006. Metal limitation of biological $N_2$ fixation and implications for the Precambrian nitrogen cycle. Geobiology 4, 285-297

Zheng, Y., Anderson, R. F., Van Geen, A. L., Kuwabara, J., 2000. Authigenic molybdenum formation in marine sediments: A link to pore water sulfide in the Santa Barbara Basin. Geochimica et Cosmochimica Acta 64, 4165-4178.

Table 1.1 Molybdenum budget and isotopic mass-balance in the modern ocean

| **Riverine Flux** | **Reservoir Mass** | **Residence Time** |
|---|---|---|
| $1.8 \times 10^{10}$ g/yr[a] | $1.4 \times 10^{16}$ g[b] | ~800,000 yr |

**Removal Term**

| **Environment:** | **Oxic** | **Anoxic** | **Suboxic** | **Euxinic** |
|---|---|---|---|---|
| Fraction of Seafloor | 0.8 | 0.18[c,d] | 0.015[e] | 0.0005 |
| Average rate of burial (μg Mo/ $cm^2$ $10^3$ y) | 2.0[f] | n/a | 200 | 1400[g] |
| Seafloor normalized[h] removal rate (μg Mo/ $cm^2$ $10^3$ y) | 1.6 | n/a | 3.0 | 0.7 |
| Percent of riverine flux removed (5 μg Mo/ $cm^2$ $10^3$ y)[i] | 35 | n/a | 50 | 15 |
| Isotopic Composition ($\delta^{98/95}$Mo) | -0.7‰[j] | n/a | +1.0 | +1.8[k] |

[a]Martin and Meybeck, 1979; [b]Collier, 1985; [c]Archer et al., 2000; [d]Morford and Emerson, 1999; [e]McManus et al., 2006; [f]Bertine and Turekian, 1973; [g]Lyons et al., 2002; [h]burial rate x seafloor fraction; [i]ocean area $3.6 \times 10^{18}$ $cm^2$. [j]Barling et al. (2001); [k]Arnold et al. (2004).

Chapter 2

*Tracing the Stepwise Oxygenation of the Proterozoic Ocean*

Originally published in *Nature*

## 2.1 Abstract

Biogeochemical signatures preserved in ancient sedimentary rocks provide clues to the nature and timing of the oxygenation of the Earth's atmosphere. Geochemical data (Karhu and Holland, 1996; Bekker et al., 2004; Farquhar and Wing, 2003; Rouxel et al., 2005; Canfield et al., 2007; Fike et al., 2006) suggest that oxygenation proceeded in two broad steps near the beginning and end of the Proterozoic eon (2,500 to 542 million years ago). The oxidation state of the Proterozoic ocean between these two steps and the timing of deep-ocean oxygenation have important implications for the evolutionary course of life on Earth but remain poorly known. Here we present a new perspective on ocean oxygenation based on the authigenic accumulation of the redox-sensitive transition element molybdenum in sulfidic black shales. Accumulation of authigenic molybdenum from sea water is already seen in shales by 2,650 Ma ago; however, the small magnitudes of these enrichments reflect weak or transient (Anbar et al., 2007) sources of dissolved molybdenum before about 2,200 Ma ago, consistent with minimal oxidative weathering of the continents. Enrichments indicative of persistent and vigorous oxidative weathering appear in shales deposited at roughly 2,150 Ma ago, more than 200 million years after the initial rise in atmospheric oxygen (Karhu and Holland, 1996; Bekker et al., 2004). Subsequent expansion of sulfidic conditions after about 1,800 Ma ago (Canfield, 1998; Poulton et al., 2004) maintained a mid-Proterozoic molybdenum reservoir below 20 per cent of the modern inventory, which in turn may have acted as a nutrient feedback limiting the spatiotemporal distribution of euxinic (sulfidic) bottom waters and perhaps the evolutionary and ecological expansion of eukaryotic organisms (Anbar and Knoll, 2002). By 551 Ma, molybdenum contents reflect a greatly expanded oceanic reservoir due to oxygenation of the deep ocean and corresponding decrease in sulfidic conditions in the sediments and water column.

## 2.2 Introduction

Numerous geochemical proxies converge on a significant and unidirectional oxygenation of the Earth's atmosphere at about 2,400 Ma (Karhu and Holland, 1996; Bekker et al., 2004; Farquhar and Wing, 2003; Rouxel et al., 2005) but the response of the ocean to this event is not well constrained. Early workers invoked deep-ocean oxygenation and titration of dissolved iron to explain the disappearance of banded iron formations after about 1,800 Ma (Holland, 1984), but Canfield (1998) proposed instead the expansion of sulfidic environments and removal of iron sulfides in response to greater oxidative continental weathering and delivery of sulfur to the ocean. This proposal, which invokes an oxidized surface ocean and a sulfidic deep ocean, finds support in C–S–Fe systematics (Poulton et al., 2004; Shen et al., 2002 and 2003), molybdenum isotope relationships (Arnold et al., 2004) and biomarker studies (Brocks et al., 2005) from Proterozoic sedimentary rocks. However, the nature and extent of these sulfidic environments is unclear. Canfield (1998) envisaged a widely euxinic deep ocean where sulfide accumulated in the water column, but the deep ocean may have been dominated by less reducing conditions (Slack et al., 2007) where sulfide was confined to pore waters beneath a low-oxygen water column. Regardless, sequestration of trace metals (Algeo and Lyons, 2006) in association with the extension of sulfidic environments has biological implications (Anbar and Knoll, 2002), as many redox-sensitive transition metals are important micronutrients (for example, Fe and Mo).

The strength of molybdenum as a tracer of the Earth's oxygenation results from its uniquely bimodal geochemical characteristics. The primary source of dissolved molybdenum in the modern ocean is riverine delivery of molybdate ($MoO_4^{2-}$) liberated during oxidative weathering of continental crust containing on average 1 to 2 ppm molybdenum (Bertine and Turekian, 1973; Taylor and McLennan, 1995). Molybdate, however, is highly conservative with an average present-day seawater concentration of ~100 nM—greater than any other transition

element—and an oceanic residence time of 700,000 yr. The only significant sink for molybdate in well-oxygenated environments is by co-precipitation and burial with Mn-oxyhydroxides (Bertine and Turekian, 1973), a slowly-occurring process.

Although oxygenated environments cover most of the sea floor today, removal of molybdate in association with Mn-oxyhydroxides accounts for only 35% of the annual riverine flux (Table 2.1). Today, the remainder of the riverine flux is removed in spatially limited sulfidic settings (Bertine and Turekian, 1973) where molybdate is converted to particle-reactive thiomolybdates ($MoO_xS_{4-x}$) (Helz et al., 1996) and Mo removal by organic matter and other reduced substrates outpaces that of oxygenated environments by a factor of 200 to 5,000. The low end of this range represents non-euxinic sites where hydrogen sulfide is restricted to the sediments, and Mo enrichment is dependent on diffusion of $MoO_4^{2-}$ (Lyons et al., 2003) into pore waters where conversion to thiomolybdates occurs. At the upper end of this range are euxinic basins where sulfide and the highly reactive tetrathiomolybdate ion ($MoS_4^{2-}$) are present in the water column.

Persistent euxinia is the extreme end-member of sulfidic conditions, and although euxinic shales are common in the rock record, few examples of euxinic basins exist today, with the Black Sea and Cariaco Basin, Venezuela, being the two largest examples (Lyons, et al., 1992 and 2003). Where dissolved Mo is readily available, as in the Cariaco Basin, sediment Mo concentrations (up to 184 ppm; Lyons et al., 2003) exceed average continental crust by two orders of magnitude, and elevated ratios of Mo to total organic carbon (average Mo/TOC ratio 26 ppm Mo per wt% C) develop (Algeo and Lyons, 2006, Lyons et al., 2003). Where Mo is exhausted in the water column, as in the highly restricted Black Sea (5nM Mo below the chemocline, Emerson and Huested, 1991) drop correspondingly (Algeo and Lyons, 2006).

These characteristics of Black Sea sediments—that is, Mo concentrations and Mo/TOC ratios that are depressed relative to most Phanerozoic euxinic shales and sediments (Figs 1 and 2)—provide an analogue for Mo-deficient ancient oceans (Algeo and Lyons, 2006). From this perspective, the magnitudes of Mo enrichments and Mo/TOC in euxinic black shales reflect the size of the oceanic Mo reservoir as determined by the weathering flux and the relative influence of the sulfidic and oxic sinks. In the modern ocean, sulfide-rich pore waters and bottom waters represent 2% of the sea floor yet account for 65% of Mo removal (Table 2.1). It follows that the expansion of sulfidic environments in the past would have depressed the concentration of dissolved Mo in the ocean until, as in the Black Sea, the magnitude of euxinic enrichment was affected.

**2.3 Materials**

Most of the samples analyzed for this study are described elsewhere as indicated in Table 2.2. Details for the south China samples and the Borden Basin are provided here. The Datangpo Formation is well developed in the border area of Hunan, Guizhou, and Chongqing, south China. Glacial diamictite of the Tiesiao Formation equivalent to the Sturtian glacial sediment (Zhou et al., 2004) is overlain by the ~200-m-thick Datangpo Formation. The basal of Datangpo Formation consists of ~6 m thin-bedded Mn-carbonate interbeded with black shale and siltstone. The following unit is ~25-m-thick black shale or carbonaceous shale. The rest is gray shale and siltstone, which is overlain by the Nantuo diamictite equivalent to the Marinoan glacial sediment (Zhou et al., 2004; Condon et al., 2005). The Datangpo Formation is thus considered to be an interglacial succession. Zircon from intercalated tuff bed of the basal rhodochrosite zone is dated 663±4 Ma (Zhou et al., 2004). Our samples were collected from the lower part of black shale of the Datangpo Formation.

The Doushantuo Formation in the Yangtze Gorges area, south China, is constrained between 635.2 ± 0.6 Ma and 551.1 ± 0.7 Ma19 (Condon et al., 2005) is divided into four lithostratigraphic members. A ~5-m-thick cap dolostone (Member I) overlies the Nantuo diamictite equivalent to the Marinoan glacial sediment. Member II is characterized by ~70 m of alternating organic-rich shale and dolostone beds with abundant pea-sized chert nodules. Member III is ~70 m thick and is composed of dolostone and bedded chert in the lower part that passes up section into alternating limestone-dolostone "ribbon rocks". The Miaohe Member, i.e., Member IV of the Doushantuo Formation, is a ~13-m-thick black, organic-rich shale unit that is widespread across the Yangtze Gorges area and defines the lithological boundary between the Doushantuo Formation and the overlying Dengying Formation. An ash bed near the contact with the overlying Dengying Formation is dated 551.1±0.7 Ma (Condon et al., 2005). All the studied samples were collected from the Miaohe Member.

Borden Basin The Bylot Supergroup of northern Baffin and Bylot Islands, Canada, was deposited between ca. 1270 and 1000 Ma (Knight and Jackson, 1994; Kah et al., 2001) in the fault-bounded Borden Basin and experienced sub-greenschist facies metamorphic grade. The Borden Basin is interpreted as a failed rift arm forming an intracratonic basin with a restricted connection to the Poseidon Ocean. The Borden Basin passed through the extensional, passive subsidence, and convergent stages. Shale samples were analyzed from three stratigraphic levels: at the base (Arctic Bay Formation), in the middle (Victor Bay Formation), and at the top (Athole Point) of the supergroup. The Arctic Bay Formation was deposited during the transgressive stage from shallow-marine shelf to subtibal basinal settings and includes beds of black to dark-grey, locally pyritized shale (Hofmann and Jackson, 1994). The lower part of the Victor Bay Formation includes beds of thinly dark-grey bedded shale, locally graphitic, and was deposited under subtidal to intertidal conditions (Jackson et al., 1978). The Athole Point Formation

contains dark-grey to black stromatolitic bioherms and turbiditic calcareous siliciclastic beds deposited in the semi-restricted basin (Hofmann and Jackson, 1994).

## 2.4 Methods

### 2.4.1 Geochemical Methods

To constrain the deep-ocean redox state in the early ocean we have measured Mo concentrations ([Mo]) and TOC and generated Mo/TOC ratios (Figs 2.1 and 2.2) for a diverse sample set of Precambrian black shales (2,700 Ma) and assembled them with published data from Precambrian and Phanerozoic black shales (Appendix A). For interpretation of the size of the oceanic Mo reservoir we focus on units shown independently to reflect the euxinic end-member based on proxies such as the degree of pyritization (DOP) and/or ratios of highly reactive to total Fe ($Fe_{HR}/Fe_T$) and total iron to aluminum (Lyons and Severmann, 2006). The motivation for this filter is the exclusion of non-euxinic black shales where the magnitude of Mo enrichment does not necessarily reflect the size of the oceanic reservoir.

For samples analyzed in this study, euxinic deposition is constrained by degree of pyritization, defined as $(Fe_{pyrite}/(Fe_{pyrite} + Fe_{HCl}))$. The term $Fe_{HCl}$ means acid soluble iron, present primarily as Fe-oxides and Fe-carbonates, which will react readily with free sulfide to form pyrite. We extracted and quantified pyrite sulfur in powdered shale samples by chromium reduction and calculated $Fe_{pyrite}$ stoichiometrically ($FeS_2$). We extracted $Fe_{HCl}$ with boiling, concentrated HCl. The concentration of HCl-soluble Fe is determined spectrophotometrically. A DOP value of 0.6 is a conservative lower limit for values delineating a sulfidic water column. Total organic carbon was determined on an Eltra CS-500 infrared carbon/sulfur analyser equipped with acidification and furnace modules. Total carbon was determined by combustion, and total inorganic carbon was measured by acidification. TOC was calculated by difference. For

trace metal analyses, samples were ashed at 850 ºC for 24 h, and the mass lost on ignition was recorded. Ashed splits were dissolved following standard $HNO_3$– HCl–HF digestion methods and analysed by quadrupole inductively coupled plasma mass spectrometry at approximately 2,000-fold dilution. We used a US Geological Survey standard Devonian reference material (SDO-1) as our external standard.

### 2.4.2 Modern Molybdenum Budget

Table 2.1 is a summary of estimates for the primary sources and sinks involved in the modern Mo cycle. In order to balance the budget we assume that the oceanic Mo reservoir is in steady-state, and we define three depositional environments that represent sinks for molybdenum: oxic, suboxic, and euxinic. Any global budget contains inherent limitations. This is particularly so for Mo, which has a residence time on the order of 700,000 years, much longer than glacial/interglacial timescales. As such, estimates for the size of the oceanic reservoir and the strength of the riverine flux are limited to first-order arguments. Our budget is therefore intended to be a general representation of the different magnitudes of sources and sinks involved in the Mo cycle. From the standpoint of the molybdenum cycle, oxic environments are those where manganese oxides are permanently buried. The coupled cycling of Mo and Mn is well described (e.g., Shimmield and Price, 1986; Bertine and Turekian, 1973). Shimmield and Price (1986) demonstrated a nearly constant Mo/Mn ratio of 0.002 in Mn oxide-rich sediments.

Combining this ratio with an average Mn oxide burial rate of 500 μg Mn/$cm^2$ 103 yr (Krishnaswami, 1976) gives a Mo burial rate of 1 μg Mo/$cm^2$ 103 yr. Bertine and Turekian (1973) estimated that Mo is buried at a rate of 2 μg Mo/$cm^2$ 103 yr in oxic environments. Since both approaches yield burial rates of the same magnitude, we use the higher rate in our budget in order to avoid overemphasizing the sulfidic sinks.

Use of the term suboxia is broad and frequently ambiguous. Many definitions are based on some minimum oxygen concentration in the bottom waters. For Mo cycling, the master variable is the presence of sulfide in the environment (Helz, et al., 1996; Zheng et al., 2000). Thus, we define suboxic environments are those where sulfide is present but restricted to the pore waters. Where sulfide is also present in the water column, we define the environment as euxinic. By this definition, suboxic conditions can form under a range of bottom water conditions, but they are typically associated with low bottom-water oxygen.

A range of Mo burial rates for non-euxinic sulfidic environments is found in the literature (Table 2.3). We choose an intermediate value of 250 μg Mo/cm$^2$ 103 yr for our budget calculations. McManus et al. (2006) suggested that Mo isotope mass balance considerations require that the area of suboxic seafloor (where Mo is permanently buried) is on the order of 1%. We use this value for suboxic environments as defined here. While burial rates of Mo in euxinic environments are as high as 10,000 μg Mo/cm$^2$ 103 yr (Table 2.3), we feel the most representative euxinic environment today is the Cariaco Basin, where Mo is buried at a rate of ~1200 μg Mo/cm$^2$ 103 yr (Lyons et al., 2003). Due to the extreme limitation of dissolved Mo in the water column, the Black Sea buries Mo at rates similar to those found in suboxic environments (Table 2.3). The euxinic fraction of our budget (0.0005) is 20 times the size of the Cariaco Basin and is intended to include upwelling regions like the Peru Margin and the Namibian Shelf, where sulfide is abundant in the uppermost pore waters and may intermittently breach the sediment water interface (Dugdale et al., 1977; Brüchert et al., 2003).

Our budget demonstrates that the size of the oceanic Mo reservoir is highly sensitive to the extent of sulfidic environments, whether in the sediments or the water column. Setting all other variables in our balanced Mo budget, we find that the expansion of suboxic depositional

environments (250 μg Mo/ $cm^2$ 103 yr) to 10% of the seafloor would drive the oceanic reservoir to 10% of its present mass in less than 200,000 years.

Similarly, were euxinic environments to expand to 1% of the seafloor, they would remove nearly 2.5 times more Mo than the rivers supply annually (Table 2.4).

### 2.4.3 Molybdenum Compilation Requirements

In order to relate Mo enrichments and Mo/TOC relationships preserved in ancient black shales to temporal changes in the oceanic Mo reservoir, we have compiled Mo and total organic carbon concentrations (TOC) from numerous literature sources (Appendix A) for comparison to our sample set from Precambrian euxinic shales. In most cases, we include only examples that are characterized as euxinic by any of a number of Fe-based paleoredox indicators (Lyons and Severmann,2006). Exceptions are shales from the Archean for which we include all black shales containing pyrite. Sulfidic pore waters beneath anoxic but non-sulfidic Archean bottom waters would favor Mo enrichment in the sediments if adequate Mo is available in the water column. For samples analyzed in this study we have chosen to use degree of pyritization as our indicator of euxinia, which is known to be consistent with other tracers of paleoredox (Lyons and Severmann, 2006).

## 2.5 Results and Discussion

From our record of [Mo] and Mo/TOC (Table 2.2) we delineate three stages of Mo cycling (Figs 2.1 and 2.2) based on marked shifts in the magnitudes of enrichment and Mo/TOC. During stage 1, [Mo] and Mo/TOC are typically variable but low, requiring only small amounts of dissolved Mo in the ocean. A prominent enrichment of Mo is recorded in the 2,500-Myr Mount McRae shale (Anbar et al., 2007), but Mo/TOC rises to only 3 ppm per wt % during this event,

relative to a background of 1.5 ppm per wt %, suggesting that dissolved Mo concentrations remained well below those of the modern deep Black Sea. Such enrichments may reflect mild oxidative weathering of continental materials during the Archean Eon, including transient events of slightly elevated $O_2$ in the surface ocean and atmosphere, consistent with evidence for the presence of oxygenic photosynthesis by 2,700 Ma (Brocks et al., 1999). Anbar et al. (2007) proposed recently that continental pyrite and molybdenite could have been oxidized even at the very low partial pressure of oxygen ($pO_2$) suggested for the atmosphere at this time (less than 10% of the present level) on the basis of temporal distributions of non-mass-dependent sulfur isotope fractionations (Kaufman et al., 2007). Other possibilities include submarine oxidative weathering in shallow photosynthetic hotspots or ephemeral atmospheric oxygenation (Anbar et al., 2007). Alternatively,

hydrothermal inputs might have supplied small amounts of dissolved Mo to local sulfidic environments. Whether oxidative or hydrothermal, [Mo] and Mo/TOC suggest that the sources of Mo during this first stage were weak or transient and do not reflect vigorous and sustained oxidative weathering of continental crust.

During the second stage of Mo cycling, a persistent oxidative source and strong oceanic sinks resulted in a Proterozoic Mo reservoir intermediate between those of the Archean and Phanerozoic Eons. Enrichments of up to 74 ppm occur in shales deposited between 2,200 and 2,000 Ma, coincident with a prominent carbon excursion thought to reflect increases in organic carbon burial and atmospheric $O_2$ content (Karhu and

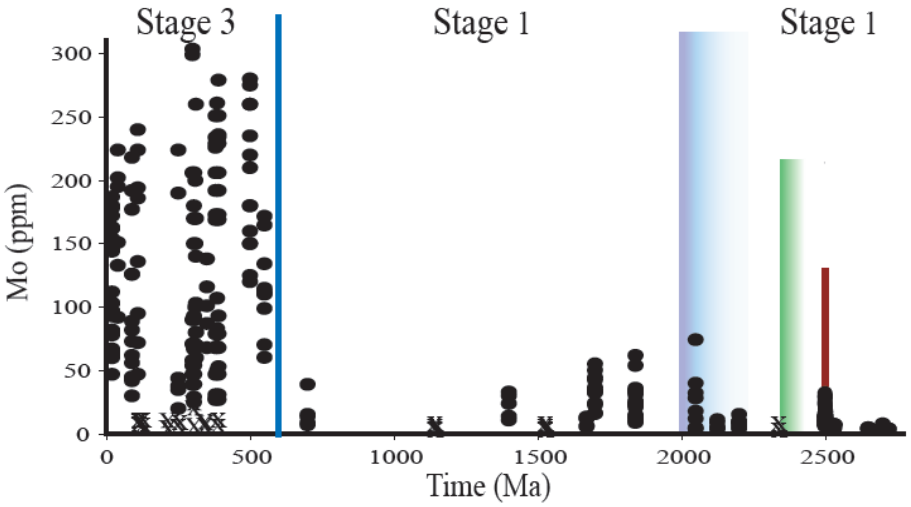


Figure 2.1: Temporal trends in Mo enrichment in black shales. Filled circles are euxinic examples; X‟s refer to non-euxinic, organic-rich shales. Blue stage boundaries are as defined in text. The red bar marks the Mt. McRae “whiff” interval8; the green gradient is the GOE as defined by sulfur isotopes3. Stratigraphic and chronologic details are provided in the Supplementary Information.

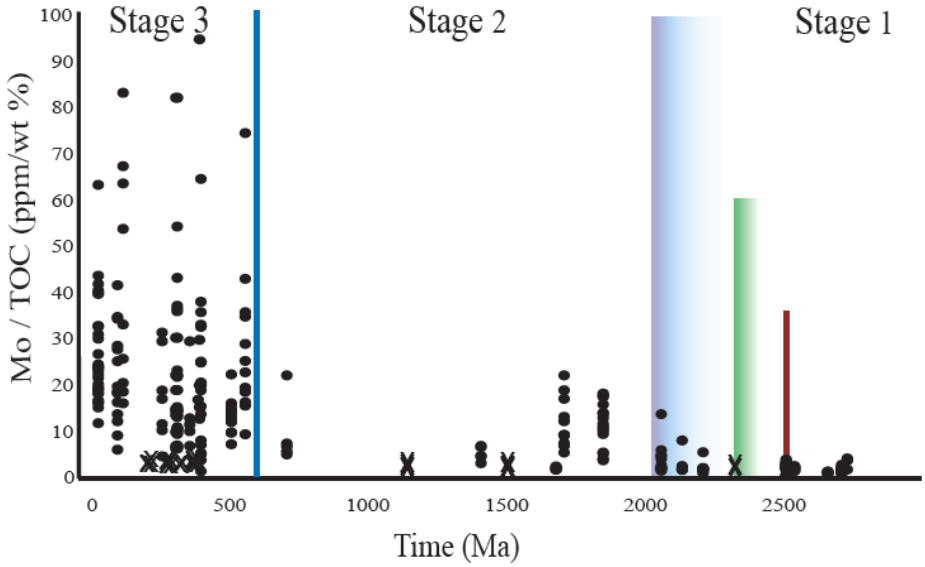


Figure 2.2: Temporal trends in Mo/TOC ratios in euxinic black shales. Symbol descriptions as in Fig. 2.1.

Holland, 1996; Bekker, et al., 2004). Coupled burial of Mo and organic carbon would act to pull down the oceanic Mo reservoir and therefore mute the level of enrichment in individual shales.

The rise in Mo and Mo/TOC in stage 2 beyond the weaker and possibly transitory enrichments seen earlier (Figs 2.1 and 2.2) suggests a larger compensating riverine flux from increased oxidative weathering. Hydrogen sulfide required for Mo uptake in the shales would also increase with the greater delivery of sulfate to the ocean. The gap of 200 million years between the Great Oxidation Event at 2,400 Ma and the first persistent enrichment of Mo in shales is intriguing and may track increasing continental sources through repeated cycles of black shale deposition, exhumation and weathering as described by Hannah et al. (2004). The 'boundary' between stages 1 and 2 is inherently diffuse (Figs 1 and 2) owing to the complexity of the ocean's initial response to atmospheric oxygenation and poor preservation of the ancient Earth record. However, across this transition, [Mo] and Mo/TOC ratios exceed those observed before and support our arguments for a fundamental shift in ocean–atmosphere redox and associated Mo cycling at that time.

With [Mo] and Mo/TOC from Black Sea sediments (Lyons and Severmann, 2006) as our analogue for Proterozoic black shales, we estimate that the concentration of dissolved Mo remained less than 10–20% of the modern ocean for at least 800 Myr following the initiation of intense Mo cycling at about 2,200 Ma. Considering arguments for an increase in weathering of Mo-bearing sulfides on the continents during the Proterozoic (Holland, 1984; Kah et al., 2004) and corresponding increase in riverine Mo flux to the ocean, we interpret the suppressed size of the oceanic reservoir as reflecting the persistence or even expansion of sulfidic sinks as opposed to a decrease in the riverine flux. It is important to stress that pervasive euxinia (that is, a sulfidic water column) is not required to exhaust the oceanic Mo reservoir. With a modern riverine flux, expansion of sulfidic pore waters, commonly found below weakly oxygenated bottom waters, to

10% of the sea floor would deplete the oceanic reservoir by 90% in 200,000 yr (see Supplementary Information). This interpretation of the modern Mo budget does not preclude a more common occurrence of euxinic conditions during the Proterozoic (Canfield, 1998; Poulton et al., 2004) but demonstrates that less extreme conditions are required to explain the Mo record. Indeed, global euxinia may have been difficult to achieve and sustain owing to the connection between Mo availability and the nitrogen cycle (Anbar and Knoll, 2002; Zerkle et al., 2006).

Recent laboratory results demonstrate that below 5% of present oceanic concentrations, Mo limitation begins to depress growth rates and rates of nitrogen fixation in cultured cyanobacteria (Zerkle et al., 2006). These results and our estimates for the size of the oceanic reservoir are consistent with the hypothesis (Anbar and Knoll, 2002) that the drawdown of Mo into sulfidic environments may have worked to restrict the occurrence and the evolutionary path of eukaryotes through the bioinorganic bridge linking Mo to N bioavailability. A corollary is that this bioinorganic bridge would also act as a negative feedback limiting the spatial and temporal extent of sulfidic conditions, because organic matter is required for the exhaustion of oxygen and other oxidants as well as subsequent bacterially mediated reduction of sulfate to sulfide.

Where productivity is depressed, sulfidic conditions are difficult to maintain. This feedback mechanism may explain the apparent decline in euxinic deposition after 1,400 Ma (Figs 2.1 and 2.2). Our sample set includes two well-preserved black shales from the Belt Supergroup in Montana, USA (1,500 Ma), and the Borden Basin, Canada (1,200 Ma), which represent restricted marine settings (Lyons et al., 2000) ideally suited for the development of a sulfidic water column. However, these units are characterized instead by degrees of pyritization (0.2–0.4), Mo concentrations (2–12 ppm) and Mo/TOC ratios typical of Phanerozoic non-euxinic shales. Although it is important to stress that artifacts of preservation and sampling complicate our search for euxinic examples, the presence of these well-preserved, non-euxinic black shales may be

telling us that similar conditions were common following 1,400 Ma. Molybdenum-sequestering conditions could drive Mo-related nitrogen stress—not only in the absence of euxinic conditions, but also to their exclusion.

In stage 3, extreme Mo enrichments and elevated Mo/TOC typical of Phanerozoic black shales reflect a greatly expanded oceanic Mo reservoir requiring deep-ocean oxygenation with only limited Mo-enriching sulfidic environments. Unlike the more diffuse stage 1–2 boundary, which reflects a complex source–sink interplay, an abrupt step to this final stage of Mo cycling is apparent in the 551-Ma Miaohe member of the Doushantuo Formation, south China (Figs 1 and 2, and Supplementary Information). Samples from the 663-Ma Datangpo Formation, also in south China, reveal [Mo] and Mo/TOC typical of the earlier Proterozoic ocean. Interpretations of the chemistry of the Datangpo Formation are complicated by its temporal proximity to the Sturtian glaciation, yet the possibility remains that it captures a continuation of stage-2 cycling. If so, the Mo record brackets the timing of deep-ocean oxygenation to between 663 and 551 Ma, consistent with recent C–S–Fe studies of Late Neoproterozoic successions arguing for deep ocean oxygenated at 580 Ma (Canfield et al., 2007; Fike et al., 2006) and subsequent radiation of large, structurally complex life forms. Our interpretation of Mo cycling in the Late Neoproterozoic suggests that modern redox and nutrient cycles were well established by 551 Ma, shortly after the initial oxidation of the deep ocean, and that the appearance of the first large animals followed not only the oxidation of the deep ocean but also the establishment of modern biogeochemical cycles.

**2.6 References**

Algeo, T. J., Lyons, T. W., 2006. Mo–total organic carbon covariation in modern anoxic marine environments: Implications for analysis of paleoredox and paleohydrographic conditions. Paleoceanography 21, doi:10.1029/2004PA001112.

Anbar, A. D. & Knoll, A. H., 2002. Proterozoic ocean chemistry and evolution: A bioinorganic bridge? Science 297, 1137–1142.

Anbar, A. D., Duan, Y., Lyons, T. W., Arnold, G. L., Kendall, B., Creaser, R. A., Kaufman, A. J., Gordon, G. W., Scott, C., Garvin, J., Buick, R., 2007. A whiff of oxygen before the great oxidation event? Science 317, 1903-1906.

Arnold, G. L., Anbar, A. D., Barling, J., Lyons, T. W., 2004. Molybdenum isotope evidence for widespread anoxia in Mid-Proterozoic oceans. Science 304, 87–90.

Bekker, A., Holland, H. D., Wang, P.-L., Rumble III, D., Stein, H. J., Hannah, J. L., Coetzee, L. L., Buekes, N. J., 2004. Dating the rise of atmospheric oxygen. Nature 427, 117-120.

Bertine, K. K., Turekian, K. K., 1973. Molybdenum in marine deposits. Geochim. Cosmochim. Acta 37, 1415–1434.

Brocks, J. J., Logan, G. A., Buick, R., Summons, R. E., 1999. Archean molecular fossils and the early rise of eukaryotes. Science 285, 1033–1036.

Brüchert, V., Jørgensen, B. B., Neumann, K., Riechmann, D., Schlösser, M., Schulz, H., 2003. Regulation of bacterial sulfate reduction and hydrogen sulfide fluxes in the

central Namibian coastal upwelling zone. Geochimica et Cosmochimica Acta 67, 4505-4518.

Canfield, D. E., 1998. A new model for Proterozoic ocean chemistry. Nature 396, 450–453.

Canfield, D. E., Poulton, S. W., Narbonne, G. M., 2007. Late-Neoproterozoic deep ocean oxygenation and the rise of animal life. Science 315, 92–95.

Collier, R. W., 1985. Molybdenum in the Northeast Pacific Ocean. Limnology and Oceanography 30, 1351-1354.

Condon, D., Zhu, M., Bowring, S., Wang, W., Yang, A., Jin, Y., 2005. U-Pb ages from the Neoproterozoic Doushantuo Formation, China. Science 308, 95-98.

Dugdale, R. C., Goering, J. J., Barber, R. T., Smith, R. L. & Packard, T. T., 1977. Denitrification and hydrogen sulfide in the Peru upwelling region during 1976. Deep-Sea Research 24, 601-608.

Emerson, S. R., Huested, S. S., 1991. Ocean anoxia and the concentrations of molybdenum and vanadium in seawater. Mar. Chem. 34, 177–196.

Farquhar, J. & Wing, B. A., 2003. Multiple sulfur isotopes and the evolution of the atmosphere. Earth and Planetary Science Letters 213, 1–13.

Fike, D. A., Grotzinger, J. P., Pratt, L. M., Summons, R. E., 2006. Oxidation of the Ediacaran ocean. Nature 444, 744–747.

Francois, R. A., 1988. Study on the regulation of the concentrations of some trace metals (Rb, Sr, Zn, Pb, Cu, V, Cr, Ni, Mn and Mo) in Saanich Inlet sediments, British Columbia, Canada. Marine Geology 83, 285-308.

Gross, M. G., 1967. Concentrations of minor elements in diatomaceous sediments of a stagnant fjord. In Estuaries, G. H. Lauff ed. AAAS publication 83, 273-278.

Hannah, J. L., Bekker, A., Stein, H. J., Markey, R. J., Holland, H. D., 2007. Primitive Os and 2316Ma age for marine shale: implications for Paleoproterozoic glacial events and the rise of atmospheric oxygen. Earth and Planetary Science Letters. 225, 43–52.

Helz, G. R., Miller, C. V., Charnock, J. M., Mosselmans, J. F. W., Patrick, R. A. D., Garner, D. D., Vaughan, D. J., 1996. Mechanism of molybdenum removal from the sea and its concentration in black shales: EXAFS evidence. Geochimica et Cosmochimica Acta 60, 3631-3642.

Hofmann, H.J., Jackson, G.D., 1994. Shelf-facies microfossils from the Proterozoic Bylot Supergroup, Baffin Island, Canada. Journal of Paleontology 68, 39.

Holland, H. D. The Chemical Evolution of the Atmosphere and Oceans (Princeton University Press, Princeton NJ, 1984).

Jackson, G.D., Iannelli, T.R., Narbonne, G.M., Wallace, P.J., 1978. Upper Proterozoic sedimentary and volcanic rocks of Northwestern Baffin Island. Geological Survey of Canada Paper 78-14, 15.

Kah, L.C., Lyons, T.W., Chesley, J.T., 2001. Geochemistry of a 1.2 Ga carbonate-evaporite succession, northern Baffin and Bylot Islands: implications for Mesoproterozoic marine evolution. Precambrian Research 111, 203-234.

Kah, L. C., Lyons, T. W., Frank, T. D., 2004. Low marine sulphate and protracted oxygenation of the Proterozoic biosphere. Nature 431, 834–838.

Karhu, J. A., Holland, H. D., 1996. Carbon isotopes and the rise of atmospheric oxygen. Geology 24, 867–870.

Kaufman, A. J., Johnston, D. T., Farquhar, J., Masterson, A. L., Lyons, T. W., Bates, S., Anbar, A. D., Arnold, G. L., Garvin, J., Buick, R., 2007. Late Archean biospheric oxygenation and atmoshpheric evolution. Science 317, 1900-1903.

Knight, R.D., Jackson, G.D., 1994. Sedimentology and stratigraphy of the Mesoproterozoic Elwin Subgroup (Aqigilik and Sinasiuvik Formations), Uppermost Bylot Supergroup, Borden Rift Basin, Northern Baffin Island. Geological Survey of Canada Bull. 455, 43.

Krishnaswami, S., 1976. Authigenic transition elements in Pacific pelagic clays. Geochimica et Cosmochimica Acta 40, 425-434.

Lyons, T. W., Berner, R. B., 1992. Carbon–sulfur–iron systematics of the upper-most deep-water sediments of the Black Sea. Chem. Geol. 99, 1–27.

Lyons, T. W., Luepke, J. J., Schreiber, M. E., Zieg, G. A., 2000. Sulfur geochemical constraints onMesoproterozic restrictedmarine deposition: lower Belt Supergroup, northwestern United States. Geochim. Cosmochim. Acta 64, 427–437.

Lyons, T. W., Werne, J. P., Hollander, D. J., Murray, R. W., 2003. Contrasting sulfur geochemistry and Fe/Al and Mo/Al ratios across the last oxic-to-anoxic transition in the Cariaco Basin, Venezuela. Chem. Geol. 195, 131–157.

Lyons, T. W., Severmann, S., 2006. A critical look at iron paleoredox proxies: New insights from modern euxinic marine basins. Geochim. Cosmochim. Acta 70, 5698–5722.

Martin, J. M., Meybeck, N., 1979. Elemental mass-balance of material carried by major world rivers. Marine Chemistry 7, 173-206.

McManus, J., Berelson, W. M., Severmann, S., Poulson, R. L., Hammond, D. E., Klinkhammer, G. P., Holm, C., 2006. Molybdenum and uranium geochemistry in continental margin sediments: Paleoproxy potential. Geochimica et Cosmochimica Acta 70, 4643-4662.

Nameroff, T. J., Balistrieri, L. S., Murray, J. W., 2002. Suboxic trace metal geochemistry in the eastern tropical North Pacific. Geochimica et Cosmochimica Acta 66, 1139-1158.

Poulton, S. W., Fralick, P. W., Canfield, D. E., 2004. The transition to a sulfidic ocean, 1.84 billion years ago. Nature 431, 173–177.

Rouxel, O. J., Bekker, A., Edwards, K. J., 2005. Iron isotope constraints on the Archean and Paleoproterozoic ocean redox state. Science 307, 1088–1091.

Shen, Y., Canfield, D. E., Knoll, A. H., 2002. Middle Proterozoic ocean chemistry: Evidence from the McArthur Basin, northern Australia. Am. J. Sci. 302, 81–109.

Shen, Y., Knoll, A. H., Walter, M. R., 2003. Evidence for low sulphate and anoxia in a mid-Proterozoic marine basin. Nature 423, 632–635.

Shimmield, G. B., Price, N. B., 1986. The Behavior of molybdenum and manganese during early sediment diagenesis – Offshore Baja California, Mexico. Marine Chemistry 19, 261-280.

Slack, J. F., Grenne, T., Bekker, A., Rouxel, O. J., Lindberg, P. A., 2007. Suboxic deep seawater in the late Paleoproterozoic: Evidence from hematitic chert and iron

formation related to seafloor-hydrothermal sulfide deposits, central Arizona, USA. Earth Planet. Sci. Lett. 255, 243–256.

Taylor, S. R., McLennan, S. M., 1995. The geochemical evolution of the continental crust. Rev. Geophys. 33, 241–265.

Zerkle, A. L., House, C. H., Cox, R. P., Canfield, D. E., 2006. Metal limitation of cyanobacterial N2 fixation and implications for the Precambrian nitrogen cycle. Geobiology 4, 285–297.

Zheng, Y., Anderson, R. F., Van Green, A., Kuwabara, J., 2000. Authigenic molybdenum formation in marine sediments: a link to pore water sulfide in the Santa Barbara Basin. Geochimica et Cosmochimica Acta 64, 4165-4178.

Zhou, C., Tucker, R., Xiao, S., Peng, Z., Yuan, X., Chen, Z., 2004. New constraints on the ages of Neoproterozoic glaciations in south China. Geology 32, 437-440.

Table 2.1 Modern Molybdenum Budget

| **Reservoir** | | |
|---|---|---|
| **Riverine Flux** | **Reservoir Mass** | **Residence Time** |
| $1.8 \times 10^{10}$ g/yr[a] | $1.4 \times 10^{16}$ g[b] | ~800,000 yr |

| **Removal Flux** | | | | |
|---|---|---|---|---|
| **Environment:** | **Oxic** | **Anoxic** | **Sulfidic** | **Euxinic** |
| Fraction of Seafloor | 0.8 | 0.18[c,d] | 0.015[e] | 0.0005 |
| Average rate of burial ($\mu$g Mo/ $cm^2$ $10^3$ y) | 2.0[f] | n/a | 200 | 1400[g] |
| Seafloor normalized[h] removal rate ($\mu$g Mo/ $cm^2$ $10^3$ y) | 1.6 | n/a | 3.0 | 0.7 |
| Percent of riverine flux (5 $\mu$g Mo/ $cm^2$ $10^3$ y)[i] removed | 35 | n/a | 50 | 15 |

[a]Martin and Meybeck, 1979; [b]Collier, 1985; [c]Archer et al., 2000; [d]Morford and Emerson, 1999; [e]McManus et al., 2006; [f]Bertine and Turekian, 1973; [g]Lyons et al., 2002; [h]burial rate x seafloor fraction; [i]ocean area $3.6 \times 10^{18}$ $cm^2$.

Table 2.2 Results

| Formation/ Sample ID | Mo (ppm) | TOC (wt.%) | Spy (wt.%) | DOP | FeHR/FeT | Reference |
|---|---|---|---|---|---|---|
| Roy Hill Shale Member, Jeerinah Formation, Fortescue Group 2.62 Ga | | | | | | |
| FVG-1 794.1 m | 3.6 | 4.7 | 2.9 | 0.7 | | Descriptive and chronological details Rouxel et al., 2005 |
| FVG-1 752.65 m | 2.4 | 6.0 | 1.4 | 0.8 | | |
| FVG-1 765.8 m | 2.2 | 9.9 | 1.9 | 0.7 | | |
| FVG-1 774.0 m | 3.3 | 4.4 | 3.4 | 0.9 | | |
| FVG-1 707.95 m | 4.8 | 10.4 | 2.1 | 0.9 | | |
| Gamohaan Formation, Fortescue Group, South Africa. 2.53 Ga | | | | | | |
| WB-98 468.89 m | 7.5 | 4.5 | 0.4 | 0.2 | | Descriptive and chronological details Rouxel et al., 2005 |
| WB-98 474.1 m | 7.7 | 4.8 | 0.3 | 0.1 | | |
| WB-98 477.5 m | 5.6 | 3.9 | 0.5 | 0.1 | | |

Table 2.2 Continued

| Formation/ Sample ID | Mo (ppm) | TOC (wt.%) | Spy (wt.%) | DOP | FeHR/FeT | Reference |
|---|---|---|---|---|---|---|
| Gamohaan Formation, Fortescue Group, South Africa. 2.53 Ga | | | | | | |
| WB-98 507.39 m | 2.9 | 3.0 | 2.5 | 0.5 | | Descriptive and chronological details Rouxel et al., 2005 |
| WB-98 512.95 m | 2.7 | 2.9 | 0.2 | 0.1 | | |
| Sengoma Argillite Formation, Pretoria Series 2.2-2.1 Ga | | | | | | |
| Strat. 2 171.5 m | 2 | 10.0 | 2.3 | 0.8 | | Descriptive and chronological details Rouxel et al., 2005 |
| Strat. 2 186.57 m | 48 | 11.0 | 3.5 | 0.7 | | |
| Strat. 2 200.7 m | 10 | 13.3 | 3.6 | 0.9 | | |
| Strat. 2 202.5 m | 7 | 15.5 | 3.0 | 0.9 | | |
| Strat. 2 205.25 | 26 | 14.2 | 3.4 | 0.9 | | |
| Strat. 2 209 m | 7 | 15.9 | 2.3 | 0.8 | | |
| Strat. 2 212.7 m | 8 | 16.0 | 2.4 | 0.7 | | |

Table 2.2 Continued

| Formation/ Sample ID | Mo (ppm) | TOC (wt.%) | Spy (wt.%) | DOP | FeHR/FeT | Reference |
|---|---|---|---|---|---|---|
| Francevillian Series, Gabon 2.1-2.0 Ga | | | | | | |
| OKP 67.6 m | 4 | 16.5 | 2.5 | 0.8 | | Descriptive and chronological details Rouxel et al., 2005 |
| OKP 46.57 m | 2 | 5.7 | 1.4 | 0.8 | | |
| OKP 62.22 m | 2 | 7.9 | 3.6 | 0.8 | | |
| BA-30B 46.5 m | 12 | 5.7 | 5.2 | 0.6 | | |
| Zaonezhskaya Fm., Ludikovian Series, Karelia, Russia 2.1-2.0 Ga | | | | | | |
| C-34 64.8 m | 74 | 10.2 | 3.7 | 0.9 | | Descriptive and chronological details Rouxel et al., 2005 |
| C-34 90.7 m | 4 | 0.4 | 1.1 | 0.9 | | |
| C-34 96.5 m | 28 | 1.8 | 1.2 | 0.8 | | |
| C-5190 75 m | 32 | 7.4 | 0.0 | 0.0 | | |
| C-5190 78 m | 30 | 5.2 | 0.1 | 0.1 | | |
| C-5190 83 m | 7 | 9.3 | 1.5 | 0.5 | | |
| C-5190 146.5 m | 43 | 10.1 | 0.1 | 0.3 | | |
| C-5190 144.7 m | 49 | 6.8 | 0.1 | 0.1 | | |

Table 2.2 Continued

| Formation/ Sample ID | Mo (ppm) | TOC (wt.%) | Spy (wt.%) | DOP | FeHR/FeT | Reference |
|---|---|---|---|---|---|---|
| Rove Formation, Animikie Group, Ontario 1.84 Ga | | | | | | |
| R-16 | 21 | 2.1 | .8 | | 0.6 | Descriptive and chronological details, TOC, Spy,FeHR/FeT (Poulton et al., 2004) |
| R-19 | 24 | 1.4 | .6 | | 0.5 | |
| R-21 | 26 | 1.5 | 1.4 | | 0.7 | |
| R-25 | 62 | 4.7 | 2.4 | | 0.8 | |
| R-26A | 9 | 0.9 | 1.9 | | 0.6 | |
| R-26C | 15 | 4.2 | 3.7 | | 0.7 | |
| R-26E | 10 | 3.1 | 1.7 | | 0.6 | |
| R-26G | 14 | 3.0 | 1.1 | | 0.7 | |
| R-26I | 12 | 2.5 | 1.0 | | 0.6 | |
| R-26P | 54 | 3.2 | 2.2 | | 0.8 | |
| R-28 | 31 | 2.5 | 0.8 | | 0.5 | |
| R-30 | 24 | 2.7 | 2.9 | | 0.5 | |
| R-32 | 36 | 3.2 | 4.4 | | 0.5 | |
| R-33 | 33 | 3.1 | 6.4 | | 0.6 | |
| R-39 | 23 | 1.7 | 3.4 | | 0.5 | |
| R-40 | 34 | 2.2 | 7.2 | | 0.6 | |

Table 2.2 Contiued

| Formation/ Sample ID | Mo (ppm) | TOC (wt.%) | Spy (wt.%) | DOP | FeHR/FeT | Reference |
|---|---|---|---|---|---|---|
| Wollogorang Formation, Tawallah Group, McArthur Basin, Australia 1.73 G | | | | | | |
| MY-1 | 16 | 1.9 | 1.5 | 0.6 | 0.34 | Descriptive and chronological details, TOC, Spy, DOP, FeHR/FeT (Shen et al., 2002). |
| MY-2 | 42.6 | 4.9 | .1 | 0.2 | 0.24 | |
| MY-3 | 16.0 | 2.5 | 1.0 | 0.5 | 0.56 | |
| MY-4 | 44.6 | 2.7 | 1.6 | 0.8 | 0.69 | |
| MY-5 | 22.8 | 3.5 | 2.7 | 0.8 | 0.75 | |
| MY-6 | 32.4 | 1.5 | 1.2 | 0.7 | 0.21 | |
| MY-7 | 33.1 | 3.8 | 1.4 | 0.6 | 0.62 | |
| MY-8 | 36.6 | 2.9 | 4.0 | 0.9 | 0.80 | |
| MY-9 | 34.8 | 5.0 | 1.4 | 0.9 | 0.76 | |
| MY-10 | 24.5 | 5.0 | 1.1 | 0.6 | 0.76 | |
| MY-11 | 50.2 | 4.3 | 1.9 | 0.9 | 0.64 | |
| MY-12 | 55.2 | 3.0 | 1.7 | 0.7 | 0.66 | |

Table 2.2 Continued

| Formation/ Sample ID | Mo (ppm) | TOC (wt.%) | Spy (wt.%) | DOP | FeHR/FeT | Reference |
|---|---|---|---|---|---|---|
| Velkerri Formation, Roper Group, McArthur Basin, 1.4 Ga | | | | | | |
| U4 156.1 m | 33.0 | 8.0 | 1.4 | 0.8 | 0.52 | Descriptive and chronological details,TOC, Spy, DOP, FeHR/FeT (Shen et al., 2003) Mo concentrations (Arnold et al. 2005) |
| U4 173.0 m | 24.0 | 3.9 | 1.0 | 0.8 | 0.51 | |
| U4 204.1 m | 14.0 | 5.4 | 3.0 | 0.8 | 0.79 | |
| U4 214.1 m | 30.0 | 4.7 | 3.0 | 0.6 | 0.54 | |
| U4 363.0 m | 11.0 | 2.7 | 2.3 | 0.7 | 0.50 | |
| Datangpo Formation, south China, 663 Ma | | | | | | |
| ML05 1 | 39.1 | 1.8 | 4.2 | 0.9 | | Chronological details (Zhou et al., 2002). |
| ML05 2 | 8.9 | 1.7 | 2.2 | 0.8 | | |
| ML05 3 | 7.2 | 1.6 | 2.3 | 0.9 | | |
| ML05 4 | 15.4 | 2.5 | 2.6 | 0.9 | | |
| ML05 5 | 13.7 | 2.0 | 0.2 | 0.2 | | |

Table 2.2 Contiuned

| Formation/ Sample ID | Mo (ppm) | TOC (wt.%) | Spy (wt.%) | DOP | FeHR/FeT | Reference |
|---|---|---|---|---|---|---|
| Miaohe Member, Doushantuo Formation, south China 551 Ma | | | | | | |
| 28.85 m | 294 | 2.4 | 1.9 | 0.9 | | Chronological details (Condon et al., 2005) |
| 29.5 m | 385 | 5.2 | 2.0 | 0.9 | | |
| 32.2 m | 110 | 4.5 | 2.6 | 0.9 | | |
| 33.8 m | 60 | 6.8 | 2.1 | 0.9 | | |
| 34.6 m | 99 | 6.3 | 2.5 | 0.9 | | |
| 36.2 m | 115 | 7.6 | 1.6 | 0.9 | | |
| 37.0 m | 70 | 3.9 | 2.3 | 0.4 | | |
| 37.8 m | 110 | 5.0 | 2.1 | 0.9 | | |
| 38.9 m | 172 | 4.9 | 2.1 | 0.9 | | |
| 39.6 m | 113 | 6.0 | 2.3 | 0.9 | | |
| 40.2 m | 165 | 3.9 | 2.1 | 0.9 | | |
| 41.0 m | 134 | 3.9 | 2.0 | 0.9 | | |

Table 2.2 Contineud

| Formation/ Sample ID | Mo (ppm) | TOC (wt.%) | Spy (wt.%) | DOP | FeHR/FeT | Reference |
|---|---|---|---|---|---|---|
| Newland Formation, Belt Supergroup, USA, 1.5 Ga | | | | | | |
| 204.8 m | 3 | 0.4 | 0.8 | 0.4 | | Descriptive and chronological details, TOC, Spy, DOP (Lyons et al., 2000) |
| 204.85 m | 2 | 0.6 | 0.9 | 0.4 | | |
| 285 m | 4 | 0.7 | 1.2 | 0.3 | | |
| 286.5 m | 3 | 0.5 | 1.2 | 0.3 | | |
| 313.6 m | 4 | 0.4 | 1.2 | 0.5 | | |
| 371.5 m | 6 | 1.2 | 1.3 | 0.4 | | |
| 372.5 m | 5 | 1.0 | 1.4 | 0.4 | | |
| 372.55 m | 5 | 1.0 | 1.5 | 0.5 | | |
| 420.9 m | 9 | 1.6 | 0.8 | 0.5 | | |
| 495 m | 6 | 1.4 | 0.9 | 0.3 | | |
| 495.05 m | 6 | 1.2 | 1.0 | 0.4 | | |
| 495.1 m | 6 | 1.2 | 0.7 | 0.3 | | |
| 492.15 m | 7 | 1.1 | 1.0 | 0.3 | | |
| 503.7 m | 4 | 2.4 | 1.1 | 0.7 | | |
| 503.75 m | 4 | 2.2 | 0.9 | 0.6 | | |
| 507.8 m | 2 | 0.3 | 0.9 | 0.6 | | |

Table 2.2 Contiuned

| Formation/ Sample ID | **Mo (ppm)** | **TOC (wt.%)** | **Spy (wt.%)** | **DOP** | **FeHR/FeT** | **Reference** |
|---|---|---|---|---|---|---|
| Borden Basin, Bylot Supergroup, Canada ca. 1.2 Ga | | | | | | |
| JD-79 138D | 10.2 | 3.1 | 0.5 | 0.4 | | Descriptive and chronological details (Jackson et al., 1978; Hoffman and Jackson, 1994; Knight and Jackson, 1994) |
| JD-79 112-C1 | 3.0 | 2.2 | 0.7 | 0.3 | | |
| JD-79 113-B | 2.5 | 1.0 | 0.6 | 0.5 | | |
| JD-77 70E | 7.4 | 2.3 | 0.6 | 0.4 | | |
| JD-79 112 C-2 | 7.0 | 3.5 | 1.5 | 0.5 | | |
| JD-79 I-112-C-2 | 12.0 | 3.8 | 1.5 | 0.6 | | |
| JD-79 186k | 3.8 | 1.0 | 0.5 | 0.6 | | |

Table 2.3 Measured and Estimated Reservoir Concentrations

| | **Black Sea[a]** | **Framvaren Fjord[a]** | **Cariaco Basin[a]** | **Stage 1** | **Stage 2** | **Stage 3** |
|---|---|---|---|---|---|---|
| $Mo_{ave}$ (ppm)[b] | 45 | 84 | 85 | 3.3 | 24 | 164 |
| $Mo/TOC_{ave}$ (ppm/wt %) | 4.5 | 9 | 25 | 2.8 | 6.4 | 27 |
| $[Mo]/[Mo]_{sw}$[c] | 0.03-0.05 | 0.20-0.30 | 0.7-.85 | <0.05 | 0.1-0.2 | >0.2 |

[a]Algeo and Lyons, 2006; [b]Bulk shale or sediments concentration; [c]Ratio of measured and estimated dissolved Mo relative to the modern open ocean average (105 nM; Collier, 1985).

Chapter 3

*A Non-Euxinic Mesoproterozoic Basin*

## 3.1 Abstract

Anoxic and sulfidic bottom waters (euxinia) are generally believed to have dominated mid-Proterozoic oceans for hundreds of millions of years, exerting a strong control on the trace metal inventories of seawater and thus on the co-evolution of life on Earth and ocean/atmosphere chemistry. Here we present a biogeochemical study of mid-Proterozoic black shales from the Newland Formation, Belt Supergroup, USA. We find multiple lines of evidence for a lack of euxinia in the Belt Basin, and perhaps even mildly oxygenated bottom waters. We conclude that euxinia was likely common during the Proterozoic, but not globally pervasive as have previously been argued.

## 3.2 Introduction

In recent years, studies of Precambrian biogeochemistry have focused on the dramatic events that characterize the beginning and end of the Proterozoic Eon. Paleoproterozoic studies are centered on the initial accumulation of oxygen in the atmosphere and the transition, by most models, from Fe-rich to sulfidic seas (Bekker et al., 2004; Poulton et al., 2004; Rouxel et al., 2005), while Neoproterozoic studies are concerned with the cause and effect relationship between global glaciations, final oxygenation of the deep ocean and the appearance of metazoans (Hoffman et al., 1998; Hurtgen et al., 2005; Fike et al., 2006; Canfield et al., 2007; Canfield et al., 2008; Scott et al., 2008). By comparison, ocean redox conditions during the Mesoproterozoic are more generally characterized. Carbon and sulfur isotopes studies of Mesoproterozoic carbonates suggest a progressive oxygenation of the Earth's surface (Kah et al., 2001;

Kah et al., 2004; Gellatly and Lyons, 2005; Johnston et al., 2005) but the magnitude and rate of change were low. In contrast to the mild, progressive oxygenation of the surface ocean and atmosphere, the deep ocean is generally characterized by far more extreme conditions.

The Mesoproterozoic is widely accepted to have captured the heart of the "Canfield Ocean", when hydrogen sulfide is alleged to have accumulated and persisted over broad portions of the deep ocean for hundreds of millions of years (Canfield, 1998). However, support for the Canfield Ocean is derived primarily from a single location, the McArthur Basin of north-central Australia (Shen et al., 2002; Shen et al., 2003; Brocks et al., 2005). Because this scenario has such profound implications for the inventories of redox-sensitive and bioessential transition metals such as Fe, Mo and Cu, and therefore the history of life on Earth (Anbar and Knoll, 2002; Saito et al., 2003), it is imperative to better constrain the extent of sulfidic deposition in the Mesoproterozoic.

The Belt Supergroup is one of the most extensive and well-studied Mesoproterozoic successions in North America. The sequence is predominately siliclastic with minor carbonates and volcanics, exposed over 130,000 $km^2$ of the western United States and Canada (Winston, 1990). The depositional setting of the Belt Basin has been a long standing subject of debate. A lacustrine model was promoted by Winston (1986) based on sedimentological and facies considerations, but the more recent addition of geochemical analyses suggests that while the basin was highly restricted, it was connected to the open ocean (Lyons et al., 2000; Gellatly and Lyons, 2005; Lyons et al., 2006). The bulk of Belt deposition occurred between ca. 1470 and 1401 Ma (Sears et al.,

1998; Evans et al., 2000) during which considerable thicknesses accumulated (greater than 15 km along the present day western margin (Winston, 1990)). Belt rocks contain numerous features that are characteristic of Proterozoic environments such as sedimentary exhalative or SEDEX deposits (Lyons et al., 2006), enigmatic molar-tooth structures (Frank and Lyons, 1998), stromatolites (Horodyski, 1977; Schieber, 1988) and the probable macroscopic eukaryotes *Grypania* and *Horodyskia* (Horodyski, 1982; Knoll et al., 2006).

From the perspective of its size and restricted nature, the modern Black Sea is an appropriate analogue for the Belt Basin. Because the Black Sea is also our best analogue for euxinic conditions in the modern, the Belt Basin is an excellent candidate to explore the potential for the development of euxinic conditions under a low-oxygen Mesoproterozoic atmosphere. In order to characterize redox conditions in the deep waters of the Belt Basin, we have applied a multi-elemental proxy approach (C-Al-S-Mn-Fe-Mo) to carbonaceous and pyritic black shales from the ca. 1470 Ma Newland Formation (Sears et al., 1998), located in the informally designated lower Belt Group. Fe speciation and Mo enrichments provide clear evidence for non-euxinic deposition in the Belt Basin while the presence of Mn carbonates suggests that the deep basin may have been mildly oxygenated.

### 3.3 Materials and Methods

Newland shale samples were selected from drill-core used in a previous C and S study (Lyons et al., 2000). The core was taken from the Helena Embayment, a fault-bounded eastern extension of the Belt Basin where metamorphism is minimal. We

performed detailed Fe speciation, to include the recently developed sequential Fe extraction of Poulton and Canfield (2005), which quantifies the contribution of four pools of highly reactive iron ($Fe_{HR}$), or iron that is biogeochemically reactive on diagenetic timescales: sulfide Fe, carbonate Fe, easily reducible iron oxides and magnetite. Due to minor metamorphic alteration of primary pyrite ($FeS_2$) to pyrrohtite (~ FeS), we modified this method to include extraction of "acid volatile sulfide" or AVS, to account for Fe sulfides with an assumed stoichiometry of Fe:S = 1:1. In addition, we determined degree of sulfidization (DOS), which considers the ratio sulfide Fe to Fe liberated by boiling concentrated HCl ($Fe_{sulfide}$ / $Fe_{sulfide}$ + $Fe_{HCl}$), an approach that is analogous to degree of pyritization (DOP; Raiswell et al., 1988) and accounts for the contribution of iron monosulfides (Boesen and Postma, 1988). We also measured bulk elemental concentrations (Al, Fe, Mn, Mo) via a standard multi-acid digestion ($HNO_3$-HCl-HF) and analysis by ICP-MS. Total inorganic carbon (TIC), or carbonate carbon, was measured using an Eltra™ IR C/S Determinator with an acidification module. $\delta^{13}C$ of carbonate minerals was measured at the University of Missouri, Columbia.

## 3.4 Results and Discussion

### 3.4.1 Fe Speciation in the Newland Formation

The term "euxinia" refers specifically to bottom waters that are both anoxic and contain hydrogen sulfide. The most common methods for identifying ancient euxinic basins are based on the speciation of biogeochemically reactive iron, or iron that is reactive towards hydrogen sulfide over diagenetic timescales (Lyons and Severmann,

2006; Lyons et al., 2009). Degree-of-sulfidization (DOS) is the ratio of Fe present in sulfide minerals relative to total reactive iron and is directly analogous to degree-of-pyritization (DOP). DOS (or DOP) in modern and ancient euxinic environments typically exceeds 0.6 and often exceeds 0.8 (Hurtgen et al., 1999; Scott et al., 2008). However, in our sample set, DOS averages 0.45 and never exceeds 0.6 (Fig. 3.1). We interpret these data as reflecting a lack of euxinic conditions during Newland deposition.

The ratio of total iron to total aluminum ($Fe_T/Al$) can also be used as an indicator of euxinia. The $Fe_T/Al$ of average shale is 0.5. However, due to scavenging of reactive Fe from the water column, $Fe_T/Al$ in euxinic environments displays a distinct enrichment, commonly exceeding 1.0. In our Newland shale samples, $Fe_T/Al$ averages 0.38, below the crustal average (Fig. 3.1). This is further evidence that euxinic conditions are not indicated in our sample set.

Poulton and Canfield (2005) developed a paleoredox proxy based on the sequential extraction of Fe from multiple phases which allows the identification of euxinic as well as ferruginous (anoxic and Fe-rich) conditions in the rock record. This method has been used successfully in Precambrian studies and revealed extraordinary enrichments of Fe from ferruginous deep waters in the Paleoproterozoic and the terminal Neoproterozoic (Poulton et al., 2004; Canfield et al., 2007; Canfield et al., 2008). In their method, euxinic conditions are indicated where the ratio of pyrite Fe to highly reactive Fe ($Fe_{PY}/Fe_{HR}$) exceeds 0.8, and the ratio of highly reactive to total Fe ($Fe_{HR}/Fe_T$) exceeds

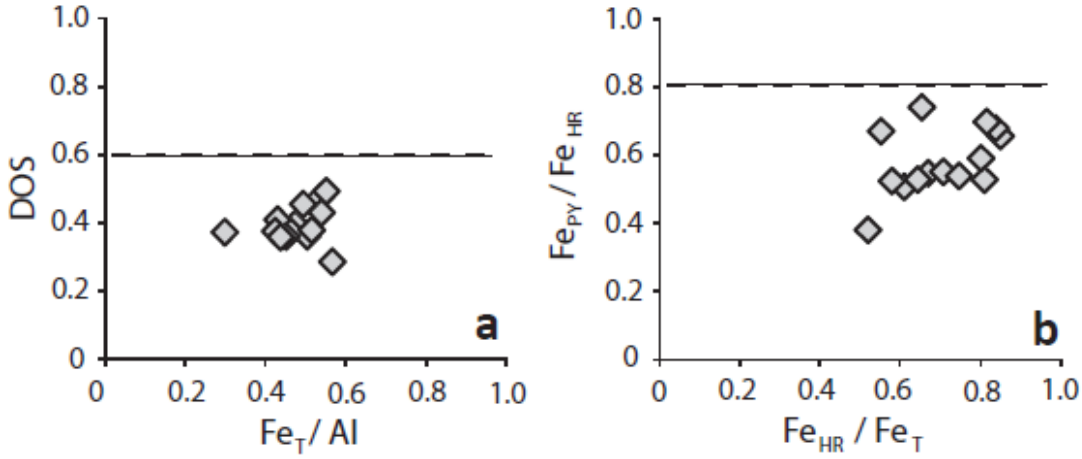


Figure 3.1. Fe speciation in Newland Formation Shales. a. Degree-of-sulfidization (DOS) versus $Fe_T$/Al. Dashed line represents a euxinic threshold of 0.6. b. Ratio of pyrite Fe to total highly reactive iron versus ratio of highly reactive iron and total iron. Dashed line represents a euxinic threshold of 0.8.

0.38. The latter value is based on the maximum ratio of $Fe_{HR}/Fe_T$ in modern "normal marine" or oxic sediments. Our data do indeed demonstrate elevated $Fe_{HR}/Fe_T$, clearly in excess of modern, normal marine environments (Fig. 3.1). However, $Fe_{PY}/Fe_{HR}$ averages 0.65 and never reaches the euxinic threshold of 0.8, indicating that pyrite formation was sulfide limited. Thus, all three commonly used Fe proxies support our interpretation of an absence of euxinia.

### 3.4.2 Molybdenum Enrichments in the Newland Formation

The transition metal Mo is a trace constituent of Earth's crust (1-2 ppm; Taylor and McLennan, 1995) but is highly enriched in euxinic black shales, characteristically reaching 10s to 100s of ppm (Scott et al., 2008). However, Mo concentrations in the Newland Formation cover a narrow range of 2-9 ppm (Fig. 3.2). We argue that this subtle enrichment of Mo is best explained by non-euxinic deposition.

If we consider the entire range of modern sulfidic environments we see a distinct bimodal distribution in Mo enrichments (Fig. 3.3). In non-euxinic sediments, where sulfide is restricted to the pore waters, Mo concentrations average ~10 ppm and rarely exceed 20 ppm. In euxinic environments, even those where sulfide is present in the bottom waters only seasonally, Mo enrichments cover a wide range of concentrations but never fall below 15 ppm. This is true even in the Black Sea, where Mo is quantitatively removed from the euxinic water column (Emerson and Huested, 1991) and sedimentation rates are high (15-20 cm/ky; Lyons and Severmann, 2006). We argue that black shales

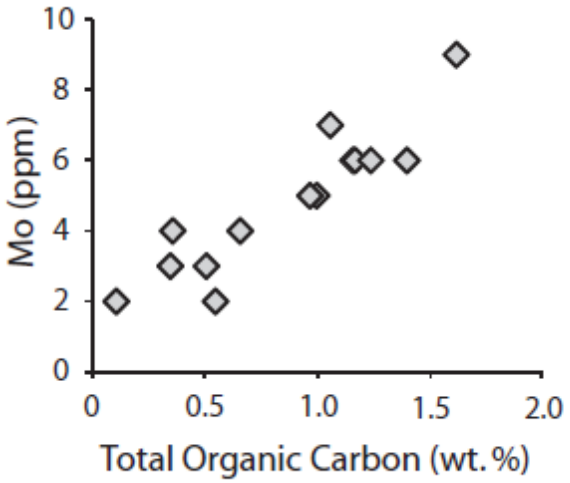


Figure 3.2. Bulk concentration of Mo (this study) and total organic carbon (Lyons et al., 2000).

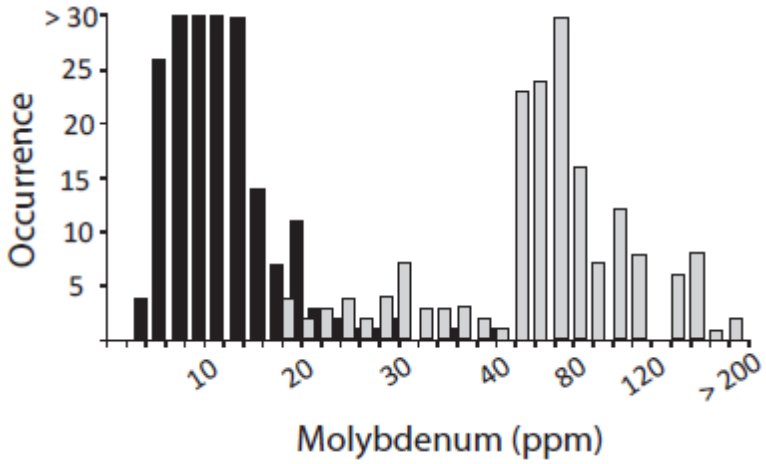


Figure 3.3. Mo concentrations in modern sulfidic sediments. Black bars represent non-euxinic sediments where hydrogen sulfide is restricted to the pore waters. Gray bars represent euxinic environments where hydrogen sulfide is intermittently or permanently present in bottom waters. Data from: Malcolm, 1985; Francois, 1988; Pedersen et al., 1989; Zheng et al., 2000; Lyons et al., 2002; Nameroff et al., 2002; Algeo and Lyons, 2006; McManus et al., 2006.

with Mo concentrations consistently below 10 ppm are indicative of non-euxinic deposition. Scott et al. (2008) recently demonstrated that Proterozoic euxinic black shales exhibit muted enrichments of Mo due to drawdown in widespread sulfidic environments.

Nevertheless, the only euxinic shale in Earth's history known to preserve Mo concentrations consistently below 10 ppm is from the Archean Jeerinah Formation, Hamersley Basin, which was deposited before the initiation of oxidative weathering as a source of Mo to the ocean (Scott et al., in prep).

### 3.4.3 Ferruginous versus Oxic Bottom Waters

Previous studies based on the sequential Fe extraction argue that where $Fe_{HR}/Fe_T > 0.38$ and $Fe_{PY}/Fe_T < 0.8$ bottom waters are ferruginous, meaning anoxic and rich in $Fe^{2+}$, a concept that is based on the ratio of $Fe_{HR}/Fe_T$ in modern "normal marine" or open ocean oxic environments (Raiswell and Canfield, 1998; Poulton and Raiswell, 2002; Poulton et al., 2004; Canfield et al., 2007; Canfield et al., 2008). We argue that the Newland Formation is an exception to this rule. The Belt Basin does not reflect normal marine conditions, rather a highly restricted epicontinental sea. Because the $Fe_{HR}/Fe_T$ of the suspended load in many modern rivers also exceeds 0.38 (e. g., Mekong River $Fe_{HR}/Fe_T = 0.66$; Poulton and Raiswell, 2002), the Belt Basin would be susceptible to enrichment of $Fe_{HR}$ from rivers emptying into the basin. Furthermore, Schieber (1995) recognized the addition of "non-detrital" Fe in Newland shales and attributed it to riverine delivery of Fe-oxyhydroxides. The ferruginous conditions described for the Neoproterozoic and Paleoproterozoic are accompanied by extraordinary enrichment of

Fe. In the Newland Formation, however, Fe is actually depleted ($Fe_T/Al < 0.5$) relative to average shale. We propose that in this instance, $Fe_{HR}/Fe_T$ greater than 0.38 does not require ferruginous bottom waters. In fact, additional data suggests that bottom waters may have been mildly oxygenated during Newland deposition.

### 3.4.4 Authigenic Carbonate Minerals

Carbonate minerals comprise between 0 and 5.0 wt. % of our Newland shale samples and $\delta^{13}C$ ranges from -3.9 ‰ to -6.1 ‰ (Fig. 3.4). Because carbonate minerals in Newland shales are depleted relative to Newland Formation limestones (~ +2‰; Hall and Veizer, 1996), we interpret these phases as reflecting authigenic precipitation of carbonate minerals from pore fluids where istopically depleted $HCO_3^{2-}$ accumulated as a result of bacterial oxidation of organic matter, coupled to the reduction of Mn-oxides, Fe-oxides and sulfate (Mozley and Burns, 1993). This complete range of oxidants is supported by the incorporation of both Mn carbonate minerals (as expressed in the strong covariation between total Mn and total inorganic carbon; Fig. 3.4) and pyrite in Newland shales.

While it is well known that post-depositional alteration of bulk carbonates will result in depletions in $\delta^{13}C$ and enrichments of Mn and Fe, this phenomenon is not described for minor carbonate minerals in pyritic black shales. The average concentrations of Mn and Fe in authigenic carbonates from the Newland Formation are ~200 and ~900 ppm, respectively, compared to an average of 3.3 wt. % authigenic

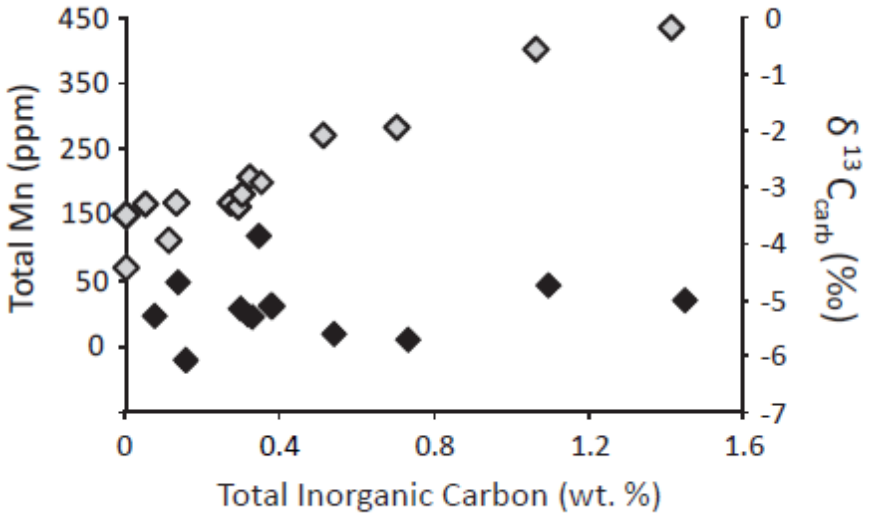


Figure 3.4. Bulk Mn versus total inorganic carbon (grey diamonds). $\delta^{13}C$ (PDB) of carbonate minerals versus total inorganic carbon (black diamond).

carbonate minerals. These concentrations are analogous to ~3,600 and 29,000 ppm, respectively, for bulk carbonates. By comparison, Mn and Fe concentrations from bulk carbonates of the Newland Formation and the younger Helena Formation, never exceed 2,000 and 3,000 ppm, respectively (Hall and Veizer, 1996; Frank et al., 1997). Because carbonates preserved in Newland shales are depleted in $\delta^{13}C$ and enriched in Mn and Fe relative to bulk carbonates from the Belt Basin, we posit that carbonate minerals in Newland shales must, to some degree, reflect primary pore water chemistry.

Calvert and Pedersen (1996), highlight the significance of the incorporation of Mn into authigenic carbonates, describing a "Mn pump", where Mn-oxides are recycled in oxygenated surface sediments. In their model, as Mn-oxyhydroxides are buried into reducing sediments, they are easily dissolved, releasing $Mn^{2+}$ into the pore waters. As $Mn^{2+}$ diffuses into overlying, oxygenated sediments, Mn particulates reprecipitate. As this cycle continues, surface sediments become enriched in Mn-oxyhydroxides, while the underlying pore waters become enriched in $Mn^{2+}$ (e.g., Canfield et al., 1993). Where $Mn^{2+}$ and $HCO_3^{2-}$ reach saturation, Mn-carbonates will precipitate, leaving behind evidence for Mn-oxide recycling even where Mn-oxides themselves do not persist. Shaw et al. (1990) found that Mn-oxides are not buried in the California Borderland Basins, where bottom water $O_2$ falls below 5-10 μM. Thus, the sum of our geochemical data suggest that the Belt Basin was not euxinic during Newland deposition and may have been mildly oxygenated, with dissolve $O_2 > 5$ μM at the sediment water interface.

### 3.5 Implications for Mesoproterozoic Ocean Chemistry

Our data describe local redox conditions in a highly restricted basin and should not be construed as evidence for an oxygenated global ocean, just as evidence for euxinia in the broadly contemporaneous McArthur Basin should not be construed as evidence for global euxinia. Nonetheless, our data set informs us on the likelihood that globally pervasive and persistent euxinia may have developed during the Mesoproterozoic. Due to its restricted nature, the Belt Basin should be more susceptible to the development of euxinic conditions than the open ocean, as is the case with the modern Black Sea. Furthermore, preservation of ~1-2 wt % organic matter in the Newland Formation informs us that the surface waters were at least moderately productive. Yet the geochemistry of the Newland Formation suggests that the basin was clearly not euxinic and was possibly fully oxygenated. Evidently, low atmospheric oxygen and moderately productive surface waters are not sufficient to produce a euxinic basin. Euxinia requires either higher productivity or lower atmospheric oxygen than reflected in Newland shales.

It is possible that productivity in the Belt Basin was limited by local nutrient supply. For example, if the connection between the Belt Basin and the open ocean were across a shallow sill, then the basin would be supplied by oligotrophic surface waters, as was the case for the Cariaco Basin during the last glacial maximum. However, it has been proposed that high productivity in the Proterozoic was likely restricted to nearshore environments where nutrients were readily available (Javaux et al., 2001; Anbar and Knoll, 2002) and it is unlikely that broad portions of the Proterozoic ocean, 100s to 1000s of kilometers from any continental source of nutrients would have been more productive

than the Belt Basin. We agree with the suggestion by Canfield (1998) that due to low $pO_2$ in the atmosphere, the Proterozoic ocean was more susceptible to the development of euxinic conditions, as is supported by the record of Mo enrichments in Proterozoic black shales (Scott et al., 2008). But we suggest that euxinic conditions were likely restricted to the vicinity of highly productive surface waters, either in restricted basins or along continental margins, and not globally pervasive. This view is consistent with recent work on REE trends in deep sea hydrothermal deposits which reflect low oxygen conditions but a lack of sulfide on the Proterozoic seafloor (Slack et al., 2007; Slack et al., 2009).

### 3.6 References

Algeo, T. J., and Lyons, T. W., 2006, Mo-total organic carbon covariation in modern anoxic marine environments: Implications for analysis of paleoredox and paleohydrographic conditions: Paleoceanography, v. 21, PA1016, doi:10.1029/2004PA001112.

Anbar, A.D., and Knoll, A.H., 2002, Proterozoic ocean chemistry and evolution: A bioinorganic bridge?: Science, v. 297, p. 1137–1142.

Bekker, A., Holland, H. D., Wang, P.-L., Rumble III, D., Stein, H. J., Hannah, J. L., Coetzee, L. L., and Beukes, N. J., 2004, Dating the rise of atmospheric oxygen: Nature, v. 427, p. 117-120.

Boesen, C. and Postma, D., 1988, Pyrite formation in anoxic environments of the Baltic: American Journal of Science, v. 288, p. 575-603.

Brocks, J. J., Love, G. D., Summons, R. E., Knoll, A. H., Logan, G., A., and Bowden, S. A., 2005, Biomarker evidence for green and purple sulphur bacteria in a stratified Paleoproterozoic sea: Nature, v. 437, p. 866-870.

Canfield, D.E., 1998, A new model for Proterozoic ocean chemistry: Nature, v. 396, p. 450–453.

Canfield, D. E., Thamdrup, B., and Hansen, J. W., 1993, The anaerobic degradation of organic matter in Danish coastal sediments: iron reduction, manganese reduction, and sulfate reduction: Geochimica et Cosmochimica Acta v. 57, p. 3867-3883.

Canfield, D. E., Poulton, S. W., and Narbonne, G. M., 2007, Late-Neoproterozoic deep-ocean oxygenation and the rise of animal life: Science, v. 315, p. 92-95.

Canfield, D. E., Poulton, S. W., Knoll, A. H., Narbonne, G. M., Ross, G., Goldberg, T., and Strauss, H., 2008, Ferruginous conditions dominated later Neoproterozoic deep-water chemistry: Science, v. 321, p. 949-952.

Calvert, S. E., and Pedersen, T. F., 1996, Sedimentary geochemistry of manganese: implications for the environment of formation of manganiferous black shales: Economic Geology, v. 91, p. 36-47.

Fike, D. A., Grotzinger, J. P., Pratt, L. M., and Summons, R. E., 2006, Oxidation of the Ediacaran ocean: Nature, v. 444, p. 744-747.

Francois, R. A., 1988, Study on the regulation of the concentrations of some trace metals (Rb, Sr, Zn, Pb, Cu, V, Cr, Ni, Mn and Mo) in Saanich Inlet sediments, British Columbia, Canada: Marine Geology, v. 83, p. 285-308.

Gellatly, A. M., and Lyons, T. W., 2005, Trace sulfate in mid-Proterozoic carbonates and the sulfur isotope record of biospheric evolution: Geochimica et Cosmochimca Acta, v. 69, p. 3813-3829.

Hall, S. M., and Veizer, J., 1996, Geochemistry of Precambrian carbonates: VII. Belt supergroup, Montana and Idaho, USA: Geochimica et Cosmochimica Acta, v. 60, p. 667-677.

Hoffman, P.F., Kaufman, A.J., Halverson, G.P., and Schrag, D.P., 1998, A Neoproterozoic snowball Earth: Science, v. 281, p. 1342–1349.

Hurtgen, M. T., Lyons, T. W., Ingall, E. D., and Cruse, A. M., 1999, Anomalous enrichments of iron monosulfide in euxinic marine sediments and the role of $H_2S$

in iron sulfide transformations: examples from Effingham Inlet, Orca Basin, and the Black Sea: American Journal of Science, v. 299, p. 556-588.

Hurtgen, M. T., Arthur, M. A., and Halverson, G. P., 2005, Neoproterozoic sulfur isotopes, the evolution of microbial sulfur species, and the burial efficiency of sulfide as sedimentary pyrite: Geology, v. 33, p. 41-44.

Javaux, E., Knoll, A. H., and Walter, M. R., 2001, Morphological and ecological complexity in early eukaryotic ecosystems: Nature, v. 412, p. 66-69.

Johnston, D.T., Wing, B.A., Farquhar, J., Kaufman, A.J., Strauss, H., Lyons, T.W., Kah, L.C., and Canfield, D.E., 2005, Active microbial sulphur disproportionation in the Mesoproterozoic: Science, v. 310, p. 1477–1479.

Kah, L.C., Lyons, T.W., and Chesley, J.T., 2001, Geochemistry of a 1.2 Ga carbonate-evaporite succession, northern Baffin and Bylot Islands: Implications for Mesoproterozoic marine evolution: Precambrian Research, v. 111, p. 203–234.

Kah, L.C., Lyons, T.W., and Frank, T.D., 2004, Low marine sulphate and protracted oxygenation of the Proterozoic biosphere: Nature, v. 431, p. 834–838.

Lyons, T. W., and Severmann, S., 2006, A critical look at iron paleoredox proxies: new insights from modern euxinic marine basins: Geochimica et Cosmochimica Acta, v. 70, p. 5698-5722.

Lyons, T.W., Luepke, J.J., Schreiber, M.E., and Zieg, G.A., 2000, Sulfur geochemical constraints on Mesoproterozoic restricted marine deposition: Lower Belt Supergroup, northwestern United States: Geochimica et Cosmochimica Acta, v. 64, p. 427–437.

Lyons, T. W., Werne, J. P., Hollander, D. J., and Murray, R. W., 2002, Contrasting sulfur geochemistry and Fe/Al and Mo/Al ratios across the lasat oxic-to-anoxic transition in the Cariaco Basin, Venezuela: Chemical Geology, v. 195, p. 131-158 (2002).

Lyons, T. W., Gellatly, A. M., McGoldrick, P. J., and Kah, L. C., 2006, Proterozoic sedimentary exhalative (SEDEX) deposits and evolving global ocean chemistry: in Evolution of Earth's atmosphere, hydrosphere and biosphere-Constrains from ore deposits Kesler, S. E. and Ohmoto, H. Geological Society of America memoir 198, p. 169-184.

Lyon, T. W., Anbar, A. D., Severmann, S., Scott, C., and Gill, B. C., 2009, Tracking euxinia in the ancient ocean: a multiproxy perspective and Proterozoic case study: Annual Review of Earth and Planetary Sciences, v. 37, p. 507-534.

Malcolm, S. J., 1985, Early diagenesis of molybdenum in estuarine sediments: Marine Chemistry, v. 16, p. 213-225.

McManus, J., Berelson, W. M., Severmann, S., Poulson, R. L., Hammond, D. E., Klinkhammer, G. P., and Holm, C., 2006, Molybdenum and uranium geochemistry in continental margin sediments: Paleoproxy potential: Geochimica. et Cosmochimica Acta, v. 70, p. 4643-4662.

Mozley, P. S., and Burns, S. J., 1993, Oxygen and carbon isotopic composition of marine carbonate concretions: an overview: Journal of Sedimentary Petrology, v. 63, p. 73-83.

Nameroff, T. J., Balistrieri, L. S., and Murray, J. W., 2002, Suboxic trace metal geochemistry in the eastern tropical North Pacific: Geochimica et Cosmochimica Acta, v. 66, p. 1139-1158.

Pedersen, T. F., Waters, R. D., and Macdonald, R. W., 1989, On the natural enrichment of cadmium and molybdenum in the sediments of Ucluelet Inlet, British Columbia: The Science of the Total Environment, v. 79, p. 125-139.

Poulton, S. W., and Raiswell, R., 2002, The low-temperature geochemical cycle of iron: from continental fluxes to marine sediment deposition: American Journal of Science, v. 302, p. 774-805.

Poulton, S. W., and Canfield, D. E., 2005, Development of a sequential extraction procedure for iron: implications for iron partitioning in continentally derived particulates: Chemical Geology, v. 214, p. 209-221.

Poulton, S. W., Frallick, P. W., and Canfield, D. E., 2004, The transition to a sulphidic ocean ~1,84 billion years ago: Nature, v. 431, p. 173-177.

Raiswell, R., Buckley, F. Berner, R. A., and Anderson, T. F., 1988, Degree of pyritization of iron as a paleoenvironmental indicator of bottom-water oxygenation: Journal of Sedimentary Research, v. 58, p. 812-819.

Raiswell, R., and Canfield, D. E., 1998, Sources of iron for pyrite formation in marine sediments: American Journal of Science, v. 298, p. 219-245.

Rouxel., O. J., Bekker, A., and Edwards, K. J., 2005, Iron isotope constraints on the Archean and Paleoproterozoic ocean redox state: Science, v. 307, p. 1088-1091.

Saito, M. A., Sigman, D. M., and Morel, F. M. M., 2003, The bioinorganic chemistry of ancient oceans: the co-evolution of cyanobacterial metal requirements and biogeochemical cycles at the Archean-Paleoproterozoic boundary?: Inorganica Chimica Acta, v. 356, p. 308-318.

Schieber, J., 1995, Anomalous iron distribution in shales as a manifestation of "non-clastic iron" supply to sedimentary basins: relevance for pyritic black shales, base-metal mineralization, and oolitic ironstone deposits, Mineralium Deposita, v. 30, p. 294-302.

Scott, C., Lyons, T. W., Bekker, A., Shen, Y., Poulton, S. W., Chu, X., and Anbar, A. D., 2008, Tracing stepwise oxygenation of the Proterozoic ocean: Nature, v. 452, p. 456-459.

Sears, J. W., Chamberlain, K. R., and Buckley, S. N., 1998, Structural and U-Pb geochronological evidence for 1.47 Ga rifting in the Belt basin, western Montana: Canadian Journal of Earth Science, v. 35, p. 467-475.

Slack, J. F., Greene, T., Bekker, A., Rouxel, O. J., and Lindberg, P. A., 2007, Suboxic deep seawater in the late Paleoproterozoic: evidence from hematitic chert and iron formation related to seafloor-hydrothermal sulfide deposits, central Arizona, USA: Earth and Planetary Science Letters, v. 255, p. 243-256.

Slack, J. F., Greene, T., and Bekker, A., 2009, Seafloor-hydrothermal Si-Fe-Mn exhalites in the Pecos greenstone belt, New Mexico, and the redox state of ca. 1729 Ma deep seawater: Geosphere, v. 5, p. 302-314.

Shaw, T. J., Gieskes, J. M., and Jahnke, R. A., 1990, Early diagenesis in differing depositional environments: the response of transition metals in pore water: Geochimica et Cosmochimica Acta, v. 54, p. 1233-1246.

Shen, Y., Canfield, D. E., and Knoll, A. H., 2002, Middle Proterozoic ocean chemistry: evidence from the McArthur Basin, Northern Australia: American Journal of Science, v. 302, p. 81-109.

Shen, Y., Knoll, A. H., and Walter, M. R., 2003, Evidence for low sulphate and anoxia in a mid-Proterozoic marine basin: Nature, v. 423, p. 632-635.

Taylor, S. R., and McLennan, S. M., 1995, The geochemical evolution of the continental crust: Reviews of Geophysics, v. 33, p. 241-265.

Winston, D., 1986, Sedimentation and tectonics of the Middle Proterozoic Belt basin and their influence of Phanerozoic compression and extension in western Montana and northern Idaho: in Paleotectonics and Sedimentation in the Rocky Mountain Region, United States (ed. J. A. Peterson) AAPG Memoir, v. 41, p. 87–118.

Winston, D., 1990, Evidence for intracratonic, fluvial and lacustrine settings of Middle and Late Proterozoic basins of western USA: in Mid-Proterozoic Laurentia-Baltica (eds. C. F. Gower, T. Rivers, and B. Ryan) Geologic Association of Canada Special Paper, v. 38, p. 535–564.

Zheng, Y., Anderson, R. F., Van Geen, A. L., and Kuwabara, J., 2000, Authigenic molybdenum formation in marine sediments: A link to pore water sulfide in the Santa Barbara Basin: Geochimica et Cosmochimica Acta, v. 64, p. 4165-4178.

Table 3.1 Results

| Core Depth | Al | Fe | Mn | Mo | TOC | TIC | $\delta^{13}C$ | S ($FeS_2$) | S (~FeS) | $\delta^{34}S$ |
|---|---|---|---|---|---|---|---|---|---|---|
| (m) | (wt. %) | (wt. %) | (ppm) | (ppm) | (wt. %) | (wt. %) | (‰) | (wt. %) | (wt. %) | (‰) |
| 204.8 | 6.7 | 2.4 | 166 | 3 | 0.4 | 0.05 | -5.4 | 0.83 | 0 | 1.4 |
| 204.85 | 6.7 | 2.6 | 168 | 2 | 0.6 | 0.13 | -6.1 | 0.86 | 0.04 | 1.8 |
| 232.8 | 8.7 | 3.2 | 149 | 2 | 0.1 | 0 | | 0.64 | 0.07 | 3.3 |
| 285 | 7.5 | 2.8 | 207 | 4 | 0.7 | 0.32 | -3.9 | 1.15 | 0.2 | 4.7 |
| 286.5 | 6.8 | 2.8 | 69 | 3 | 0.5 | 0 | | 1.23 | 0.24 | -0.5 |
| 313.6 | 6.2 | 2.9 | 402 | 4 | 0.4 | 1.06 | -4.8 | 1.17 | 0.04 | 3.2 |
| 371.5 | 5.6 | 2.4 | 111 | 6 | 1.2 | 0.11 | -4.8 | 1.26 | 0.26 | 4.8 |
| 372.5 | 5.6 | 2.5 | 199 | 5 | 1.0 | 0.35 | -5.2 | 1.36 | 0.26 | 4.9 |
| 372.55 | 5.8 | 2.8 | 271 | 5 | 1.0 | 0.51 | -5.7 | 1.45 | 0.37 | 3.2 |
| 420.9 | 5.4 | 1.5 | 435 | 9 | 1.6 | 1.41 | -5.1 | 0.8 | 0.04 | 11.8 |
| 495 | 6.8 | 2.5 | 168 | 6 | 1.4 | 0.27 | -5.2 | 0.9 | 0.1 | 2.1 |
| 495.05 | 6.5 | 2.4 | 162 | 6 | 1.2 | 0.29 | -5.4 | 0.95 | 0.1 | 2.5 |
| 495.11 | 6.5 | 2.3 | 181 | 6 | 1.2 | 0.3 | -5.4 | 0.74 | 0.2 | 1.2 |
| 495.15 | 6.4 | 2.4 | 283 | 7 | 1.1 | 0.7 | -5.8 | 0.95 | 0.1 | 2.5 |

Table 3.1 Continued

| Core Depth | Fe ($FeS_2$) | Fe (~FeS) | Sulfide Fe | Carbonate Fe | Oxide Fe | Oxalate-reducible Fe | HCl-soluble Fe | DOS | $Fe_T/Al$ | $Fe_{PY}/Fe_{HR}$ | $Fe_{HR}/Fe_T$ |
|---|---|---|---|---|---|---|---|---|---|---|---|
| (m) | (wt. %) | (wt. %) | (ppm) | (ppm) | (wt. %) | (wt. %) | (‰) | | | | |
| 204.8 | 0.74 | 0.0 | 0.74 | 0.06 | 0.13 | 0.28 | 0.73 | 0.50 | 0.36 | 0.61 | 0.51 |
| 204.85 | 0.73 | 0.07 | 0.80 | 0.11 | 0.22 | 0.25 | 0.89 | 0.47 | 0.40 | 0.58 | 0.52 |
| 232.8 | 0.51 | 0.12 | 0.63 | 0.08 | 0.20 | 0.31 | 1.50 | 0.30 | 0.37 | 0.52 | 0.38 |
| 285 | 0.85 | 0.36 | 1.20 | 0.08 | 0.18 | 0.02 | 1.40 | 0.46 | 0.37 | 0.81 | 0.53 |
| 286.5 | 0.88 | 0.43 | 1.31 | 0.04 | 0.24 | 0.04 | 1.74 | 0.43 | 0.41 | 0.80 | 0.59 |
| 313.6 | 1.01 | 0.07 | 1.08 | 0.13 | 0.15 | 0.25 | 0.93 | 0.54 | 0.47 | 0.67 | 0.55 |
| 371.5 | 0.89 | 0.46 | 1.35 | 0.04 | 0.21 | 0.0 | 1.15 | 0.54 | 0.43 | 0.85 | 0.66 |
| 372.5 | 0.98 | 0.46 | 1.44 | 0.04 | 0.23 | 0.0 | 1.48 | 0.49 | 0.45 | 0.84 | 0.68 |
| 372.55 | 0.96 | 0.66 | 1.62 | 0.06 | 0.30 | 0.0 | 1.31 | 0.55 | 0.49 | 0.82 | 0.70 |
| 420.9 | 0.68 | 0.07 | 0.75 | 0.07 | 0.30 | 0.03 | 0.57 | 0.57 | 0.28 | 0.65 | 0.74 |
| 495 | 0.69 | 0.21 | 0.91 | 0.40 | 0.18 | 0.16 | 1.10 | 0.45 | 0.36 | 0.55 | 0.67 |
| 495.05 | 0.75 | 0.20 | 0.94 | 0.06 | 0.20 | 0.12 | 1.28 | 0.42 | 0.37 | 0.71 | 0.55 |
| 495.11 | 0.53 | 0.27 | 0.79 | 0.07 | 0.30 | 0.07 | 1.02 | 0.44 | 0.36 | 0.64 | 0.53 |
| 495.15 | 0.72 | 0.25 | 0.97 | 0.06 | 0.22 | 0.05 | 0.91 | 0.52 | 0.38 | 0.75 | 0.54 |

# Chapter 4

*Biogeochemical Evidence for a Late Archean Nitrogen Crisis*

## 4.1 Abstract

Elemental and isotopic analyses of ~2630 million year old (Ma) shales from the Jeerinah Formation, Hamersley Basin, Western Australia reveal a sustained episode of Fe-limited pyrite formation under an anoxic and sulfidic water column. In the absence of oxidative weathering, oceanic sulfur was derived primarily from volcanic emissions, and trace metal inventories favored denitrification over nitrogen fixation, highlighting a potential link between nitrogen limitation and the delayed arrival of the Great Oxidation Event.

## 4.2 Introduction

Oxygenation of Earth's oceans and atmosphere resulted from a prolonged competition between oxygenic photosynthesis in surface waters and reducing power released from the Earth's interior (Catling and Claire, 2005). Because free oxygen is both the product of biological activity and an absolute requirement for animals, the mechanisms and timing of oxygenation are important components of the history of life on Earth (Knoll, 2003). However, as ocean/atmosphere redox conditions evolve, so too must the chemical composition of the oceans as redox-controlled sources and sinks are activated or are lost. Because seawater contains trace concentrations ($10^{-12}$ to $10^{-7}$ moles/L) of transition metals that are vital micronutrients (e.g., Ni, Cu, and Mo), tracking the composition of Earth's oceans through time is equally important in elucidating the evolutionary pathways that ultimately led to complex, multi-cellular life.

Oxygen first exceeded 0.001% of present atmospheric levels (Pavlov and Kasting, 2002) between 2450 and 2320 million years ago (Ma), early in the Proterozoic Eon (2500 to 542 Ma), a transition commonly referred to as the Great Oxidation Event or GOE (Holland, 2002; Bekker et al., 2004). However, there is evidence (Buick, 2007; Anbar et al., 2007; Reinhard et al., in press), disputed by some (Kopp et al., 2005; Kirschvink and Kopp, 2008), that oxygenic photosynthesis appeared on Earth during the Archean Eon (3500 to 2500 Ma), millions of years before the GOE. This evidence includes biomarker work (Brocks et al., 1999), recently challenged on the basis of potential contamination (Rasmussen et al., 2008), that placed cyanobacteria in the Hamersley Basin by 2700 Ma. If real, this lag implies a long-lived intermediate state where oxygen was produced in the surface waters, and thus was impacting ocean chemistry, but did not accumulate in the atmosphere.

The factors responsible for this delay are still unknown and represent one of the great paradoxes in Earth history. An important step in resolving this paradox is to better understand biogeochemical cycling of major and trace elements in late Archean surface environments. Furthermore, considering the intimate link between redox-controlled trace metal inventories and primary productivity, it is important to explore the extent to which late Archean ocean chemistry behaved as a barrier or a trigger to the initial accumulation of oxygen in the atmosphere. In order to constrain crucial variables in ocean chemistry during this important interval, we present here a geochemical study of the ca. 2630 Ma Roy Hill Member of the Jeerinah Formation, Hamersley Basin, Western Australia, an organic carbon- and sulfide-rich black shale.

## 4.3 Samples and Methods

### 4.3.1 Samples

Samples of the Roy Hill Member were collected from the drill core FVG-1 (Ilbianna Well; 22°33'S, 119°30'E). The age of the Jeerinah Formation is bracketed by a 2629 ± 5 Ma SHRIMP U-Pb zircon age of andesitic ignimbrite at the top of the Roy Hill Shale Member, the upper Jeerinah Formation (Nelson et al., 1999), and 2715 ± 2 Ma and 2713 ± 3 Ma SHRIMP U-Pb zircon ages for felsic tuffs within the underlying Maddina Basalt (Blake et al., 2004). Arndt et al. (1991) obtained 2684 ± 6 Ma and 2690 ± 16 Ma SHRIMP U-Pb zircon ages for the andesitic ignimbrite and tuffaceous sandstone of the upper Jeerinah Formation. The Hamersley Province where the Jeerinah Formation was deposited is mildly deformed and metamorphosed, with depth of burial being the primary control on metamorphic grade (Thorne and Trendall, 2001). The FVG-1 drill core was collared in the area that experienced prehnite-pumpellyite-epidote facies of metamorphism (Thorne and Trendall, 2001). The Jeerinah Formation was deposited during the transition from the rift to drift stage in an open-marine setting and consists of upward-fining sequence of sandstone, siltstone, shale, and carbonaceous pyritic shale with minor chert, dolomite, and mafic and felsic volcanic and volcanoclastic rocks (Canfield et al., 1996).

### 4.3.2 Analytical Methods

Iron speciation measures the relative contribution of three reactive Fe pools (sulfide, carbonate, and oxides) to the total Fe of the sample. First, pyrite sulfur is

measured by chromium reduction (Canfield et al., 1993), and pyrite Fe is calculated stoichiometrically ($FeS_2$). A separate sample split is then subjected to a sequential extraction of Fe from minerals developed by (Poulton and Canfield, 2005). A buffered sodium acetate solution is used to extract Fe from carbonate minerals. This is followed by an extraction of easily reducible Fe oxides using sodium dithionite. Because magnetite, a mixed-valence Fe oxide, is resistant to sodium dithionite, it is extracted using a solution of ammonium oxalate.

Total concentrations of Fe, Al, Mo and Cu were determined at Institute for Chemistry and Biology of the Marine Environment, University of Oldenburg, Germany. About 700 mg of the sample powder were mixed with 3600 mg of lithium tetraborate were oxidized at 500°C with $NH_4NO_3$, fused into glass beads and analyzed using X-ray fluorescence analysis (XRF). The beads were analyzed on a Philips PW 2400 spectrometer, calibrated with 46 carefully selected geostandards. Analytical precision, as checked by parallel analysis of international reference material and in-house standards, is better than 1% for Al and Fe, 5% for Mo and 5-10% for Cu.

Isotope analysis of pyrite sulfur begins with the extraction of reduced sulfur using chromium reduction (Canfield et al., 1996) and precipitation of $Ag_2S$. At the Geophysical Laboratory, Carnegie Institution of Washington, between 2 and 4 mg $Ag_2S$ was reacted with elemental fluorine at 25-30 torr with the assistance of a 25W $CO_2$ infrared laser in a vacuum chamber. The produced $SF_6$ was purified by gas chromatography before being introduced into a Thermo Electron Inc. MAT 253 mass-spectrometer for multiple sulfur isotope measurements in a dual-inlet mode (Ono et al., 2006). The sulfur isotope

compositions are reported with respect to VCDT. The intra-laboratory precision for $\delta^{34}S$, $\delta^{33}S$, and $\Delta^{33}S$ values based on multiple S isotope analysis of CDT material and internal laboratory reference materials was better than 0.36, 0.20, and 0.03‰, respectively.

Total organic carbon was determined on an Eltra Infrared C/S Determinator. Powdered sample is first combusted in a furnace at 1500 ºC, and evolved $CO_2$ represent total carbon. A second split of powdered sample is then acidified and stirred at 50 ºC. Evolved $CO_2$ represent total inorganic carbon. Total organic carbon is calculated as the difference between total carbon and total inorganic carbon.

## 4.4 Results and Discussion

### 4.4.1 Iron Speciation

In order to characterize local redox conditions for the Roy Hill Member, we rely on well-established methods, based on the speciation of Fe in ancient shales, that allow us to differentiate between oxic, anoxic or euxinic (anoxic and sulfidic) marine conditions (Poulton et al., 2004; Canfield et al., 2007; Canfield et al., 2008; Reinhard et al., in press). These methods first identify the relative abundances of highly reactive Fe ($Fe_{HR}$), or iron present in mineral phases that are biogeochemically reactive on diagenetic timescales (sulfides, oxides and carbonate), and total iron ($Fe_T$). In modern sediments deposited under oxygenated waters, $Fe_{HR}$ is dominated by the detrital fraction, and does not exceed 38% of total iron ($Fe_{HR}/Fe_T \leq 0.38$) (Raiswell and Canfield, 1998), with the remaining Fe present primarily in unreactive silicate minerals. In Precambrian black shales, $Fe_{HR}/Fe_T$ commonly exceeds 0.38, and augmentation of $Fe_{HR}$ from an anoxic or

euxinic water column is inferred (Canfield et al., 1996). We identify ancient euxinia by considering the extent to which $Fe_{HR}$ has been converted to pyrite iron ($Fe_{PY}$). Because $H_2S$ and $Fe^{2+}$ cannot coexist in abundance in solution, where euxinic conditions develop, pyrite formation is limited by availability of $Fe_{HR,}$ and $Fe_{PY}/Fe_{HR}$ will approach 1.0. Conversely, when a substantial fraction of the additional $Fe_{HR}$ remains unpyritized, iron-rich or ferruginous conditions are implied for the water column, with the residual $Fe_{HR}$ deposited as oxide or carbonate phases. We use a threshold of $Fe_{PY}/Fe_{HR} > 0.8$ as an indicator of euxinic conditions, when $Fe_{HR}/Fe_T$ also exceeds 0.38 (Poulton et al., 2004; Canfield et al., 2007; Canfield et al., 2008; Reinhard et al., in press).

Iron speciation from the Roy Hill Member reveals a sustained, 30 m thick, episode of Fe-limited pyrite formation under a euxinic water column (high $Fe_{HR}/Fe_T$ and $Fe_{PY}/Fe_{HR}$; Fig. 4.1), bracketed by periods of ferruginous conditions (high $Fe_{HR}/Fe_T$ and low $Fe_{PY}/Fe_{HR}$). This is the oldest of two known euxinic episodes in the Hamersley Basin, the second captured by the 2501 Ma Mt. McRae Shale (Reinhard et al., in press). By exploring key differences between these two euxinic episodes, the Hamersley Basin provides us a unique glimpse into the biogeochemical evolution of Archean seawater over a span of approximately 130 million years.

Based on periodic deposition of BIFs and the isotopic record of pyrite sulfur ($\delta^{34}S$), Archean seawater is classically considered to have been iron rich, with $Fe^{2+}$ reaching 100s of μM (Holland, 1984) and sulfate poor, such that $Fe^{2+} >> SO_4^{2-}$. However, Fe speciation data from the Roy Hill Member and Mt. McRae Shale (Reinhard et al., in press), point to significant spatial and/or temporal heterogeneities in the relative

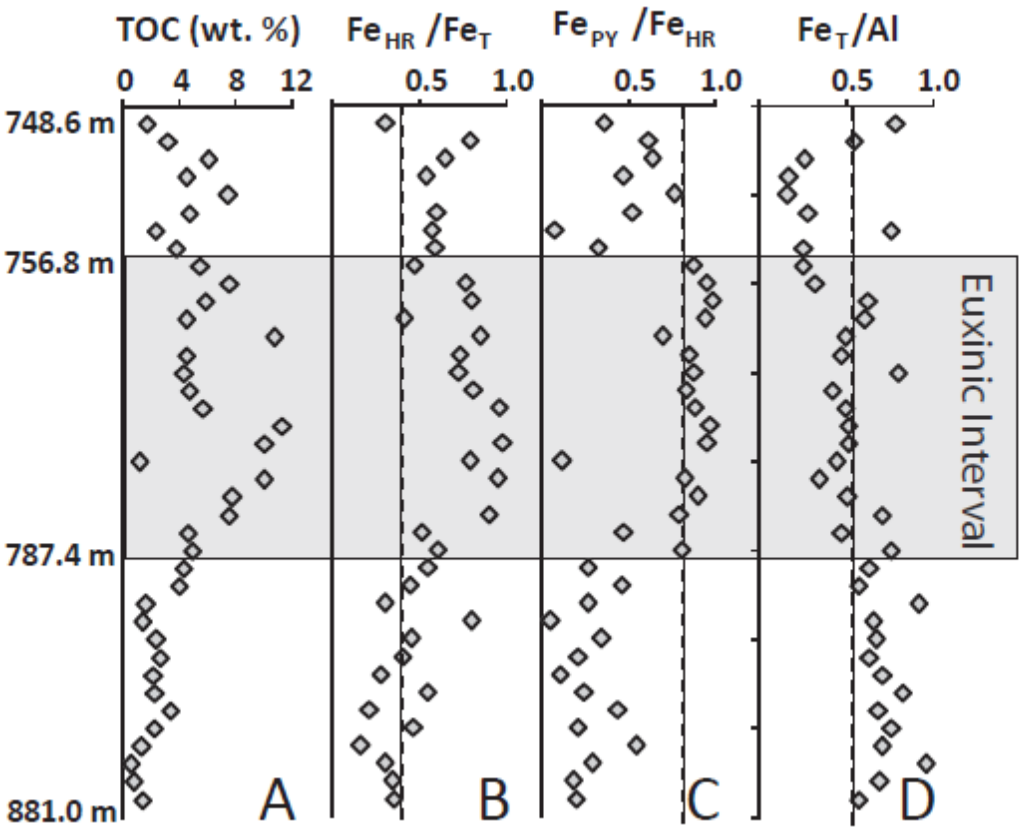


Figure 4.1. Total organic carbon and Fe speciation data from the Roy Hill Member. Dashed line in (B) represents the siliciclastic background of 0.38. Dashed line in (C) represents the euxinic threshold of 0.8. Dashed line in (D) is the average crustal value of 0.5. Shaded region is the euxinic interval.

concentrations of $Fe^{2+}$ and $SO_4^{2-}$ throughout Hamersley Basin deposition. We use a third Fe proxy, $Fe_T/Al$, which simply compares the concentration of total iron to total aluminum (Lyons and Severmann, 2006), as an indicator of the magnitude of $Fe_{HR}$ enrichment from seawater. The $Fe_T/Al$ ratio of average continental crust is 0.5. Due to scavenging of $Fe_{HR}$ from the water column, modern euxinic sediments and ancient shales typically display $Fe_T/Al > 1.0$, and portions of the Mt. McRae Shale exceed 3.0 (Reinhard et al., in press). By comparison, $Fe_T/Al$ in the Roy Hill Member reveals only minor enrichments of Fe relative to average crust (Fig. 4.1), with values well below those seen in the Mt. McRae Shale or even many Phanerozoic black shales. These data indicate that the flux of $Fe_{HR}$ to the basin was considerably higher during Mt. McRae deposition than during Roy Hill deposition. Each unit also captures an episode of euxinia, where the rate of $Fe_{HR}$ delivery was outpaced by the rate of sulfide production via bacterial sulfate reduction. Thus, the Hamersley Basin captures a range of bottom water conditions, as represented by BIFs, ferruginous shales, and euxinic shales, where the concentration of $Fe^{2+}$ varied significantly, and on occasion, $Fe^{2+} < SO_4^{2-}$.

### 4.4.2 Pyrite Sulfur Isotopes

A unique feature of sedimentary pyrite deposited prior to the GOE is the preservation of large, non-mass dependent (NMD) S isotopes fractionations ($\Delta^{33}S > |0.4|$ ‰; Farquhar et al., 2000). NMD fractionations are produced during photolysis of volcanic $SO_2$ in the absence of ozone, producing $S_8$ and $H_2SO_4$. In addition, preservation requires very low levels of oxygen ($pO_2 < 0.001\%$ PAL; Pavlov and Kasting, 2002) in

order to prevent re-oxidation of the resultant sulfur species and subsequent isotopic mixing. Thus, large NMD fractionations are an unambiguous indicator of an anoxic atmosphere. Because sulfate derived from oxidative weathering of the continents and hydrothermally-sourced hydrogen sulfide each lack this isotopic signature, we use the isotopic composition of disseminated pyrites from the Roy Hill Member to determine the source of S in the basin.

Disseminated pyrite in the Roy Hill Member displays a robust NMD signature ($\Delta^{33}S$ = -1.4 to + 7.9 ‰) that correlates positively with $\delta^{34}S$ (Fig. 4.2), falling along a linear array that is characteristic of Archean pyrites (Reinhard et al., in press; Kaufman et al., 2007; Ono et al., 2009). There is no stratigraphic trend in $\Delta^{33}S$, or between ferruginous and euxinic intervals. This range of isotopic values, and their insensitivity to local redox conditions, suggests that sulfide in the Roy Hill Member is primarily derived from atmospherically processed S.

While we cannot exclude the possibility that hydrothermal or continental sulfur was present in the basin, there is no clear evidence that either was a significant constituent of the local sulfur pool during Roy Hill deposition. Reinhard et al., (in press) argued that the trigger for euxinia in the Mt. McRae Shale was an oxidative pulse of sulfate to the basin, spurring high rates of sulfate reduction. Their argument relies on the diminished expression of the NMD S signal and the conspicuous enrichment of Mo during the euxinic interval (Anbar et al., 2007). Neither of these two features is expressed in the Roy Hill Member, where the trigger for euxinia was likely a more subtle shift in the relative delivery of $Fe_{HR}$ and reduced sulfur, and not an oxidative pulse of sulfate to

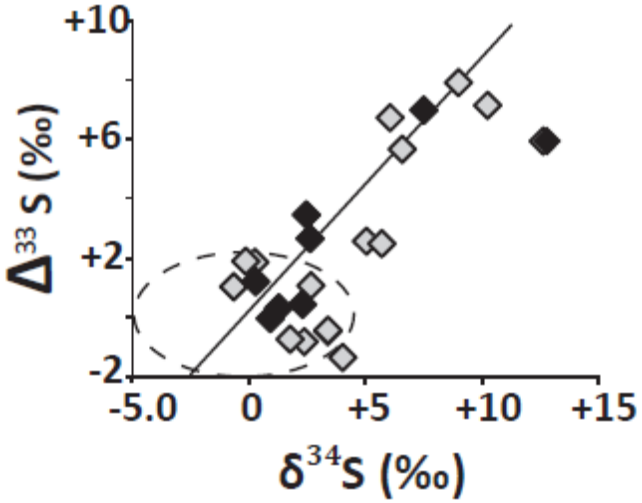


Figure 4.2. Sulfur isotope data for disseminated pyrites from the Roy Hill Member. Grey diamonds are from the euxinic interval. Black diamonds are from the ferruginous intervals. Solid line is the Archean reference array (Kaufman et al., 2007; Ono et al., 2009). Dashed field represents sulfur isotope data for the Mt. McRae Shale euxinic interval (Reinhard et al., 2009).

the ocean — suggesting there is nothing unique about S delivery to the basin during this time. If so, we expect that euxinic conditions could develop at any point during the Archean, provided $Fe_{HR}$ input was low and primary productivity and sulfate reduction were comparatively high.

### 4.4.3 Evidence for Oxygenic Photosynthesis

The geochemistry of the Roy Hill Member also reveals clues to the source of abundant organic carbon in the basin. All photosynthesizers require a reductant (e. g., $Fe^{2+}$, $H_2S$, or $H_2O$) in order to convert $CO_2$ to organic matter (Canfield, 2005). Anoxygenic photosynthesis coupled to oxidation of ferrous iron produces four moles of $Fe_{HR}$ for every mole of organic matter,

$$4Fe^{2+} + CO_2 + H_2O \rightarrow CH_2O + 4Fe(OH)_3 + 8H^+.$$

If $Fe^{2+}$ was the dominant reductant in the surface waters, we would expect $Fe_{HR}$ > TOC, even if most of the resultant $Fe_{HR}$ escaped burial. This ratio would be further elevated as TOC is preferentially lost from the system. However, $Fe_{HR}$/TOC averages 0.7 in the Roy Hill Member. We argue that the Fe chemistry of the Roy Hill Member is inconsistent with high productivity coupled to $Fe^{2+}$ oxidation. Furthermore, hydrogen sulfide is clearly not present in the surface waters during the non-euxinic intervals, and pyrite S isotopes argue against a hydrothermal source of hydrogen sulfide during the euxinic interval. This means that the presence of hydrogen sulfide in the basin was not the driver of high productivity. Rather, the most plausible reductant utilized in Roy Hill surface waters is $H_2O$, which releases free oxygen as a waste product:

$$H_2O + CO_2 \rightarrow CH_2O + O_2.$$

Thus, C-S-Fe systematics of the Roy Hill Member provide further, although indirect, evidence that oxygenic cyanobacteria were extant and influencing ocean chemistry by 2630 Ma, 200 million years prior to the GOE.

### 4.4.4 Euxinia as a Window into Seawater Trace Metal Inventories

Euxinic conditions provide an opportunity to gauge the concentrations of redox-sensitive micronutrients in the overlying water column. Molybdenum is the best studied example and is relevant to early nutrient cycles because it is utilized during biological N fixation (Howard and Rees, 1996; Anbar and Knoll, 2002). Mo is a minor constituent of the crust (Taylor and McLennan, 1995) but is the most abundant transition metal in the modern ocean due to its conservative behavior in oxygenated waters (Bertine and Turekian, 1973). The primary source of Mo to the oceans is oxidative weathering of continental crust, and its primary sink is in sulfidic settings (Scott et al., 2008). In euxinic sediments, Mo can become highly enriched (Scott et al., 2008), commonly two orders of magnitude above the average crustal abundance of 1-2 ppm (Taylor and McLennan, 1995), and co-varies conspicuously with TOC concentrations. Furthermore, it is well established that Mo/TOC ratios in euxinic sediments are proportional to the concentration of dissolved Mo in the euxinic water column (Algeo and Lyons, 2006). Scott et al. (2008) used this relationship to characterize Proterozoic oceans as Mo deficient due to widespread sulfidic deposition (both euxinic and non-euxinic yet sulfidic sediments) outpacing the oxidative source. The Roy Hill euxinic interval provides an excellent

opportunity to constrain the abundance of Mo in late Archean oceans, prior to the initiation of oxidative weathering.

Bulk Mo concentrations in the Roy Hill Member range from 1 to 6 ppm (average 2.7 ppm), barely distinguishable from average crust, and display no covariation with the abundance TOC and no trend between euxinic and non-euxinic intervals (Fig. 4.3). Distinct covariation between Mo and TOC is expressed in the Black Sea where the concentration of Mo in the euxinic basin is 3 nM (Algeo and Lyons, 2006), or < 5 % of the open ocean average (Collier, 1985). Covariation with TOC and clear enrichments above the crustal background are also expressed in the Mt. McRae Shale and are interpreted as evidence that dissolved Mo approached the Black Sea value, due to mild oxidative weathering of continental materials (Anbar et al., 2007; Reinhard et al., in press). Yet no significant enrichment of Mo or co-variation with organic matter are apparent in the Roy Hill Member. We therefore suggest that the concentration of Mo in the Roy Hill euxinic basin was well below the 3 nM observed in the Black Sea euxinic water column, consistent with the absence of a significant oxidative source of Mo to the surface waters.

Recent work demonstrates that cultured diazatrophs are less efficient at N fixation when dissolved Mo falls below 5 nM (Zerkle et al., 2006; Glass et al., 2009). To the degree that Mo concentrations in the Roy Hill euxinic basin are representative of the global ocean, it is likely that primary productivity was limited by the availability of fixed N, as was previously suggested for the Proterozoic ocean (Anbar and Knoll, 2002). Furthermore, if seawater Mo concentrations remain below the biological threshold in the

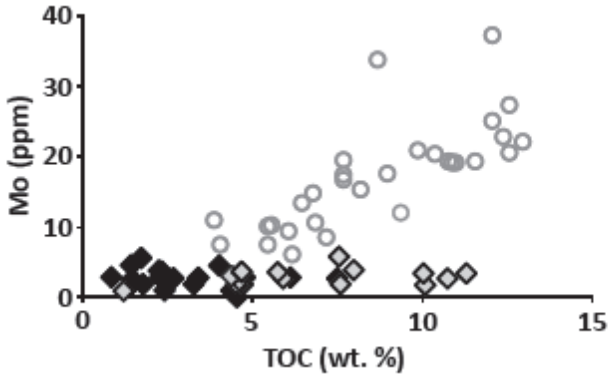


Figure 4.3. Concentrations of Mo vs. TOC in the Roy Hill Member. Grey diamonds represent the euxinic interval and black diamonds represent the ferruginous interval. Open circles are from the Mt. McRae Shale euxinic interval (Anbar et al., 2007, Reinhard et al., 2009).

absence of oxidative weathering, Mo nitrogenase likely evolved only after oxygen production by early cyanobacteria overcame reducing sinks in the ocean and atmosphere, and initiated oxidative weathering of continental crust and increased Mo delivery, sometime after 2630 Ma.

While Mo enrichments are essentially absent, Cu is clearly elevated in the Roy Hill Member, exceeding the concentration of Cu in bulk continental crust (75 ppm; Taylor and McLennan, 1995) and equivalent facies from representative Phanerozoic euxinic basins (Fig. 4.4). The sources and sinks for oceanic Cu and its behavior in euxinic versus non-euxinic environments are not yet as well established as they are for Mo. However, Cu concentrations in ancient black shales co-vary with the concentration of TOC, just as Mo does (Werne et al., 2002; Cruse and Lyons, 2004). If Cu/TOC covariation is sensitive to the concentration of Cu in seawater, then dissolved Cu in the Hamersley Basin was at least equal to that of Phanerozoic oceans, and thus, Cu delivery must have been decoupled from oxidative weathering.

Cu is utilized for a number of important cellular functions, including denitrification – the sequential reduction of bioavailable $NO_3^-$ to biologically inert $N_2$ (Zumft, 1997). Based on the trace metal chemistry of the Roy Hill Member and the Mt. McRae Shale, it is possible that the denitrification pathway evolved prior to Mo nitrogenase. This scenario would combine efficient denitrification with inefficient N fixation (possibly utilizing Fe-Fe nitrogenase; Anbar and Knoll, 2002), resulting in extreme N limitation in late Archean oceans. Further work on Cu cycling is required to test this scenario, but recent work on N isotopes in the Mt. McRae Shale (Garvin et al.,

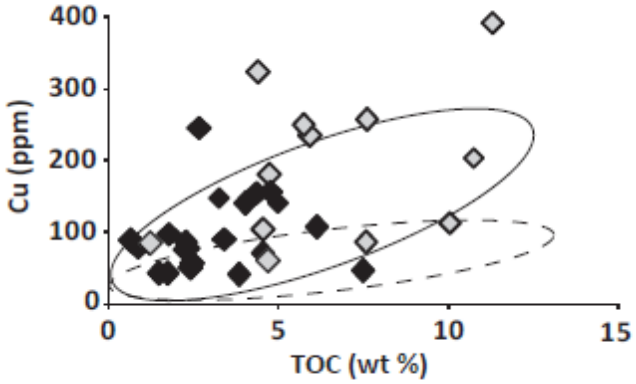


Figure 4.4. Cu concentrations versus TOC in the Roy Hill Member. Grey diamonds represent the euxinic interval and black diamonds represent the ferruginous intervals. Solid and dashed regions represent Cu/TOC relationship in the Devonian Oatka Creek Formation and the Carboniferous Hushpuckney Shale, respectively (Werne et al., 2002, Cruse and Lyons, 2004).

2009) suggests that denitrifiers were already established by 2501 Ma, coincident with the first evidence for appreciable dissolved Mo in the Hamersley Basin.

Our data support the appearance of oxygenic photosynthesis in the late Archean, at least 200 million years before the GOE. This delay represents one of the great paradoxes in the history of life on Earth and probably reflect numerous, and interrelated, contributing factors. Based on the trace metal chemistry of euxinic black shales in the Hamersley Basin, we propose that among the interrelated triggers for the GOE was a nitrogen revolution, occurring sometime after 2501 Ma, when rates of N fixation first exceeded rates of N loss through denitrification.

## 4.5 References


Algeo, T. J., Lyons, T. W., 2006. Mo–total organic carbon covariation in modern anoxic marine environments: Implications for analysis of paleoredox and paleohydrographic conditions. **Paleoceanography** *21*, doi:10.1029/2004PA001112.

Anbar, A. D., Knoll, A. H., 2002. Proterozoic ocean chemistry and evolution: A bioinorganic bridge? **Science** *297*, 1 137–1142.

Anbar, A. D., Duan, Y., Lyons, T. W., Arnold, G. L., Kendall, B., Creaser, R. A., Kaufman, A. J., Gordon, G. W., Scott, C., Garvin, J., Buick, R., 2007. A whiff of oxygen before the great oxidation event? *Science* **317**, 1903-1906.

Bekker, A., Holland, H. D., Wang, P.-L., Rumble III, D., Stein, H. J., Hannah, J. L., Coetzee, L. L., Buekes, N. J., 2004. Dating the rise of atmospheric oxygen. *Nature* **427**, 117-120.

Bertine, K. K., Turekian, K. K., 1973. Molybdenum is marine deposits. *Geochimica et Cosmochimica Acta **37***, 1415-1434.

Brocks, J. J., Logan, G. A., Buick, R. Summons, R. E., 1999. Archean molecular fossils and the early rise of eukaryotes. *Nature* **285**, 1033-1036.

Buick, R., 2008. When did oxygenic photosynthesis evolve? *Philosophical Transactions of the Royal Society B* **363**, 2731-2743.

Canfield, D. E., 2006. The early history of atmospheric oxygen: homage to Robert M. Garrels. *Annual Review of Earth and Planetary Science* **33**, 1-36.

Canfield, D. E., Raiswell, R., Westrich, J. T., Reaves, C. M., Berner, R. A., 1986. The use of chromium reduction in the analysis of reduced inorganic sulfur in sediments and shales. *Chemical Geology* **54**, 149-155.

Canfield, D. E., Poulton, S. W., Narbonne, G. M., 2007. Late-Neoproterozoic deep ocean oxygenation and the rise of animal life. *Science* **315**, 92–95 .

Canfield, D. E., Poulton, S. W., Knoll, A. H., Narbonne, G. M., Ross, G., Goldberg, T., and Strauss, H., 2008. Ferruginous conditions dominated later Neoproterozoic deep-water chemistry: *Science* **321**, 949-952.

Catling, D. C., Claire, M. W., 2005. How Earth's atmosphere evolved to an oxic state: A status report. *Earth and Planetary Science Letters* **237**, 1-20.

Collier, R. W., 1985. Molybdenum in the Northeast Pacific Ocean. *Limnology and Oceanography* **306**, 1351-1354.

Cruse, A. M., Lyons, T. W., 2004. Trace metal records of regional paleoenvironmental variability in Pennsylvanian (Upper Carboniferous) black shales. *Chemical Geology* **206**, 319-345.

Emerson, S. R., Huested, S. S., 1991. Ocean anoxia and the concentrations of molybdenum and vanadium in seawater. *Marine Chemistry* **34**, 177-196.

Farquhar, J., Bao, H., Thiemens, M., 2000. Atmosphere influence of Earth's earliest sulfur cycle. *Science* **289**, 756-758.

Garvin, J., Buick, R., Anbar, A. D., Arnold, G. L., Kaufman, A. J., 2009. Isotopic evidence for an aerobic nitrogen cycle in the latest Archean. *Science* **232**, 1045-1048.

Glass, J. B., Wolfe-Simon, F., Anbar, A. D., 2009. Coevolution of metal availability and nitrogen assimilation in cyanobacteria and algae. *Geobiology* **7**, 100-123.

Holland, H. D., 1984. The chemical evolution of the atmosphere and oceans. Princeton University Press, Princeton, N. J.

Holland, H. D., 2002. Volcanic gases, black smokers, and the great oxidation event. *Geochimica et Cosmochimica Acta* **66**, 3811 (2002).

Howard, J. B., Rees, D. C., 1996. Structural basis for biological nitrogen fixation. *Chemical Review* **96**, 2965-2982.

Kaufman, A. J., Johnston, D. T., Farquhar, J., Masterson, A. L., Lyons, T. W., Bates, S., Anbar, A. D., Arnold, G. L., Garvin, J., Buick, R., 2007. Late Archean biospheric oxygenation and atmoshpheric evolution. *Science* **317**, 1900-1903.

Knoll, A. H., 2003. The geological consequences of evolution. *Geobiology* **1**, 3-14.

Kopp, R. E., Kirschvink, J. L., Hilburn, I. A., Nash, C. Z., 2005. The Paleoproterozoic snowball Earth: a climate disaster triggered by the evolution of oxygenic photosynthesis. *Proceedings of the National Academy of Sciences* **102**, 11131-11136.

Kirschvink, J. L., Kopp, R. E., 2008. Paleoproterozoic icehouses and the evolution of oxygen-mediating enzymes: the case for a late origin of photosystem II. *Philosophical Transactions of the Royal Society B* **363**, 2755-2765 (2008).

Lyons, T. W., Severmann, S., 2005. A critical look at iron paleoredox proxies: new insights from modern euxinic marine basins. *Geochimica et Cosmochimica Acta* **70**, 5698-5722.

Olson, J. M., 2006. Photosynthesis in the Archean Era. *Photosynthesis in the Archean Era* **88**, 109-117.

Ono, S., Kaufman, A. J., Farquhar, J., Sumner, D. Y., Buekes, N. J., 2009. Lithofacies control on multiple-sulfur isotope records and Neoarchean sulfur cycles. *Precambrian Research* **169**, 58-67 (2009).

Pavlov, A. A., Kasting, J. M., 2002. Mass-independent fractionation of sulfur isotopes in Archean sediments: strong evidence for an anoxic Archean atmosphere. *Astrobiology* **2**, 27-41.

Poulton, S. W., Canfield, D. E., 2005. Development of a sequential extraction procedure for iron: implications for iron partitioning in continentally derived particulates. *Chemical Geology* **214**, 209-212.

Poulton, S. W., Fralick, P. W., Canfield, D. E., 2004. The transition to a sulphidic ocean ~1.84 billion years ago. *Nature* **431**, 173-177.

Raiswell, R., Canfield, D. E., 1998. Sources of iron for pyrite formation in marine sediments. *American Journal of Science* **298**, 219-245.

Raiswell, R., Buckley, F., Berner, R. A., Anderson, T. F., 1988. Degree of pyritization of iron as a paleoenvironmental indicator of bottom-water oxygenation. *Journal of Sedimentary Research* **58**, 812-819.

Rasmussen, B., Fletcher, I. R., Brocks, J. J., Kilburn, M. R., 2008. Reassessing the first appearance of eukaryotes and cyanobacteria. *Nature* **455**, 1101-1104.

Reinhard, C., Raiswell, R., Scott, C., Anbar, A. D., Lyons, T. W., 2009. A late-Archean euxinic basin. *Science* (in press).

Scott, C., Lyons, T. W., Bekker, A., Shen, Y., Poulton, S. W., Chu, X., Anbar, A. D., 2008. Tracing the stepwise oxygenation of the Proterozoic ocean. *Nature* **452**, 456-459.

Taylor, S. R., McLennan, S. M., 1995. The geochemical evolution of the continental crust. *Reviews of Geophysics* **33**, 241-265.

Werne, J. P., Sageman, B. B., Lyons, T. W., Hollander, D. J., 2002. An integrated assessment of a "type euxinic" deposit: evidence for multiple controls on black shale deposition in the middle Devonian Oatka Creek Formation. American Journal of Science **302**, 110-143.

Zerkle, A. L., House, C. H., Cox, R. P., Canfield, D. E., 2006. Metal limitation of biological $N_2$ fixation and implications for the Precambrian nitrogen cycle. *Geobiology* **4**, 285-297.

Zumft, W. G., 1997. Cell biology and the molecular basis of denitrification. *Microbiology and Molecular Biology Reviews* **61**, 533-616.

Table 4.1 Results

| Core depth | TOC | Pyrite S | $\delta^{34}S$ | $\delta^{33}S$ | $\Delta^{33}S$ | Al | Mo | Cu |
|---|---|---|---|---|---|---|---|---|
| (m) | (wt. %) | (wt. %) | (‰) | (‰) | (‰) | (wt. %) | (ppm) | (ppm) |
| 748.3 | 1.8 | 0.9 | 1.2 | 1.37 | 0.27 | 8.4 | 2 | 98 |
| 749.65 | 3.3 | 2.7 | 2.2 | 1.96 | 0.42 | 8.6 | 2 | 147 |
| 750.56 | 6.1 | 1.2 | 0.9 | 0.99 | -0.02 | 9.0 | 3 | 108 |
| 751.15 | 4.5 | 0.5 | 2.5 | | | 8.8 | 0 | 72 |
| 752.65 | 7.5 | 1.4 | 12.7 | 13.37 | 5.94 | 8.8 | 3 | 50 |
| 753.95 | 4.8 | 0.6 | 7.7 | | | 6.0 | 3 | 157 |
| 755.2 | 2.4 | 0.1 | 3.8 | 1.72 | -0.47 | 2.9 | 1 | 54 |
| 756.6 | 3.8 | 0.3 | 8.6 | 2.04 | 0.16 | 5.4 | 1 | 42 |
| 756.8 | 5.6 | 0.7 | 4.0 | 1.66 | -1.35 | 5.5 | | |
| 760.7 | 7.6 | 2.0 | 3.3 | 1.72 | -0.47 | 7.3 | 2 | 258 |
| 761.8 | 5.9 | 3.6 | 2.6 | 2.86 | 1.08 | 6.2 | 3 | 237 |
| 764.45 | 4.6 | 1.7 | 2.3 | 0.77 | -0.82 | 6.1 | | |
| 765 | 10.7 | 1.9 | 6.0 | 9.52 | 6.76 | 5.5 | 3 | 203 |
| 767.6 | 4.6 | 1.6 | 5.0 | 5.91 | 2.58 | 4.5 | 2 | 105 |
| 774 | 4.4 | 3.4 | 1.7 | 0.74 | -0.73 | 5.7 | 3 | 323 |
| 775.55 | 4.7 | 2.0 | 3.3 | 1.60 | -0.43 | 6.0 | 2 | 181 |
| 776.4 | 5.8 | 3.0 | 5.6 | 5.72 | 2.50 | 6.2 | 4 | 249 |
| 777.8 | 11.3 | 3.5 | -0.7 | 1.07 | 1.04 | 5.8 | 3 | 392 |
| 779.45 | 10.1 | 3.3 | 0.2 | 2.24 | 1.87 | 5.8 | 2 | 420 |
| 780.3 | 1.2 | 0.5 | -0.1 | 2.06 | 1.90 | 9.0 | 1 | 86 |
| 780.95 | 10.0 | 2.3 | 8.9 | 13.33 | 7.94 | 7.2 | 3 | 114 |
| 782.9 | 7.8 | 3.8 | 10.2 | 13.10 | 7.17 | 6.1 | | |
| 787.4 | 7.6 | 3.8 | 6.5 | 9.33 | 5.69 | 6.4 | 6 | 84 |
| 791 | 4.7 | 1.1 | -0.4 | | | 7.7 | 4 | 61 |
| 794.1 | 4.7 | 2.9 | 1.7 | 6.40 | 4.82 | 6.7 | 4 | 141 |
| 796.2 | 4.4 | 0.8 | 1.1 | | | 7.1 | 4 | 156 |
| 797.05 | 4.0 | 1.1 | 7.5 | 11.30 | 6.98 | 7.9 | 6 | 141 |
| 802.1 | 1.7 | 0.5 | 3.5 | | | 5.6 | 3 | 44 |
| 813.25 | 1.5 | 0.2 | 1.5 | | | 6.3 | | |
| 813.6 | 2.5 | 0.8 | 3.7 | | | 6.4 | 3 | 60 |
| 815.2 | 2.7 | 0.5 | 2.4 | 5.06 | 3.44 | 7.7 | 4 | 246 |
| 818.8 | 2.2 | 0.2 | 2.5 | | | 7.4 | 4 | 76 |
| 822.45 | 2.3 | 0.8 | 0.2 | 1.56 | 1.19 | 5.8 | 3 | 76 |
| 823.3 | 3.4 | 0.5 | 2.8 | | | 6.6 | 3 | 91 |

| | | | | | | | | |
|---|---|---|---|---|---|---|---|---|
| 829.9 | 2.3 | 0.6 | 2.6 | 4.33 | 2.65 | 6.8 | 5 | 84 |
| 849.6 | 1.4 | 0.5 | 0.0 | | | 6.7 | | |
| 855.65 | 0.7 | 0.8 | -0.3 | | | 7.8 | 3 | 88 |

Table 4.1 Continued

| **Core Depth** | **Total Fe** | **Acetate Fe** | **Dithionite Fe** | **Oxalate Fe** | **Pyrite Fe** | **Total $Fe_{HR}$** | **$Fe_{HR}/Fe_T$** | **$Fe_{PY}/Fe_{HR}$** | **$Fe_T/Al$** |
|---|---|---|---|---|---|---|---|---|---|
| **(m)** | **(wt. %)** | **(wt. %)** | **(wt. %)** | **(wt. %)** | **(wt. %)** | **(wt. %)** | | | |
| 748.3 | 6.6 | 0.3 | 0.3 | 0.7 | 0.7 | 2.0 | 0.3 | 0.4 | 0.8 |
| 749.65 | 4.7 | 0.3 | 0.2 | 1.0 | 2.3 | 3.7 | 0.8 | 0.6 | 0.5 |
| 750.56 | 2.4 | 0.1 | 0.1 | 0.3 | 1.0 | 1.5 | 0.6 | 0.6 | 0.3 |
| 751.15 | 1.5 | 0.1 | 0.2 | 0.2 | 0.4 | 0.8 | 0.5 | 0.5 | 0.2 |
| 752.65 | 1.4 | 0.1 | 0.2 | 0.1 | 1.2 | 1.6 | 1.1 | 0.8 | 0.2 |
| 753.95 | 1.7 | 0.2 | 0.1 | 0.2 | 0.5 | 1.0 | 0.6 | 0.5 | 0.3 |
| 755.2 | 2.2 | 0.4 | 0.1 | 0.6 | 0.1 | 1.2 | 0.6 | 0.1 | 0.8 |
| 756.6 | 1.4 | 0.4 | 0.1 | 0.1 | 0.3 | 0.8 | 0.6 | 0.3 | 0.3 |
| 756.8 | 1.4 | 0.0 | 0.1 | 0.0 | 0.6 | 0.7 | 0.5 | 0.9 | 0.3 |
| 760.7 | 2.4 | 0.0 | 0.1 | 0.0 | 1.7 | 1.8 | 0.8 | 0.9 | 0.3 |
| 761.8 | 3.9 | 0.0 | 0.0 | 0.0 | 3.0 | 3.1 | 0.8 | 1.0 | 0.6 |
| 764.45 | 3.7 | 0.1 | 0.0 | 0.0 | 1.4 | 1.5 | 0.4 | 0.9 | 0.6 |
| 765 | 2.7 | 0.4 | 0.2 | 0.1 | 1.6 | 2.3 | 0.8 | 0.7 | 0.5 |
| 767.6 | 2.1 | 0.1 | 0.0 | 0.1 | 1.3 | 1.5 | 0.7 | 0.8 | 0.5 |
| 774 | 4.5 | 0.2 | 0.1 | 0.1 | 2.9 | 3.3 | 0.7 | 0.9 | 0.8 |
| 775.55 | 2.5 | 0.1 | 0.1 | 0.1 | 1.7 | 2.0 | 0.8 | 0.8 | 0.4 |
| 776.4 | 3.0 | 0.2 | 0.1 | 0.1 | 2.5 | 2.9 | 1.0 | 0.9 | 0.5 |
| 777.8 | 3.0 | 0.0 | 0.1 | 0.0 | 3.0 | 3.1 | 1.0 | 1.0 | 0.5 |
| 779.45 | 3.0 | 0.0 | 0.1 | 0.0 | 2.7 | 2.9 | 1.0 | 0.9 | 0.5 |

| | | | | | | | | | |
|---|---|---|---|---|---|---|---|---|---|
| 780.3 | 4.0 | 2.0 | 0.1 | 0.7 | 0.4 | 3.1 | 0.8 | 0.1 | 0.4 |
| 780.95 | 2.5 | 0.2 | 0.2 | 0.1 | 1.9 | 2.3 | 0.9 | 0.8 | 0.3 |
| 782.9 | 3.1 | 0.2 | 0.1 | 0.1 | 3.2 | 3.5 | 1.1 | 0.9 | 0.5 |
| 787.4 | 4.5 | 0.7 | 0.1 | 0.1 | 3.2 | 4.0 | 0.9 | 0.8 | 0.7 |
| 791 | 3.6 | 0.6 | 0.1 | 0.3 | 0.9 | 1.9 | 0.5 | 0.5 | 0.5 |
| 794.1 | 5.0 | 0.2 | 0.1 | 0.3 | 2.4 | 3.0 | 0.6 | 0.8 | 0.8 |
| 796.2 | 4.5 | 1.0 | 0.1 | 0.8 | 0.7 | 2.5 | 0.5 | 0.3 | 0.6 |
| 797.05 | 4.5 | 0.3 | 0.1 | 0.7 | 0.9 | 2.0 | 0.4 | 0.5 | 0.6 |
| 802.1 | 5.1 | 0.4 | 0.2 | 0.6 | 0.4 | 1.5 | 0.3 | 0.3 | 0.9 |
| 813.25 | 4.1 | 2.5 | 0.2 | 0.4 | 0.2 | 3.3 | 0.8 | 0.1 | 0.7 |
| 813.6 | 4.3 | 0.2 | 0.1 | 0.9 | 0.7 | 1.9 | 0.5 | 0.3 | 0.7 |
| 815.2 | 4.9 | 0.5 | 0.1 | 0.9 | 0.4 | 2.0 | 0.4 | 0.2 | 0.6 |
| 818.8 | 5.2 | 0.6 | 0.1 | 0.6 | 0.2 | 1.5 | 0.3 | 0.1 | 0.7 |
| 822.45 | 4.7 | 0.7 | 0.1 | 1.1 | 0.6 | 2.6 | 0.5 | 0.2 | 0.8 |
| 823.3 | 4.5 | 0.3 | 0.1 | 0.2 | 0.4 | 1.0 | 0.2 | 0.4 | 0.7 |
| 829.9 | 5.1 | 1.2 | 0.2 | 0.4 | 0.5 | 2.4 | 0.5 | 0.2 | 0.8 |
| 849.6 | 4.7 | 0.2 | 0.1 | 0.1 | 0.4 | 0.8 | 0.2 | 0.5 | 0.7 |
| 855.65 | 7.5 | 1.1 | 0.1 | 0.4 | 0.7 | 2.3 | 0.3 | 0.3 | 1.0 |
| 861.05 | 5.8 | 0.4 | 0.1 | 1.1 | 0.4 | 2.0 | 0.3 | 0.2 | 0.7 |
| 881.7 | 4.8 | 0.2 | 0.1 | 1.1 | 0.3 | 1.7 | 0.4 | 0.2 | 0.6 |

**Appendix A. Molybdenum Compilation References**


Alberdi-Genolet, M. & Tocco, R. Trace metals and organic geochemistry of the Machiques Member (Aptian-Albian) and La Luna Formation (Cenomanian-Campanian), Venezuela. *Chemical Geology* **160**, 19-38 (1999).

Caplan, M. L & Bustin, R. M. Palaeoceanographic controls on geochemical characteristics of organic-rich Exshaw mudrocks: role of enhanced primary production. *Organic Geochemistry* **30**, 161-188 (1998).

Cruse, A. M. & Lyons, T. W. Trace metal records of regional paleoenvironmental variability in Pennsylvanian (Upper Carboniferous) black shales. *Chemical Geology* **206**, 319-345 (2004).

Hatch, J. R. & Leventhal, J. S. Relationships between inferred redox potential of the depositional environment and geochemistry of the Upper Pennsylvanian (Missourian) Stark Member of the Dennis Limestone, Wabaunsee County, Kansas, U.S.A. *Chemical Geology* **99**, 65-82 (1992).

Hatch, J. R. & Leventhal, J. S. Early digenetic partial oxidation of organic matter and sulfides in the Middle Pennsylvanian (Desmoinesian) Excello Shale Member of the Fort Scott Limestone and equivalents, northern Midcontinent region, USA. *Chemical Geology* **134**, 215-235 (1997).

Hirner, A. V. & Xu, Z. Trace metal speciation in Julia Creek oil shale. *Chemical Geology* **91**, 115-124 (1991).

Leventhal, J. S. Comparison of organic geochemistry and metal enrichment in two black shales: Cambrian Alum Shale of Sweden and Devonian Chattanooga Shale of United States. *Mineralium Deposita* **26**, 104-112 (1991).

Mongenot, T., Tribovillard, N., Desprairies, A., Lallier-Vergés & Laggonun-Defarge, F. Trace elements as paleoenvironmental markers in strongly mature hydrocarbon source rocks: the Cretaceous La Luna Formation of Venezuela. *Sedimentary Geology*, **103**, 23-37 (1996).

Sageman, B. B., Murphy A. E., Werne, J. P., Ver Straeten, C. A., Hollander, D. J. & Lyons, T. W. A tale of shales: the relative roles of production, decomposition, and dilution in the accumulation of organic-rich strata, Middle-Upper Devonian, Appalachian basin. *Chemical Geology* **195**, 229-273 (2003).

Werne, J. P., Sageman, B. B., Lyons, T. W. & Hollander, D. J. An integrated assessment of a "type euxinic" deposit: evidence for multiple controls on black shale deposition in the Middle Devonian Oatka Creek Formation. *American Journal of Science* **302**, 110-143 (2002).

Yamaguchi, K. Geochemistry of Archean-Paleoproterozoic black shales: the early evolution of the atmosphere, oceans, and biosphere (2002).